



University
of Glasgow

<https://theses.gla.ac.uk/>

Theses Digitisation:

<https://www.gla.ac.uk/myglasgow/research/enlighten/theses/digitisation/>

This is a digitised version of the original print thesis.

Copyright and moral rights for this work are retained by the author

A copy can be downloaded for personal non-commercial research or study,
without prior permission or charge

This work cannot be reproduced or quoted extensively from without first
obtaining permission in writing from the author

The content must not be changed in any way or sold commercially in any
format or medium without the formal permission of the author

When referring to this work, full bibliographic details including the author,
title, awarding institution and date of the thesis must be given

Enlighten: Theses

<https://theses.gla.ac.uk/>
research-enlighten@glasgow.ac.uk



Synthesis of New Flavin – based Rotaxanes

**Catherine E. Maclean
0104919.**

**Msc Research Thesis
2007**

Supervisor: Dr G. Cooke

ProQuest Number: 10753830

All rights reserved

INFORMATION TO ALL USERS

The quality of this reproduction is dependent upon the quality of the copy submitted.

In the unlikely event that the author did not send a complete manuscript and there are missing pages, these will be noted. Also, if material had to be removed, a note will indicate the deletion.



ProQuest 10753830

Published by ProQuest LLC (2018). Copyright of the Dissertation is held by the Author.

All rights reserved.

This work is protected against unauthorized copying under Title 17, United States Code
Microform Edition © ProQuest LLC.

ProQuest LLC.
789 East Eisenhower Parkway
P.O. Box 1346
Ann Arbor, MI 48106 – 1346

**GLASGOW
UNIVERSITY
LIBRARY:**

GUL

25 JAN 2008

14723

UNIVERSITY OF GLASGOW
MSc(R)
THESIS ACCESS DECLARATION

Candidate's Name:CATHERINE ...MACLEAN.....
(BLOCK CAPITALS)
Registration number:.....0104919.....

Thesis Title: Synthesis of New Flavin – based Rotaxanes

Department and

Faculty:.....CHEMISTRY.....

Name of supervisor(s):.....Dr G. COOKE.....

IMPORTANT NOTES

In the interests of scholarship, theses of the University of Glasgow are normally made freely available, for example for consultation in the University Library, or within another Library, immediately after deposit. Electronic copies are normally made available online to increase the access to, and visibility of, the University's research.

Candidates should consult <http://theses.gla.ac.uk/gettingstarted> and talk to their supervisor before completing and signing this form to establish whether there is likely to be a valid reason for restricting access to their thesis for a limited period of time.

The Freedom of Information (Scotland) Act 2002 ("FOISA") and the Environmental Information (Scotland) Regulations 2004 ("EI(S)Rs") ensure access to any information held by the University of Glasgow, including theses, unless an exemption or exception applies.

Reasons for restricting access to a thesis should be derived from exemptions under FOISA or exceptions under EI(S)Rs. Further restrictions, as described below, can be applied to online availability of the electronic version.

Candidates should consult any sponsoring organisations that may hold intellectual property rights in a thesis before completing this form.

Candidates will be required to declare at the point of electronic deposit that the copy being deposited is the same in all respects as the print copy with the exception of any 3rd party copyright material removed because permission for its inclusion has not been granted.

Does any organisation other than the University of Glasgow have an interest in the intellectual property rights to your work? If yes, please specify the organisation and the nature of their interest:

.....

.....

.....

Candidates who believe there is a valid reason to restrict access to both the hard copy and the electronic copy of their thesis should consult the list of exemptions permitted by the Freedom of Information (Scotland) Act 2002 and the list of exceptions permitted by the Environmental Information (Scotland) Regulations 2004 available at <http://theses.gla.ac.uk> and give specific details below of the relevant exemption/exception and why an exemption/exception is necessary (continue on an attached sheet of paper as necessary).
Please select one of the following two options:

No exemption/exception requested – make the thesis available immediately
Exemption/exception requested (please give details):....

The following further reason may be applied to the electronic copy only. Please tick the box below if applicable.

- The thesis contains material whose copyright belongs to a third party and the gaining of approval to publish the material electronically would be onerous or expensive; and the removal of the copyright material would compromise the thesis.

In normal circumstances any thesis to which access has been restricted will be made available after three years (this does not apply to theses restricted for reasons of copyright). Candidates who believe access to their thesis should be restricted for more than three years should state their reason here:

Please note that the University of Glasgow may be required to overturn any request for restricted access to any thesis.

To be completed by the student:

I confirm that the information I have given on this form is complete and accurate.

Signed (Author): Catherine MacLean:

Address (Author):... 14 BISHOP GARDENS.....

.....HAMILTON.....
MI 37YE.....

E-mail address
(Author):.....catmac@chem.gla.ac.uk.....

Date: 8/11/07

This section must be completed by your primary supervisor:

I confirm that I agree with the decision indicated on this form by the author of the thesis with respect to access to the thesis.

Signature (Supervisor): G. Smits

Signature (Supervisor):
Date: 8/11/07

Please return this form to your Graduate School

For more information, visit www.ams.org.

Graduate School use only:

Embargo granted Yes No

Abstract

In recent years the development of interlocked structures has been of significant importance for the expansion of molecular machines. In particular those that incorporate the rotaxane architecture, so as to utilise the shuttling properties associated with the class of structure.

The research described herein is of the synthesis of a new class of flavin based [2] rotaxanes, such that the flavin moiety acts as the rotaxane stoppers. The construction of the rotaxane threads from two modified flavin architectures are reported within.

With the use of trifluoromethyl flavin and dimethoxy flavin units, the symmetric bis-trifluoromethyl-flavin stoppered axle, and the asymmetric trifluoromethyl – dimethoxy flavin stoppered axle units were synthesised, and the corresponding interlocked [2] rotaxane structures are described.

The expectation is that these systems will lead to the development of new flavin based molecular machines, by the virtue of the redox induced shuttling properties that are inherent in these types of systems.

Acknowledgements.

I would like to thank Dr. G. Cooke for all his help, patience and expertise over the past year whilst I was working on my MSc.

I would also like to thank all in the Cooke research group for all their help within the lab.

In particular Dr. G. Rabani and Dr. S. Caldwell the postdocs in the group for their help, input, patience and good humour through out.

I would like to thank Ms N. Kryvokhyzha for elucidating the experimental pathway that was set before me.

I would also like to thank Mr. J. Tweedie, Ms I. Freer, and Mr D. Adams for their continual help with Mass Spec and NMR work.

Most of all I would like to thank my family and friends for their continual support over the past twelve months and beyond.

Glossary

CHCl ₃ / CDCl ₃	Chloroform / d ₁ -Chloroform.
CF ₃ -Flavin	10-Isobutyl-7-(trifluoromethyl)benzo[g]pteridine-2,4-dione.
Dimethoxy flavin	10-Isobutyl-7,8-dimethoxybenzo[g]pteridine-2,4-dione.
DCM	Dichloromethane.
DAP	Diaminopyridine
DMAP	4-Dimethylaminopyridine.
DB24C8	Dibenzo [24]-crown-8 ether
DMF	Dimethyl formamide.
DMSO	Dimethyl sulfoxide.
DTT	1,4-Dithio-DL-threitol.
EDCI	1-(3-Dimethylaminopropyl)-3-ethyl carbodiimide.
Et ₃ N	Triethylamine.
EtOH	Ethanol.
MeOH	Methanol.
EtOAc	Ethyl acetate.
FAB	Fast Atom Bombardment.
HCl	Hydrochloric acid.
LiAlH ₄	Lithium aluminium hydride.
MgSO ₄	Magnesium sulfate.
NaOH	Sodium hydroxide.
NOBA	Nitro benzyl alcohol.
Pd / C	5% Palladium on carbon.
TLC	Thin layer chromatography.
THF	Tetrahydrofuran.
CBPQT ⁴⁺	Tetracationic cyclophane cyclobis(paraquat- <i>p</i> -phenylene)
MALDI	Matrix assisted laser desorption ionisation.

Contents Page

1.0 Introduction

<u>1.0.1 Supramolecular Chemistry.</u>	1
<u>1.0.1.1 Intermolecular Interactions.</u>	1
<u>1.0.1.2 Important Factors in Supramolecular Chemistry.</u>	7
<u>1.2.0 Rotaxanes and Catenanes.</u>	9
<u>1.3.0 Molecular Devices And Machines.</u>	12
<u>1.3.1 Molecular Wires.</u>	12
<u>1.3.2 Switches and Sensors.</u>	14
<u>1.3.3 Rotors And Motors.</u>	15
<u>1.3.4 Maxwells Demons.</u>	17
<u>1.3.5 Dynamic Random Access Memory Devices.</u>	19
<u>1.3.6 Hydrogen bonded Rotaxane Systems.</u>	20
<u>1.3.7 Other Rotaxane systems.</u>	27
<u>1.4 Flavins.</u>	28
<u>1.5 Aims And Objectives.</u>	34
<u>2.0 Results And Discussions.</u>	36
<u>2.1 Synthesis of The First Half Of The Asymmetric Axe.</u>	37
<u>2.2 The Second Half of The Asymmetric Axe Synthesis.</u>	43
<u>2.3 Coupling To Form The Axe And Subsequent Rotaxane Fomation.</u>	52

<u>3.0 Conclusions and Future Work.</u>	58
<u>3.1 Conclusions.</u>	58
<u>3.2 Future Work.</u>	58
<u>4.0 Experimental.</u>	59
<u>4.1 General Experimental.</u>	59
<u>4.2 Chemical Experimental.</u>	60
<u>5.0 Appendices.</u>	75
<u>1. ^1H NMR</u>	75
10-Isobutyl-3-(4-nitrobenzyl)-7-(trifluoromethyl)benzo[g]pteridine-2,4-dione	
<u>2. ^1H NMR</u>	76
3-(4-Aminobenzyl)-10-isobutyl-7-(trifluoromethyl)benzo[g]pteridine-2,4-dione	
<u>3. ^1H NMR</u>	77
4-(4-((10-Isobutyl-2,4-dioxo-7-(trifluoromethyl)benzo[g]pteridin-3-yl)methyl) phenylamino)-4-oxobutanoic acid	
<u>4. ^1H NMR</u>	78
Perfluorophenyl 4-(4-((10-isobutyl-2,4-dioxo-7-(trifluoromethyl)benzo[g]pteridin-3-yl)methyl)phenylamino)-4-oxobutanoate	
<u>5. ^{13}C NMR CPD</u>	79
Perfluorophenyl 4-(4-((10-isobutyl-2,4-dioxo-7-(trifluoromethyl)benzo[g]pteridin-3-yl)methyl)phenylamino)-4-oxobutanoate	
<u>6. ^{19}F NMR</u>	80
Perfluorophenyl 4-(4-((10-isobutyl-2,4-dioxo-7-(trifluoromethyl)benzo[g]pteridin-3-yl)methyl)phenylamino)-4-oxobutanoate	
<u>7. ^{19}F NMR CPD</u>	81
Perfluorophenyl 4-(4-((10-isobutyl-2,4-dioxo-7-(trifluoromethyl)benzo[g]pteridin-3-yl)methyl)phenylamino)-4-oxobutanoate	
<u>8. ^1H NMR</u>	82
6-chloropyrimidine-2,4(1H,3H)-dione	

<u>9. $^1\text{H NMR}$</u>	83
N-(3,4-dimethoxyphenyl)isobutyramide	
<u>10. $^1\text{H NMR}$</u>	84
N-isobutyl-3,4-dimethoxyaniline	
<u>11. $^1\text{H NMR}$</u>	85
10-isobutyl-7,8-dimethoxy-2,4-dioxo-2,3,4,10-tetrahydrobenzo[g]pteridine 5-oxide	
<u>12. $^1\text{H NMR}$</u>	86
10-isobutyl-7,8-dimethoxybenzo[g]pteridine-2,4-dione	
<u>13. $^1\text{H NMR}$</u>	87
10-isobutyl-7,8-dimethoxy-3-(4-nitrobenzyl)benzo[g]pteridine-2,4-dione	
<u>14. $^1\text{H NMR}$</u>	88
3-(4-aminobenzyl)-10-isobutyl-7,8-dimethoxybenzo[g]pteridine-2,4-dione	
<u>15. $^1\text{H NMR}$</u>	89
N1-(4-((10-isobutyl-2,4-dioxo-7-(trifluoromethyl)benzo[g]pteridin-3- yl)methyl) phenyl)-N4-((4-((10-isobutyl-7,8-dimethoxy-2,4- dioxobenzo[g]pteridin-3-yl) methyl)phenyl)succinamide	
<u>16. $^1\text{H NMR}$</u>	90
Asymmetric [2] Rotaxane	
<u>17. Mass Spec.</u>	91
Mass Spectrum of The Asymmetric Rotaxane Page 1	
<u>18. Mass Spec.</u>	92
Mass Spectrum of The Asymmetric Rotaxane Page 2	
<u>19. Mass Spec.</u>	93
Mass Spectrum of The Symmetric Rotaxane.	
<u>References.</u>	94

<u>Figures.</u>	<u>Page</u>
<u>Figure 1</u>	2
<u>Figure 2</u>	2
<u>Figure 3</u>	3
<u>Figure 4</u>	3
<u>Figure 5</u>	4
<u>Figure 6</u>	5
<u>Figure 7</u>	5
<u>Figure 8</u>	6
<u>Figure 9</u>	6
<u>Figure 10</u>	7
<u>Figure 11</u>	8
<u>Figure 12</u>	8
<u>Figure 13</u>	9
<u>Figure 14</u>	10
<u>Figure 15</u>	10
<u>Figure 16</u>	11
<u>Figure 17</u>	11
<u>Figure 18</u>	11
<u>Figure 19</u>	12
<u>Figure 20</u>	13
<u>Figure 21</u>	13
<u>Figure 22</u>	14
<u>Figure 23</u>	15
<u>Figure 24</u>	16
<u>Figure 25</u>	17
<u>Figure 26</u>	18
<u>Figure 27</u>	19
<u>Figure 28</u>	20
<u>Figure 29</u>	20
<u>Figure 30</u>	21
<u>Figure 31</u>	23

<u>Figure 32</u>	25
<u>Figure 33</u>	26
<u>Figure 34</u>	26
<u>Figure 35</u>	27
<u>Figure 36</u>	28
<u>Figure 37</u>	29
<u>Figure 38</u>	30
<u>Figure 39</u>	30
<u>Figure 40</u>	31
<u>Figure 41</u>	33
<u>Figure 42</u>	34
<u>Figure 43</u>	35
<u>Figure 44</u>	35
<u>Figure 45</u>	38
<u>Figure 46</u>	40
<u>Figure 47</u>	42
<u>Figure 48</u>	44
<u>Figure 49</u>	45
<u>Figure 50</u>	47
<u>Figure 51</u>	48
<u>Figure 52</u>	49
<u>Figure 53</u>	49
<u>Figure 54</u>	51
<u>Figure 55</u>	55
<u>Table 1</u>	32
<u>Scheme 1.</u>	24
<u>Scheme 2.</u>	37
<u>Scheme 3.</u>	38
<u>Scheme 4.</u>	39
<u>Scheme 5.</u>	40
<u>Scheme 6.</u>	41
<u>Scheme 7.</u>	43

<u>Scheme 8.</u>	44
<u>Scheme 9.</u>	44
<u>Scheme 10.</u>	45
<u>Scheme 11.</u>	46
<u>Scheme 12.</u>	46
<u>Scheme 13.</u>	47
<u>Scheme 14.</u>	48
<u>Scheme 15.</u>	49
<u>Scheme 16.</u>	50
<u>Scheme 17.</u>	50
<u>Scheme 18.</u>	52
<u>Scheme 19.</u>	53
<u>Scheme 20.</u>	54
<u>Scheme 21.</u>	55
<u>Scheme 22.</u>	56
<u>Scheme 23.</u>	57

1.0 Introduction.

1.0.1 Supramolecular chemistry.

Supramolecular chemistry is the study of molecular assemblies of two or more molecules associated with each other using non covalent interactions such as hydrogen bonding, the hydrophobic effect, donor-acceptor interactions. Examples of naturally occurring supramolecular structures include DNA, tobacco mosaic virus and chlorophyll in plant leaves.

In 1987 Charles J. Pedersen and Donald J. Cram, and Jean-Marie Lehn won the nobel prize for chemistry for their work within the area of supramolecular chemistry. Jean-Marie Lehn described supramolecular chemistry as:

"the chemistry of the intermolecular bond covering the structures and functions of the entities formed by association of two or more chemical species."^[1]

He described these interactions as the basis for the highly specific recognition processes found in biology such as found in substrate binding to a receptor protein.

Donald J Cram, Lehns fellow nobel laureate defined host guest complexes as:

"Complexes are composed of two or more molecules or ions held together in unique structural relationships by electrostatic forces other than those of full covalent bonds." "High structural organization is usually produced only through multiple binding sites." "A host-guest relationship involves a complimentary stereo-electronic arrangement of binding sites in host and guest."^[2]

1.0.1.1 Intermolecular Interactions.

Host guest complexes involve reversible binding of a substrate to a receptor using non-covalent interactions such as Hydrogen bonding,

electrostatic interactions and, π - π stacking interactions. A diagrammatic illustration is shown in Figure 1.

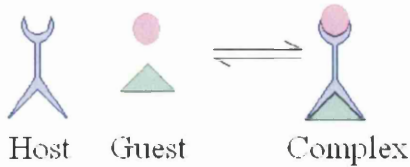


Figure 1. Schematic diagram of host – guest binding

In 1894 Fischer hypothesised the lock and key principle for the visualisation of substrate- enzyme interactions. The principle describes the complimentary nature of the host guest binding site, which is dependent on size, shape and position of host to guest in the complex. The binding site must be both sterically and electronically complementary to the substrate requiring to bind. A schematic of the fischer lock and key is shown below in Figure 2.^[3,4]

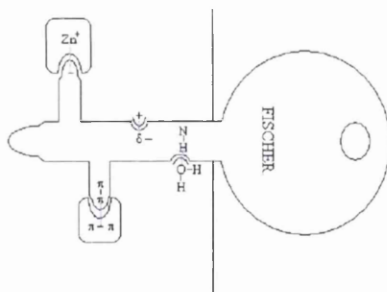


Figure 2. Schematic diagram showing Fischers' lock and key principle.

Examples include the complimentary association of the two strands in DNA where hydrogen bonding and π -stacking occur between the nucleobases, Adenine and Thymine and Guanine and Cytosine respectively as shown in Figure 3.

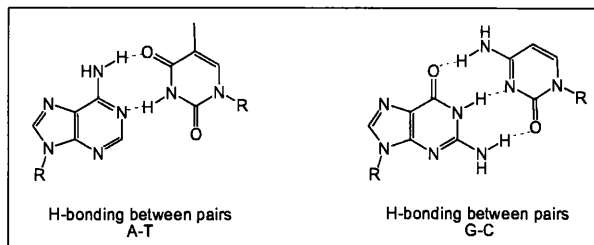


Figure 3. Hydrogen bonding found between the nucleoside base pairs of DNA.

Non covalent interactions are weaker forces than covalent interactions with a strength in the range of 2kJmol^{-1} to 250kJmol^{-1} compared 350kJmol^{-1} for covalent bonding. Each interaction has different ranges in strength.

Electrostatic Interactions.

Electrostatic interactions are a high strength interaction based on the Coulombic attraction between opposite charges. They can be found in ionic bonding complexes, between dipoles, and through the attraction of lone pairs in highly electronegative atoms to electron rich atoms in another molecule. Hydrogen bonding is a specific type of electrostatic interaction found in supramolecular chemistry.^[3,4,5] The different types of interaction is shown in Figure 4.

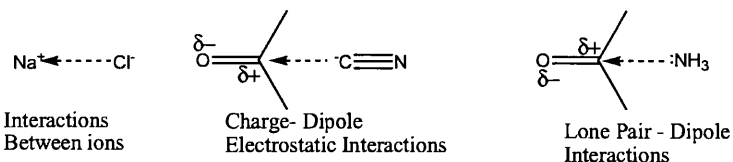


Figure 4. Shows the different types of electrostatic interaction.

Van der Waals Forces.

Van der Waals forces, are general weak interactions that are typically $<5\text{kJmol}^{-1}$. An electron cloud can be polarised by its proximity to

an adjacent nucleus causing a weak, temporary electrostatic interaction. Van der Waals forces are not used for the design of supramolecular structures due to the unspecific and low strength of these interactions.^[3,4]

Ion-Dipole Interactions

Ion-Dipole interactions are strong, and relatively directional, with interactions of between 50- 200kJmol⁻¹. The strongest interactions occur when suitable alignment of the dipole and charge is present. They are found in the binding of metal cations to crown ethers, where the oxygen lone pairs are attracted to the positive charge of metal cation. An example of ion-dipole interactions can be seen in Figure 5.^[3,4]

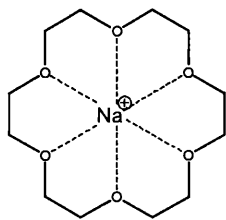


Figure 5. The binding of Na⁺ within the cavity of [18]-Crown-6.

Dipole- Dipole Interactions.

Dipole- Dipole interactions require the alignment of dipoles, which can result in an attractive force in the range of 5-50kJmol⁻¹. Alignment can be of a single pair of poles or opposing alignments of dipoles. Opposing alignments of dipole gives the strongest interactions. Figure 6 shows both single and opposing dipole interactions.^[3,4]

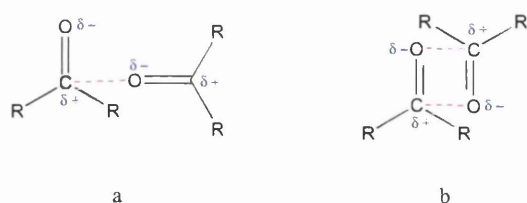


Figure 6. 6a), singular dipole interactions. 6b), opposing dipole interactions.

Hydrophobic Interactions.

Hydrophobic Interactions are the specific driving force for non-polar species to associate together in aqueous solutions. As the species associate together there is an increase in entropy as water molecules become more disordered. There is also an increase in enthalpy as the hydrogen bonding between water molecules becomes stronger. The schematic below in Figure 7 shows the expulsion of water from a hydrophobic centre, as a result of binding from a general hydrophobic species.^[3,4]

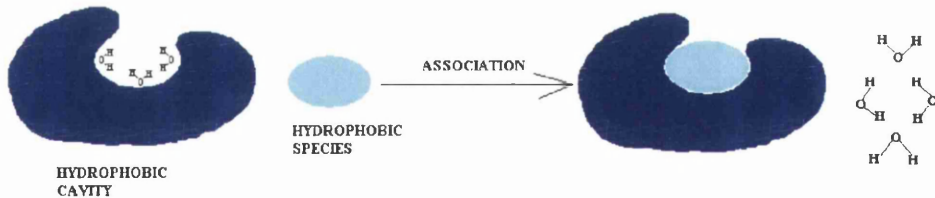


Figure 7. Schematic representation of the hydrophobic effect

Hydrogen Bonding Interactions

Hydrogen bonding is an important type of intermolecular interaction found between hydrogen atoms attached to a highly electronegative atom that can be N, O, P, and halogens, and the non-bonding electron pair on another electronegative atom, which can also be N, O, P, and halogens. They are highly specific directional electrostatic

forces, which are precise and can have a wide range of strengths, varying from $4 - 12\text{ kJmol}^{-1}$ for weak bonds up to $60-120\text{ kJmol}^{-1}$ for strong hydrogen bonds. Hydrogen bonding is utilised in biological systems including enzymes and DNA. They are found in receptors where coordination of neutral organic species such as amides and short chain alcohols to amino acids at the active site occur.

The bonding in the donor complex is highly polarised with the donor atom being δ^- and the hydrogen atom is δ^+ , as shown in Figure 8.

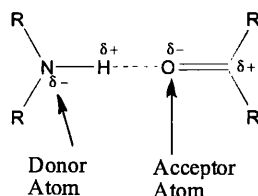


Figure 8. The donor acceptor interactions found in hydrogen bonding.

Hydrogen bonding can be spread over multiple atoms and have a number of different angles in relation to the position of the hydrogen to the acceptor atom. The more linear the hydrogen bond the stronger the bond: angles of $175-180^\circ$ have strengths of between $60-120\text{ kJmol}^{-1}$, angles of $130-180^\circ$ tend to have strengths of $16-60\text{ kJmol}^{-1}$ and the weakest interactions of $<12\text{ kJmol}^{-1}$ tend to occur when the angle of H-bonding is between $90-150^\circ$. Bond distances can vary between $1.2 - 3.2\text{ \AA}$ for $\text{H} - \text{A}$ and $2.2-4.0\text{ \AA}$ for $\text{D}-\text{H}$, where the closer the atoms, the stronger the interaction. Hydrogen bonding angles are shown in Figure 9.^[3,4]

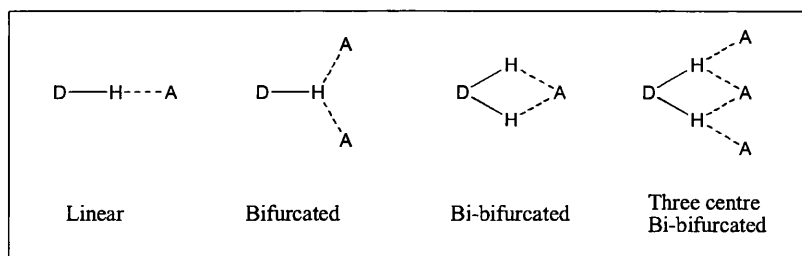


Figure 9. The different possible angles for H-bonding

π - π Stacking Interactions.

π - π Stacking Interactions are the weak electrostatic interaction between aromatic rings. The strength of these interactions ranges from 0-50kJmol⁻¹. There are two types of π stacking interactions, they are face-to-face and edge-to-face. Face-to-face π -stacking is the interaction between the electron clouds of the aromatic rings where the clouds are parallel to each other. Face-to-face π stacking is found between the nucleobases in DNA. Edge-to-face π stacking is where there is an interaction between an electron deficient hydrogen of one aromatic ring to the electron rich π cloud of another aromatic ring. Crystallisation of edge to face aromatic rings yields a herringbone distribution pattern. Edge-to-face and face-to-face alignment structures are shown below in Figure 10.^[3,4]



Figure 10.

- 10a) The edge-to-face π stacking. 10b) The face-to-face π stacking.

1.0.1.2 Important Factors in Supramolecular Chemistry.

The Chelate Effect.

The chelate effect is where the stability of a complex increases with the number of binding sites on a guest in comparison to the equivalent monodentate ligand bound to the same substrate. For example the chelation of ethylene diamine to Ni²⁺ is 10⁸ times stronger than the chelation of ammonia to Ni²⁺, due to the enhanced stability of the complex. As shown in Figure 11.^[3,4]

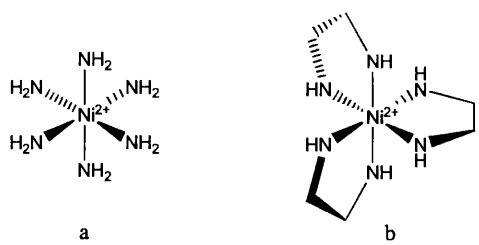


Figure 11. Binding of Ni^{2+} complexes. 11a) $[\text{Ni}(\text{NH}_3)_6]^{2+}$
And 11b) $[\text{Ni}(\text{en})_3]^{2+}$

Preorganisation

Preorganisation is where the host is in a conformation that requires very little or no rearrangement to bind the substrate. Preorganised structures exhibit slower binding kinetics to less preorganised structures, however, binding tends to be stronger in preorganised complexes, such that the spherand binds up to 10^{10} times more strongly than the equivalent crown ether. This is exemplified in Figure 12.^[3,4]

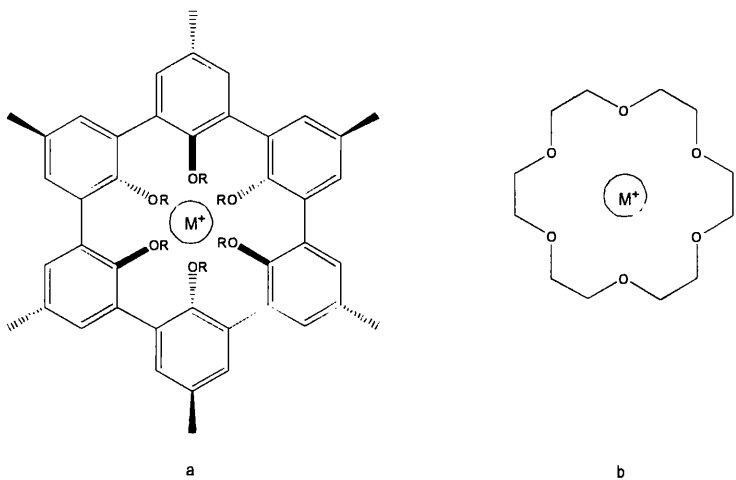


Figure 12. The binding of a metal cation to 12a) a spherand and 12b) a crown ether.

Self Assembly.

When two or more components aggregate spontaneously and reversibly together to give a non-covalently bound complex, using intermolecular forces to hold the complex together. Coordination of substrates can give appropriate alignment for covalent interactions to occur between individual substrates to form a macrocycle *insitu* of complexation.^[3,4] An example of a self assembled structure is the double helix found in DNA. The two strands are held together by a combination of hydrophobic interactions, hydrogen bonding and π -stacking between the nitrogen base pairs attached to the phosphate backbone. An illustration of the conformation shape of DNA is shown in Figure 13.^[6]

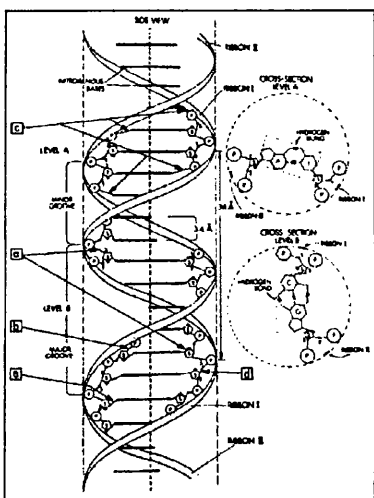


Figure 13, Illustration of DNA.

1.2 Rotaxanes and Catenanes.

Rotaxanes and catenanes are interlocked structures, such that the components are joined together such that separation is blocked by mechanical bonds. For rotaxanes the structure is composed of an axle, typically containing at least two sites of intermolecular interactions, and a macrocyclic ring that can bind to the sites on the axle. For catenanes, the

structure is composed of two macrocyclic rings intertwined together. Figure 14 below shows the basic form of these structures. Naming of these structures comes from the number of interlocked components, such as the rotaxane and catenane below are [2] rotaxane and [2] catenane structures. It is possible to have more than two components in these structures and the names change accordingly.

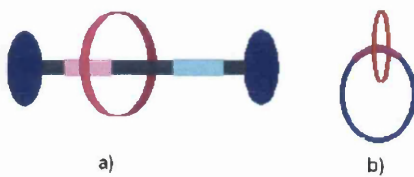


Figure 14. 14a) [2]-rotaxane 14b) [2]-catenane

Rotaxane and catenanes are supramolecular architectures which have gained interest in recent years due to their potential as molecular machines, switches, motors and molecular memory devices. The components of these structures can freely move relative to each other, without breaking covalent bonds. Motion of the macrocyclic ring relative to the axle can be in two forms, the lateral shuttling from one site of intermolecular interactions to another, and rotation around one site with no lateral movement observed^[7]. This is shown diagrammatically in Figure 15.

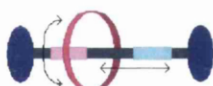


Figure 15. Motions found in [2] rotaxanes.

By modulating the structure, they can be tuned to take advantage of particular properties such as fluorescence, electrochemical potential, optical properties and the strength of non-covalent interactions in relation to each component, and so can control of the movement of the ring.^[8,9]

There are a number of ways of synthesising rotaxanes. The first is via the formation of a pseudo-rotaxane with the blocking of the ends with

bulky stopper groups. This is not always successful in great yields as the ring can move freely on and off the axle. See Figure 16.



Figure 16. Mechanism for ring threading then capping of ends.

The second method is by clipping the macrocyclic ring around the axle with stopper groups already attached. This is the preferred route as the halves of the ring associate with axle at a site of non-covalent interactions and then joins together to give the required rotaxane. See Figure 17.

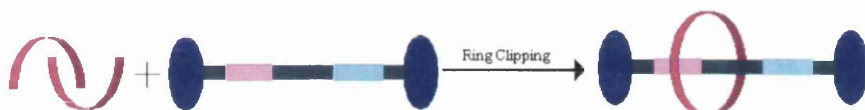


Figure 17. Clipping mechanism.

The third method is by capping of bulky substituents to the axle followed by a ring slipping reaction at high temperatures to yield the rotaxane. The axle may have thermal stability problems so not always an appropriate method of rotaxane synthesis. See Figure 18.



Figure 18. Ring slippage mechanism

Catenanes can be made by first synthesising the initial ring then clipping the second around it in a similar manner to the clipping of the ring to the rotaxane. They can also be made by clipping both rings together simultaneously. As shown in Figure 19.



Figure 19. Clipping of Catenanes

1.3 Molecular Devices and Machines

As mentioned in the previous sections, supramolecular systems fabricated from interlocked structures are finding considerable interest in the construction of molecular machines and devices. In this section the terminology will be introduced and examples of how the structures have been used to make machines and devices given.

Molecular devices are molecular assemblies that can carry out a function of some sort using non-covalent interactions in host / guest complexes. Molecular machines are molecular assemblies that with the addition of a stimulus cause a net nuclear displacement of one molecule relative to another in the complex, which in turn can cause affect the external environment in a way that can be utilised. Such as the ON/OFF of fluorescence by a molecular switch in the presence of a quenching agent.

1.3.1 Molecular Wires.

Molecular wires are typically semi-conducting polymer chains that can carry out electron- or charge-transfer steps. The wires can be branched and self insulating such as the self assembled arylene - ethynylene 7nm molecular wire shown below. It was assembled onto a gold surface. It was shown that a single molecule has an electrical current of 0.35 ± 0.05 nA at a 0.3V. The structure of the wire is shown Figure 20.^[10]

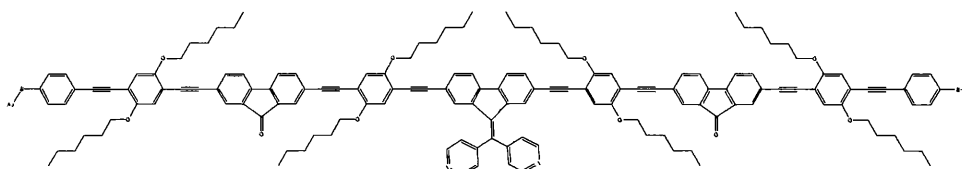


Figure 20. 7nm Molecular Wire.

Wires can also be insulated by other polymeric structures such as the insulation of poly (4,4'-diphenylenevinylene) {PDV} derivatives, with α - and/or β - cyclodextrins { α -CD or β -CD}. It has been found that insulating the semi-conductive wires show the retention of the basic semi-conductance and optical properties found in the non-rotaxinated chains. Insulation by the cyclodextrin rings avoids the aggregation of the polymer chains, yielding a minimum separation of cofacial π systems which tends to be greater than the maximum distance required to stop self quenching of photoluminescence. As a direct result of this, there is a blue-shift in rotaxinated wires compared to the un-insulated chains, this is exemplified by β -CD-PDV having a \sim 142meV (\sim 30nm) shift in energy to PDV by itself. Photoluminescence efficiency is also increased with insulation, with β -CD-PDV having $17 \pm 1\%$ efficiency, whereas PDV wire itself has $4.3 \pm 0.3\%$ efficiency. Although efficiency of photoluminescence has increased and a blue-shift in light emitted, charge transfer still occurs along the chain. Polymer LEDs were made from the photoluminescent wires and was found that luminescence levels went up to several candela per metre² with just over 10V used. Diagram of the wire is shown in Figure 21.^[11]

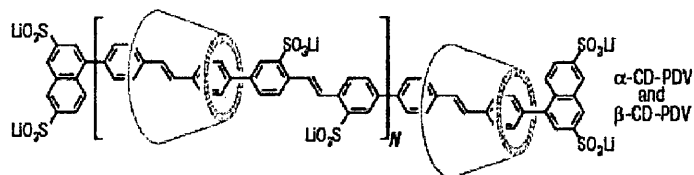


Figure 21 Cyclodextrin threaded onto a molecular wire.

1.3.2 Switches and Sensors.

Switches are molecules that can inter-convert between two or more stable forms. They can have many forms and can be used for a great variety of functions, varying from molecular logic gates, sensors, to molecular dye pigments and within molecular memory circuits.

Sensors can be in the form of rotors for measuring viscosity and flow^[12], as well as crown ethers for the measurement of potassium ions.^[13]

The structures for switches can be rotaxanes, as found in some molecular memory devices, and catenanes as exemplified in dye pigment molecules for the production of RGB electronic paper displays. The first ring contains three donor sites, a green tetrathiafulvalene (TTF) unit, a red 1,5-dioxynaphthalene (DNP) unit, and a blue difluorinated benzidine (FBZD) unit. The acceptor ring in the form of cyclobis (parquat-*p*-phenylene) CBPQT⁴⁺ sits at ground state on the green TTF unit. Application of voltage giving a stepwise oxidation causes the CBPQT⁴⁺ to move from the green site to the blue site and then to the red. Reduction will then revert the position back to the initial starting position at the green site. A schematic of the proposed movement is shown below in Figure 22.^[14]

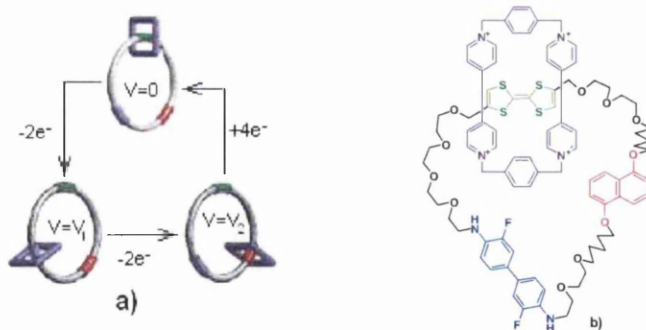


Figure 22. 22a) Electrochemical mechanism for shuttling and 22b) Final structure of catenane.

1.3.3 Rotors and Motors

Rotors are systems with high degrees of internal molecular mobility, that can be multidirectional. An example of a rotational molecule is propeller shaped hexa-*tert*-butyldecacylene, which can rotate freely

in solution. Other rotational molecules include triptycene units. The general structures are shown in Figure 23.

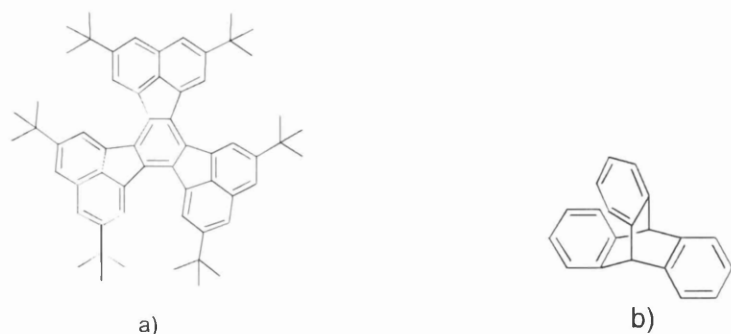


Figure 23. The structures of rotational molecules. 23a) Hexa-*tert*-butyldecacylene and b) Triptycene.

Rotors can be diversified to make more complicated structures, such as cog wheels, gears, paddle wheels, brakes, and ratchets as well as rotary motors.^[15,16,17] Motors use an energy source to produce a controllable movement. In rotary motors an energy source is used to produce controlled rotary motion. The energy source can be chemical, photochemical, or electrochemical. motors are predominately solution based, but there are examples where the motor can be successfully tethered to a silicon wafer, and still keep its activity as a molecular motor.^[18]

An example of a chemical reaction driven motor is shown below. The unidirectional rotation of the ratchet is driven by the use of carbonyl dichloride to prime the ratchet giving an isocyanate group via a carbamoyl chloride molecule. After priming the ratchet rotates clockwise using random thermal motion, where the isocyanate readily reacts with the alcohol group tethered to the helicene pawl unit. This reaction gives a conformationally restricted urethane unit which then causes rotation to occur to relieve steric interactions. Cleavage removes the fuel source as urethane to give the ratchet in almost the starting position. As with all chemically fuelled motors waste products are formed. The Mechanism for rotation is shown in Figure 24.^[19]

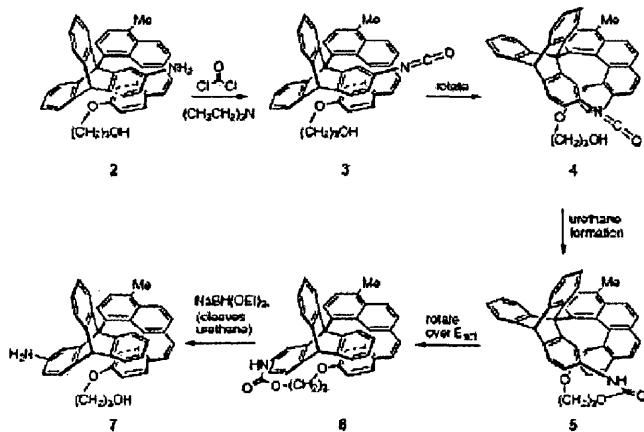


Figure 24. Mechanical rotation in molecular motor

UV light can be used for rotation across double bonds (C=C, C=N) transforming the conformation from cis to trans and trans to cis. The light stimulus can be rapidly switched on and off with no waste products.^[15]

An example of an UV light driven rotational motor is shown in Figure 25. It involves a four individual steps made up of a UV light induced cis-trans isomerisation of the C-C double bond followed by a thermally controlled helicity inversion. The inversion blocks reverse rotation, such that the four steps lead to a full 360° rotation about the axis. It was found that axial chirality and two chiral centres were essential for the monodirectional rotation of this motor.^[20]

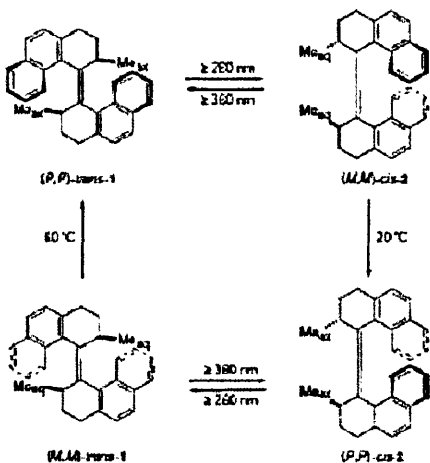
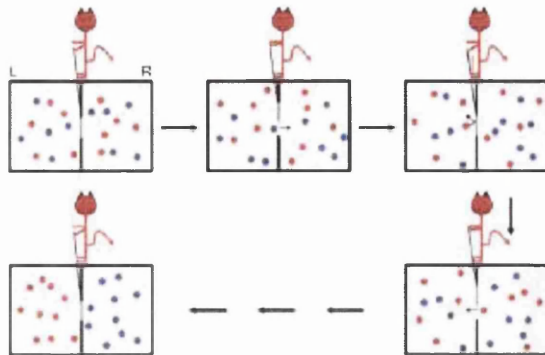


Figure 25 Mechanism for rotation in the light driven motor.

Electrochemical potentials can be used for redox active molecules, where the potential switched on and off rapidly, the structures can also be reverted back to their starting position by reversing the electro-potential. Electrochemical fuel sources also have no waste products as a result of work done. An example of the use of electrochemical fuel sources for switching is shown in section 1.3.6.

1.3.4 Maxwells Demon.

In 1867, James Clerk Maxwell, produced a hypothesis based upon the assumption that a container of gas from which no heat or matter could flow to or from, would have no gradient of temperature or pressure as follows from the 2nd law of thermodynamics. He postulated that if the container was separated into two parts, and the divider could be controlled by a ‘demon’ such that the barrier could allow the movement of gas particles of a velocity greater than a particular value one way and particles of a lower velocity the other way, until full separation has occurred; such that the number of particles in each half of the container, and the total energy of the particles within the container remain the same throughout, leading to a temperature gradient without any work done. See Figure 26 for a schematic of action.^[21]



Maxwell's "temperature demon" in which a gas at uniform temperature is sorted into "hot" and "cold" molecules. Particles with energy higher than the average are represented by red dots while blue dots represent particles with energies lower than the average. All mechanical operations carried out by the demon involve no work—that is, the door is frictionless and it is opened and closed infinitely slowly.

Figure 26. Illustration of Maxwells Demon

An example of a Supramolecular Maxwells Demon in practice is a [2]-rotaxane which acts as an information ratchet. Light acts as the Maxwells demon on the system, whereby after irradiation with 350nm light, the ring moves away from the point of equilibrium. The system mimics biological machinery, such as the enzymes involved in active transport of ions against the concentration gradient into cells.

The rotaxane has a α -methyl stilbene gate, which in the ground state is closed with the ring predominately on the left hand side of the gate. After irradiation with 350nm light, there is an isomerisation of the α -methyl stilbene unit, opening the gate. The ring is then able to move freely along the axle from one amino binding site to the other. The α -methyl stilbene gate then re-closes, with the ring predominately on the right hand side of the gate, thus shifting the position of equilibrium. ^1H NMR studies show that movement occurs in only one direction. This is shown in Figure 27.^[21]

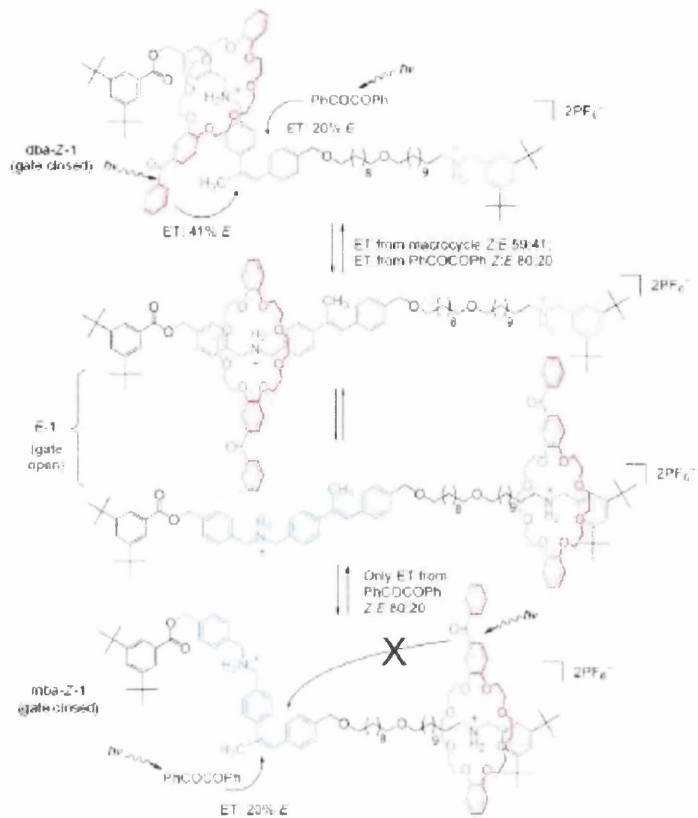


Figure 27. Showing the mechanism of movement in the light driven information ratchet.

1.3.5 Dynamic Random Access Memory Devices

Stoddart et al have recently described a molecular dynamic random access memory device that consists of a monolayer of [2]-rotaxanes with a periodic crossbar geometry of 400 titanium top-nanowire electrodes and 400 silicon bottom-nanowire electrodes, where the monolayer of rotaxanes is the data storage units. The overall size of the circuit is approximately $13 \times 13 \mu\text{m}^2$, which is comparable in size to a white blood cell. Schematic image of the cross bar is shown in Figure 28.^[22,23]

Each bit of the crossbar corresponds to an individual molecular switch tunnel junction, defined by a Si bottom-nanowire and Ti top nanowire, containing about one hundred [2]rotaxane molecules. By applying a voltage of $\pm 1.5\text{V}$ the e-bits will either be turned on or off.

Switching on or off is an indication of the movement of the macrocyclic ring from one site to another. Structure of the rotaxane switch is shown in Figure 29.^[22]

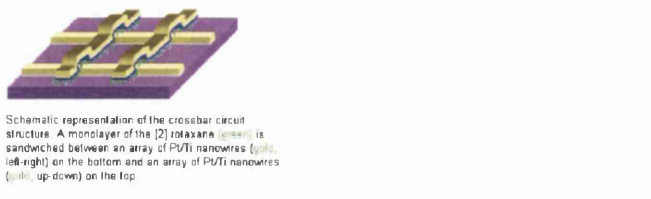


Figure 28. Schematic representation of the crossbar circuit.

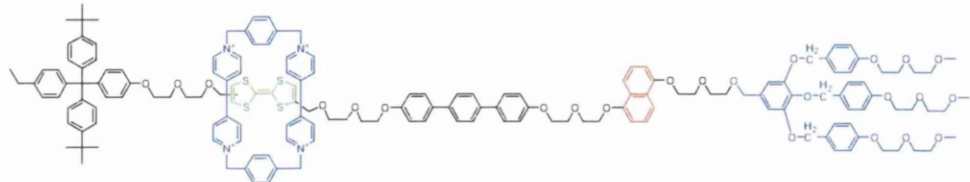


Figure 29. Structure of the [2] rotaxane used as the memory storage unit.

As this thesis describes the synthesis of new hydrogen bonded rotaxanes incorporating the flavin unit, a brief description of hydrogen bonded rotaxanes and the properties of flavin units pertinent to their incorporation into rotaxanes are now provided.

1.3.6 Hydrogen Bonded Rotaxane Systems.

The macrocyclic ring found in rotaxanes can interact with the thread in a number of ways for example by donor / acceptor interactions, and / or hydrogen bonding interactions.

The axle can be modified so as to take advantage of the possible interactions with the wheel. Movement can be induced by the presence of a stimulant, which can be thermal in some cases, chemical, photochemical or electrochemical. Photochemical shuttling is exemplified in the Maxwell's demon as previously described in section 1.3.4.

Shuttling between two non-degenerate intramolecular interaction sites can also occur in rotaxanes at room temperature, such that the

macrocyclic ring has equal preference to both sites at room temperature. This is illustrated by the shuttling motions found in the [2]rotaxane shown in Figure 30, where the binding sites are two bis(pyridinium)ethane units with a dibenzo-[24]-crown-8 ether, DB24C8, macrocyclic ring.

At room temperature the ring shuttles freely from one site to another, with equal preference for binding. At lower temperatures the ring has a 2:1 precedence for the bis(4,4'-bipyridinium)ethane site over the other bis(pyridinium)ethane site. It is thought that this is due to the sterically hindered *tert*-butyl group attached to the pyridinium group on the second binding site, and that there is more favourable π -stacking interactions on the first binding site.^[24]

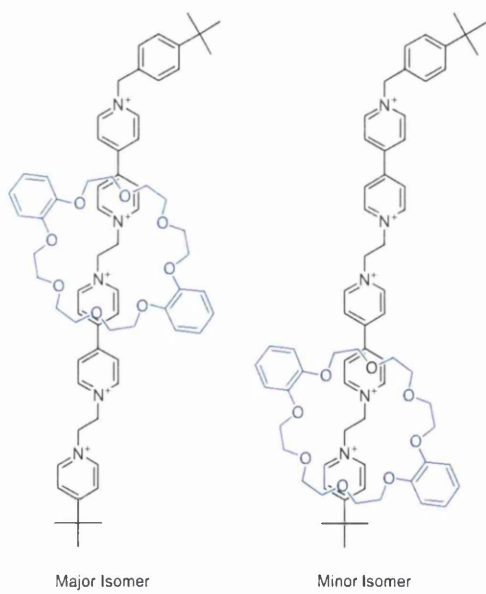


Figure 30. Position of DB24C8 ring on the thread at low temperatures.

The addition of a stimulant to induce movement of the ring along a thread can work by either stabilising the interactions at a second intermolecular binding site, making the second binding site stronger than the first causing shuttling to occur. Alternatively, destabilising the interactions at the first preferred binding site forcing the ring to move to the more stable previously weaker binding site is also an attractive

strategy. Removal of the stimulant or addition of a neutralising species then allows the structure to revert back to its starting position.

An example of this is when shuttling in the rotaxane shown in Figure 31, occurs as a result of deprotonation at the phenol group, changing the interaction from a weak hydrogen bonding acceptor or donor phenol unit to a very strong hydrogen bond acceptor as the phenolate anion site. As the interaction is stronger at the phenolate anion station than at the succinamide station, the ring shuttles along the thread to the phenolate site. Regeneration of the initial starting position can occur by the addition of trifluoro-acetic acid, which protonates the phenolate anion, causing the ring to shuttle back to the succinamide station.

Shuttling occurs irrespective of the deprotonating base and counter ion used. However it has been found that shuttling is highly solvent dependant such that shuttling only occurs in polar solvents. It is thought that this is due to the polar solvents are able to successfully solvate the second isophthalamide hydrogen bonding site, which is not used in the binding of the phenolate station, and stops the succinamide station folding up towards the phenolate binding site, as seen in non-polar solvents.^[25]

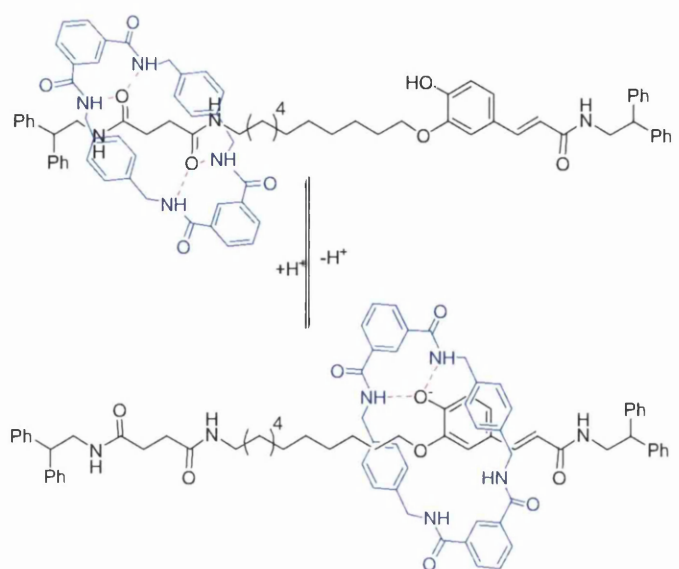
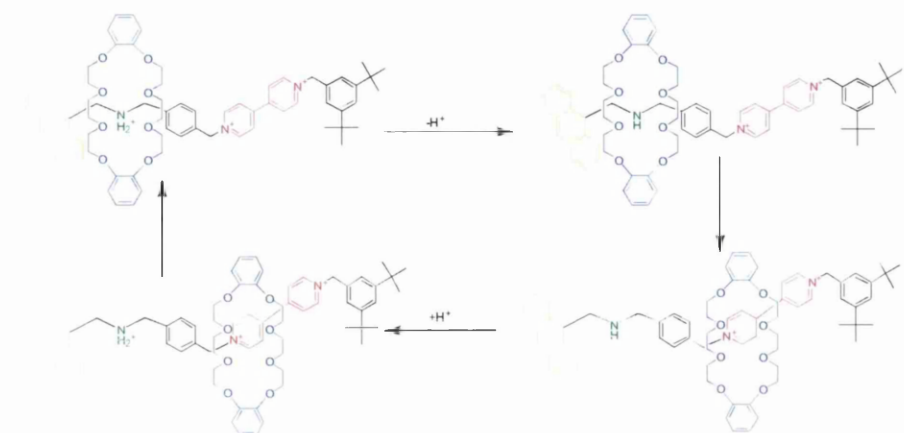


Figure 31. The shuttling of the macrocyclic ring from the succinamide to phenolate stations. Red dotted line denotes H-Bonding interactions.

Another example where shuttling motions occur by the presence of a chemical stimulant, is the acid-base shuttling motions in a [2]rotaxane consisting of a dibenzo[24]crown-8-ether, DB24C8, a π -electron donating macrocyclic ring, threaded on an axle containing two sites of non-covalent interactions. The first station is an ammonium unit that strongly binds to the ring via hydrogen bonding, the other is a bipyridinium unit, bipy^{2+} , which interacts with the crown ether by a charge transfer interaction. The ends of the axle are blocked by an anthracene, and a 3,5-di-*tert*-butyl phenyl unit.

In the ground state the DB24C8 sits at the ammonium station where the interactions between the axle and ring are strongest. When base is introduced to the system, the ammonium group is deprotonated and converted to the amine form. The ring then shuttles from the weakened hydrogen bonding site to the stronger charge transfer site on the bipyridinium station. The addition of acid then reprotonates the amine converting the site back to the strong hydrogen bonding ammonium station, whereby the DB24C8 ring flows back to its initial starting position.

The clear cut on / off acid-base switching behaviour has been shown to be fast and fully reversible by NMR, absorption, luminescence spectroscopic and electrochemical experiments. Scheme 1 shows the shuttling mechanism for this rotaxane.^[26]



Scheme 1. The acid-base switch shuttling mechanism of DB24C8 from a NH_2^+ site to a bipy^{2+} site with the removal and addition of protons to the system.

Where redox active units are incorporated into the axle, electrochemical stimuli can be used as a reagent and waste product free method for rapid on off switching. An example of this type of stimulant induced shuttling is shown by Leigh and co-workers work with [2]rotaxanes where a 3,6-di-*tert*-butyl-1,8-naphthalimide unit was incorporated into an axle containing a succinamide unit. The structure of the rotaxane involved is shown in Figure 32^[27]. The two stations for hydrogen bonding were separated by an aliphatic C₁₂ chain. As the naphthalimide unit in neutral states is a poor hydrogen bond acceptor, the ring sits at the succinamide, the stronger hydrogen bond acceptor site on the rotaxane thread. It was found that the solvent used had no effect on the position of the ring in the neutral state. By electrochemically reducing by one electron to produce the naphthalimide radical anion, the electron density on the imide carbonyls increase and in turn increase the strength of the hydrogen bonding acceptor interactions. The increase causes the

ring to shuttle from the succinamide unit to the naphthalimide radical anion station. Cyclic Voltammetry experiments on the axle showed a reversible one electron reduction redox wave. Whereas for the rotaxane there was no signal for the reoxidation of the naphthalimide group. This indicated that the ring stabilised the radical anion state, and predominately sat at the naphthalimide station. The re-oxidation back to the neutral form showed a shift of the wheel back to the succinamide group.^[27]

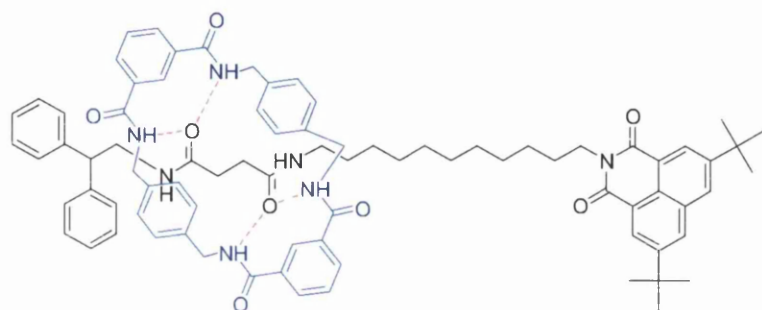


Figure 32. Showing the redox active naphthalimide containing [2] rotaxane

Photochemical sources can be used for inducing movement in rotaxanes. An example of this is within a chiroptical switch where UV light induces a cis-trans isomerisation of a fumaramide C-C double bond. As a result of the isomerisation the macrocyclic ring shuttles to the asymmetric centre at the glycine-L-leucine station. The hydrogen bonding between the macrocyclic ring and the glycine-L-leucine station causes an inequivalency in the aromatic rings, which gives a large measurable change in the induced circular dichroism response. The fumaramide unit upon photoisomerisation is converted to the self-hydrogen bonding maleamide unit, where the amide carbonyl groups are no longer in the correct orientation for binding the macrocyclic ring. Figure 33 shows the mechanism for photochemical switching.^[28]

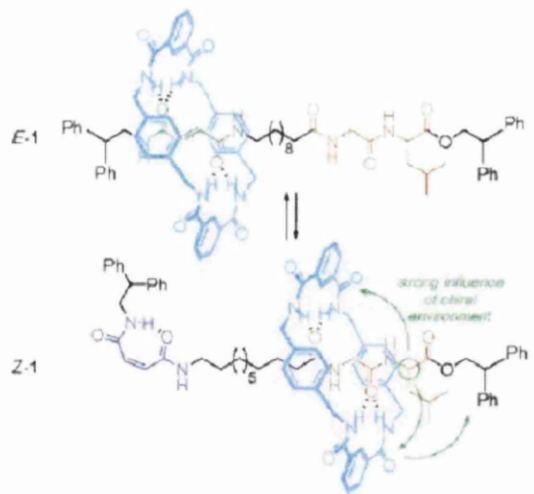


Figure 33. Mechanism for light induced switching.

It is possible to induce shuttling by the competitive binding of metal ions to a preferred binding site, forcing the macrocyclic ring to shuttle to a vacant, weaker binding station. This is shown in Figure 34.^[16]

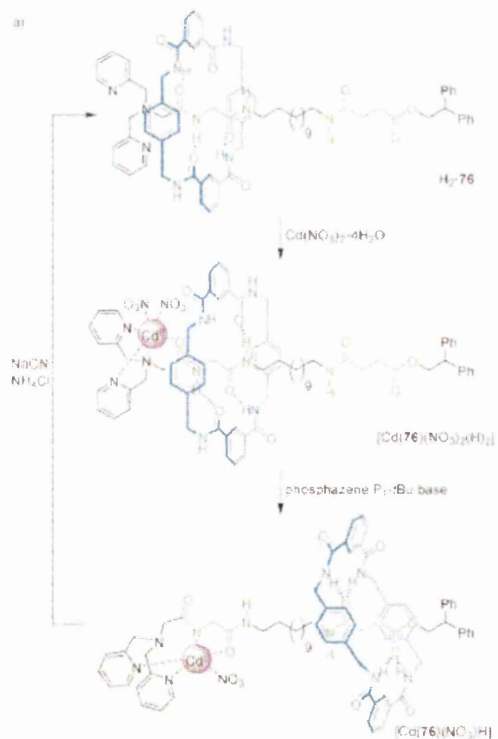
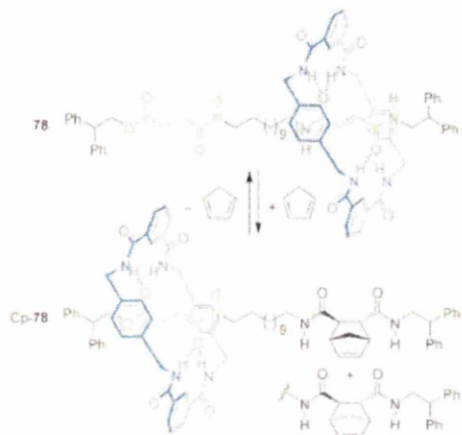


Figure 34. Mechanism for shuttling via Competitive binding of metal ions.

It has also been found that shuttling can occur as a result of reversible covalent bond formation between the axle and an external reagent. This is shown by the Diels Alder reaction exemplified in Figure 35.^[16]



Scheme 43. Shutting through reversible formation of covalent bonds.^[16] The absolute stereochemistry for Cp-78 is depicted arbitrarily.

Figure 35. Mechanism of shuttling by covalent bond formation

1.3.7 Other rotaxane systems

The axle of a rotaxane can be modified in such a way as to control the motions of the macrocyclic ring. One such change is where the sites of intramolecular interactions are degenerate, which can induce spontaneous shuttling of the ring from one site to another. This is exemplified by an early example of molecular shuttles from Stoddart et al, where a CBPQT⁴⁺ ring shuttles spontaneously along a polyether chain stoppered with bulky tri-isopropylsilyl groups from one hydroquinol unit to another at room temperature. The shuttling motion is temperature dependant such that at high temperatures the NMR signals for the hydroquinol units become completely equivalent as shuttling is very fast on an NMR timescale. At low temperatures shuttling can be frozen out and two sets of hydroquinol peaks are seen. At room temperature the hydroquinol peaks are spread out over a between the two sets of peaks

indicating that the rate of shuttling is reasonably fast on a NMR timescale. Figure 36 shows the structure of the [2] rotaxane.^[29]

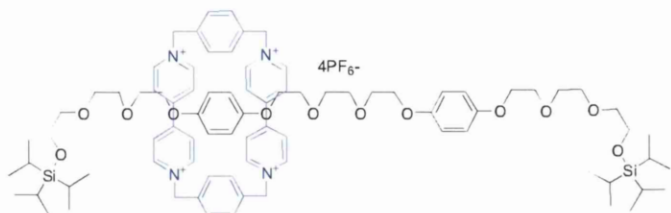
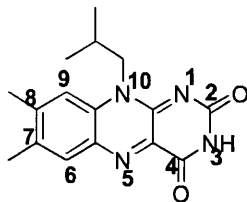


Figure 36. Showing the structure of the [2] rotaxane containing degenerate binding sites

1.4 Flavins.

Flavins are redox active compounds that are found in the cofactors of redox enzymes. These cofactors include FAD, flavin adenine dinucleotide and FMN, flavin mononucleotide. The cofactors non covalently bind to the active site of the enzymes using electrostatic interactions such as Hydrogen bonding, π -stacking and dipolar interactions. Flavoenzymes carry out a diverse array of applications such as metabolic processes, neurotransmitter regulation, and electron transport.^[30]

The name flavin is the trivial name for these complex structures that are also known as isoalloxazines or benzo[g]pteridine-2,4-diones. Each name has a basis by the method of synthesis, with isoalloxazines being derived from alloxane. The benzo[g]pteridine-2,4-dione name comes from the biosynthetic pathway where flavin synthesis is via pteridines. The numbering scheme used is shown below in Figure 37 for the isobutyl-flavin, based upon benzo[g]pteridine naming format.^[31] For ease the name flavin will be used when discussing the structure generally.



10-isobutyl-7,8-dimethylbenzo[g]pteridine-2,4-dione

Figure 37. Isobutyl flavin.

Flavins can be reduced to give the neutral flavin radical, Fl^{\bullet} , or the flavin radical anion, $\text{Fl}^{\bullet\bullet}$. Reduction can occur in two ways, by a direct two electron transfer or by two one electron transfer process via the flavohydroquinone radical, which can be either anionic or neutral. Figure 38 shows the mechanism for redox behavior.

The one electron reduction process results in the increase in electronegativity of the carbonyl oxygens on the flavin, from -45kcalmol^{-1} in Fl_{ox} to -116kcalmol^{-1} in Fl^{\bullet} which leads to a strengthening of hydrogen bond acceptor ability which in turn leads to stronger hydrogen bonding. However, the aryl core of the flavin, once reduced changes from electron deficient Fl_{ox} , $+26\text{kcal/mol}$ to electron rich Fl^{\bullet} , -77kcalmol^{-1} , which causes a destabilisation of the π -stacking interactions with electron rich aromatic rings found in the active site of the enzyme. The change in electronegativities is shown in Figure 39, with the changes in electrostatic potential.

In enzymes the flavin cofactor is non covalently bound to the reaction centre which results in control of the retention and orientation of the flavin moiety in the active site, control over the stabilisation of oxidation and protonation states and the redox behaviour of the flavin, thus controls the reduction potential over 500mV range $\sim 12\text{kcalmol}^{-1}$.^[30]

By modifying the electrostatic interactions, the stabilisation of the flavin and the flavin radical anion can be controlled, which in turn can then control the redox properties of the flavin and so make flavins tunable redox compounds.

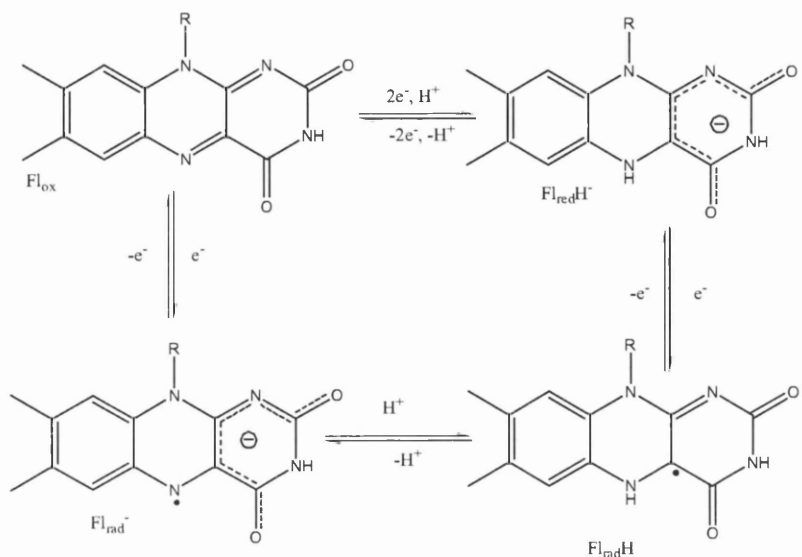


Figure 38. Redox Mechanism in Flavins from Fl_{ox} to Fl_{rad}^- species.

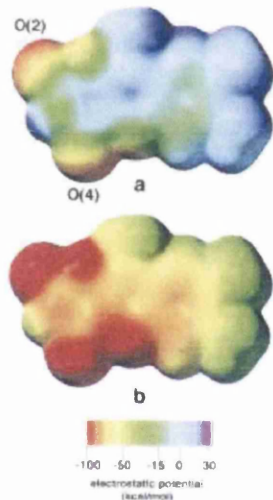


Figure 39. Changes in Electrostatic potential from a) Fl_{ox} to b) Fl_{rad}^- .

Binding of flavins to diaminopyridine (DAP) can be used to mimic the interactions found between flavin cofactors and apoproteins. Recognition occurs a three point hydrogen bonding interaction, where the flavin imide contributes two hydrogen bond acceptor sites and one hydrogen bond donor site. The DAP group has complimentary sites that interact with these stations on the flavin. Interaction between the two compounds is shown in Figure 40.

It has been found that DAP stabilises the radical anion form of the flavin and this interaction can be seen by a substantial shift in the reduction potential of the flavin unit. This interaction has been found to occur with derivatised flavin units, with variable binding constants depending on the substituents at positions 7 and 8. It has been found that generally, the binding constants increase with the increase in electron donating capacity of the substituents at these points. This is thought to be due to the increase in electron density on the carbonyl oxygen atoms, increasing the strength of the hydrogen bond acceptor interactions. Although this increase in electron density diminishes the strength of the hydrogen bond donor interactions from the imide nitrogen atom the strength of the acceptor groups is significantly stronger, such that the net result is an enhanced binding association.^[32]

Example of the changes in binding constants can be seen with the comparison of the dimethyl flavin and the dimethoxy flavin where a significant increase in strength occurs. $K_a (M^{-1})$ Fl_{ox} + DAP for the dimethyl flavin is 517, whereas the dimethoxy flavin has a $K_a (M^{-1})$ Fl_{ox} + DAP of 606. It may also be noted that the un-substituted flavin where positions 7 and 8 have hydrogen only has a $K_a (M^{-1})$ Fl_{ox} + DAP of 432, a drop in strength from the dimethyl flavin.

In addition to modulation of binding constants, the reduction potential $E_{1/2}$ is also varied with substitution pattern. This can be seen in Table 1. The cyclic voltammetry graphs for flavins (a) to (d) in the table is shown figure 41.

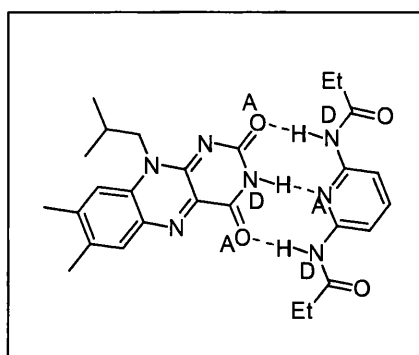


Figure 40 Interactions between Flavin and DAP.

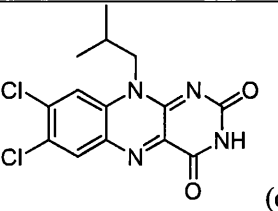
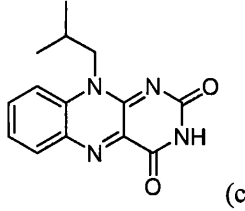
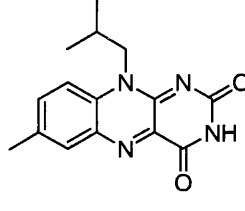
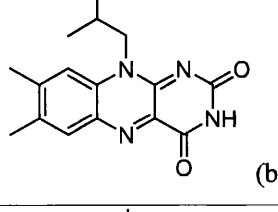
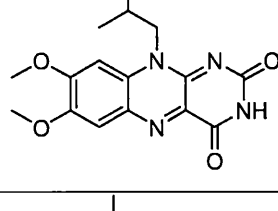
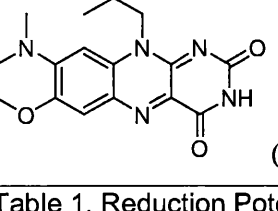
Structure	Flavin $E_{1/2}$ (mV)	Flavin + DAP $E_{1/2}$ (mV)
	-1048	-949
	-1206	-1109
	-1235	-1146
	-1286	-1194
	-1358	-1278
	-1378	-1304

Table 1. Reduction Potentials of a number of substituted flavins.

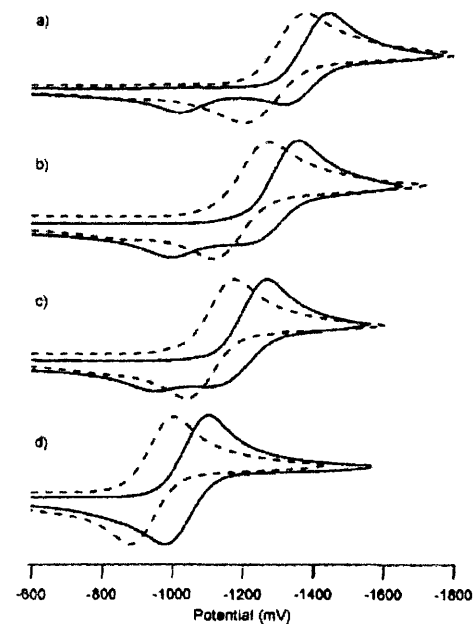


Figure 41. CV graphs of flavins (a) to (d).

1.5 Aims And Objectives of present work.

It has been proven that it is possible to incorporate the flavin moiety into [2]Rotaxanes, to take advantage of its interesting optical, redox and hydrogen bonding properties. Mono-flavin stoppered [2] rotaxanes have been previously made within the Cooke group, where by the flavins useful characteristics have been utilised to induce and detect lateral motion of the ring along the rotaxane thread. The structure shown in Figure 42, is an example of mono-flavin stoppered [2] rotaxanes made previously by the Cooke group.^[33]

When the flavin moiety is reduced to the flavin radical anion, the strength of hydrogen bonding is increased and the ring shuttles from the succinamide group to the flavin unit, where the intermolecular interactions are strongest. The oxidation back to the neutral flavin species then forces the ring to shuttle back to succinamide unit.^[33]

The aim of this project was to follow on from the previous work carried out on the mono-flavin stoppered [2] rotaxanes to make bis-flavin [2] rotaxanes, in particular symmetric [2] rotaxane a and the asymmetric [2] rotaxane b. The structures of (17) and (15) are shown below in Figure 43 and 44

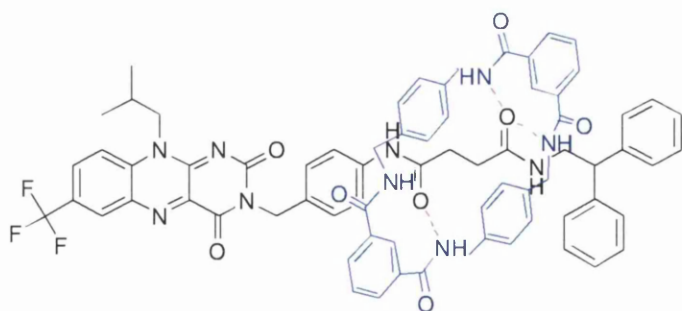


Figure 42. A mono-flavin [2] rotaxane.

Rotaxanes (17) and (15) are intriguing as they are stoppered by flavin units. The symmetrical system a, would allow the production of an electrochemically driven molecular machine whereby the simultaneous generation of the flavin radical anion, at the same potential, will allow the

wheel unit to shuttle from one flavin to another. The asymmetrical system b, due to the different redox potentials of the flavins involved, will allow a greater control over the wheels' position on the axle by the sequential generation of the radical anion for the disparate flavin units.

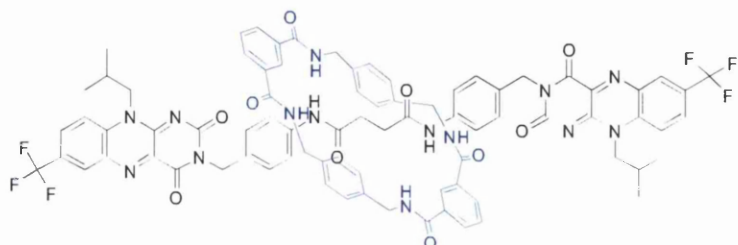


Figure 43. Symmetric [2] rotaxane (17).

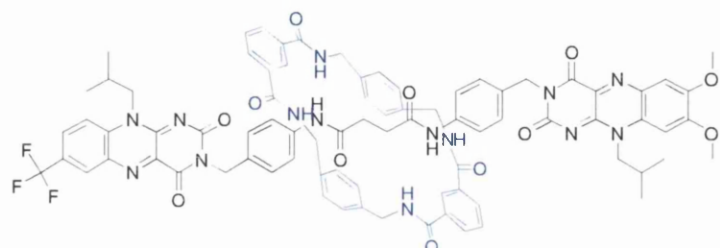


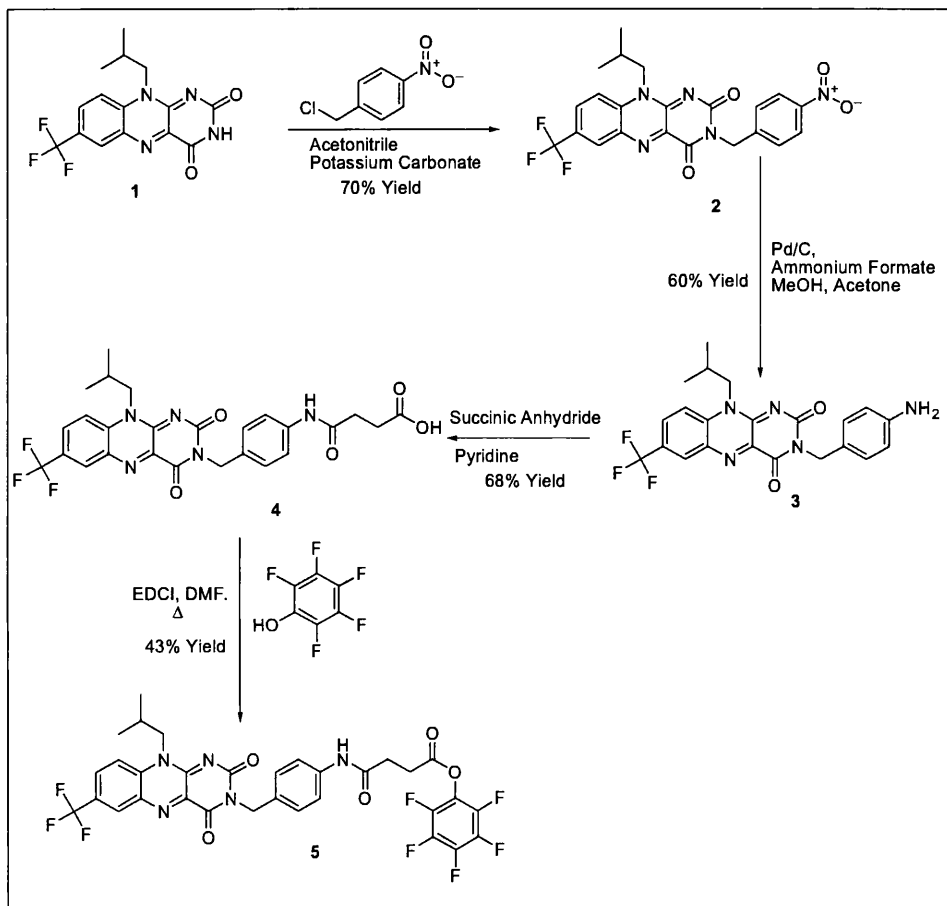
Figure 44. Asymmetric [2] rotaxane (15).

2.0 Results and Discussions.

The synthesis of the rotaxanes can be split into three sections. The first being the synthesis of the first half of the asymmetric axle, this includes the synthesis of key intermediate for the synthesis of the symmetric axle, compound (3). The second section is the synthesis of the second half of the asymmetric axle, which involves the synthesis of the dimethoxy flavin. The final section is the coupling of the two halves of the axles to form the required asymmetric and symmetric axles, followed by the formation of the [2] rotaxanes.

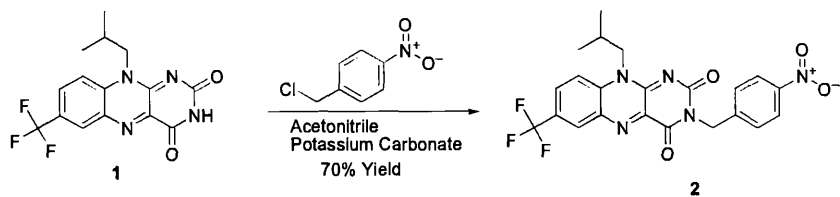
2.1 Synthesis of the first half of the asymmetric axle.

Scheme 2 below shows the overall reaction scheme for the synthesis of the first half of the asymmetric axle from the flavin starting material (1).



Scheme 2. The reaction scheme for the synthesis of the first half of the asymmetric axle.

Reaction of CF₃- Flavin with 4-Nitrobenzylchloride.



Scheme 3. Reaction scheme for benzylation.

The reaction of 10-isobutyl-7-(trifluoromethyl)benzo[g]pteridine-2,4-dione (1) starting material with 4-nitro benzyl chloride is shown in scheme 3. The alkylation was a straightforward reaction which could be carried out on a large scale, with few impurities, of which are easily removed by column chromatography. Previous alkylations' had been carried out using DMF refluxed and at room temperature, however, these methods gave a large amounts of impurities and the product appeared to be thermally unstable, with extended heating times the impurities increased and the yield dropped considerably, however it was found that acetonitrile as the solvent improved the yields as removal was possible at lower temperatures, and so reduced the thermal instability problems, increasing the yields.

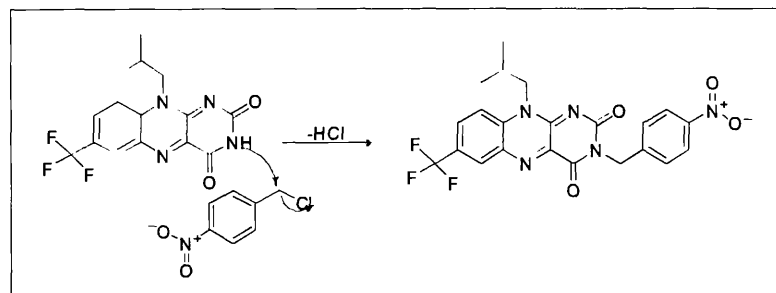
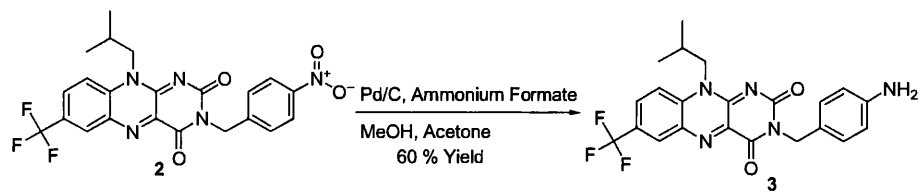


Figure 45. The possible mechanism for alkylation.

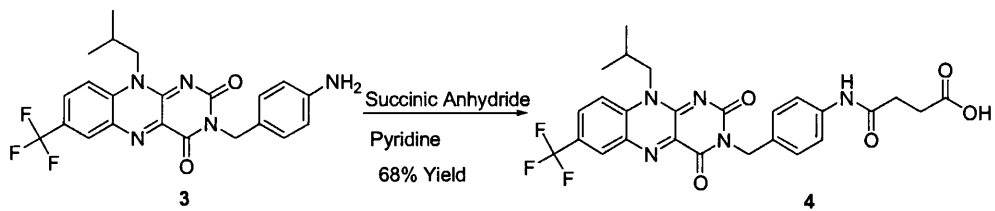
Reduction of 3-(4-nitrobenzyl)-10-isobutyl-7-(trifluoromethyl) benzo[g]pteridine-2,4-dione.



Scheme 4. Palladium reduction of NO₂ group.

The reduction of the nitro group with ammonium formate^[33] showed some solubility issues as the alkylated flavin starting material failed to dissolve in methanol, the solvent required for the ammonium formate, and the ammonium formate was insoluble in acetone which the starting material dissolved in. It was found, however that it was possible to dissolve the alkylated flavin in acetone and the ammonium formate in methanol, with no precipitation out of solution of either compound when the two were mixed together. DMF could have been used as the reaction solvent, though this may then have led to problems later on with removal of solvent and the subsequent chromatography for recovering clean product. A tlc of the reaction mixture showed that the starting material and product ran very close together, making separation by silica gel column chromatography difficult.

Reaction of 3-(4-Aminobenzyl)-10-isobutyl-7-(trifluoromethyl)benzo[g]pteridine-2,4-dione With Succinic Anhydride.



Scheme 5. Conversion of (3) to (4)

Reaction of 3-(4-aminobenzyl)-10-isobutyl-7-(trifluoromethyl)benzo[g]pteridine-2,4-dione (3) with succinic anhydride gave good yields of about sixty percent. Crystallisation overnight from DCM was sufficient to remove impurities from the product.

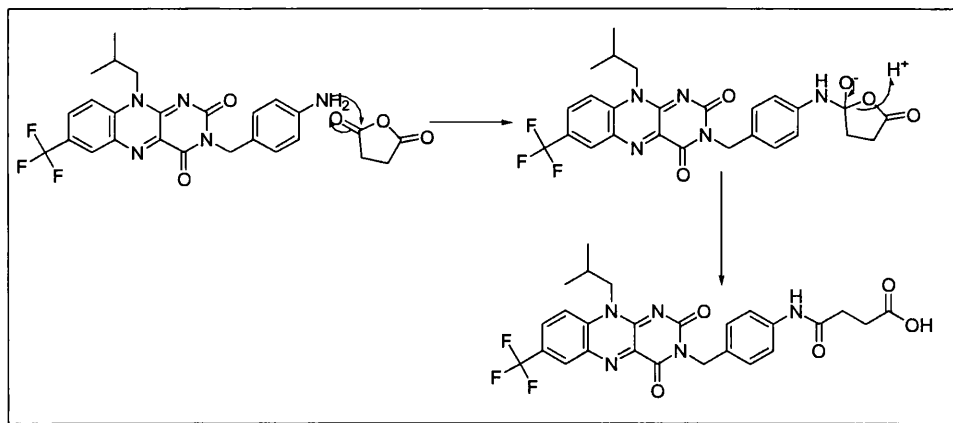
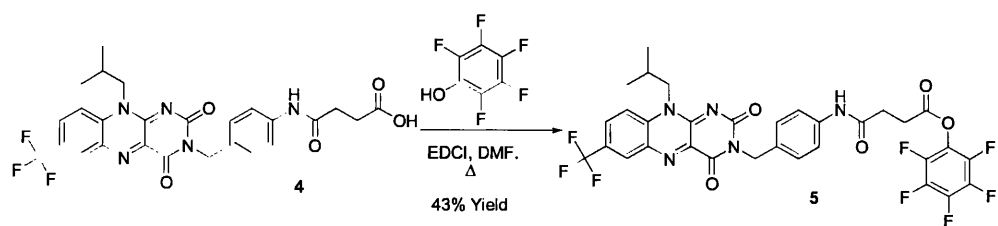


Figure 46. The possible mechanism for the conversion of (3) to (4)

Reaction with Pentafluorophenol.



Scheme 6. Esterification of the succinamic acid compound (4) with pentafluorophenol.

The reaction of 4-(4-((10-isobutyl-2,4-dioxo-7-(trifluoromethyl)benzo[g]pteridin-3-yl)methyl)phenylamino)-4-oxobutanoic acid (4) with pentafluorophenol gave a bright yellow solid that was stable at room temperature. There was a good separation by tlc of starting material and product, making separation by column chromatography favourable. ^{19}F NMR showed the presence of both sets of fluorine environments within the molecule. However the reaction was only moderate yielding.

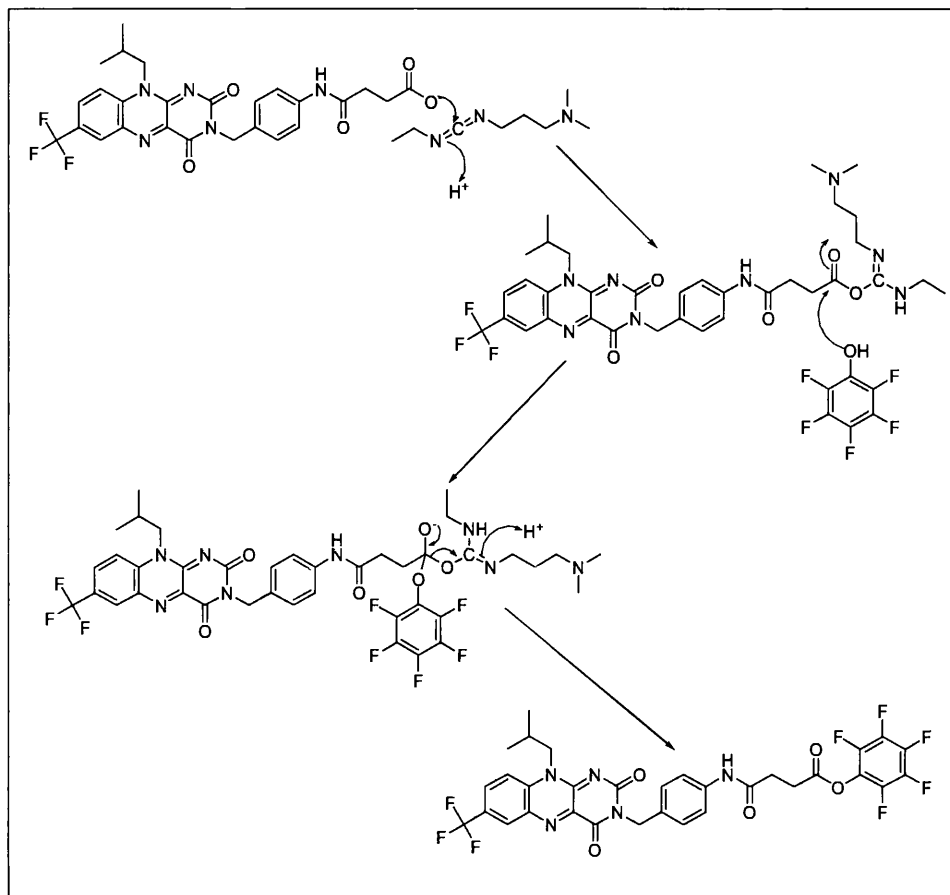
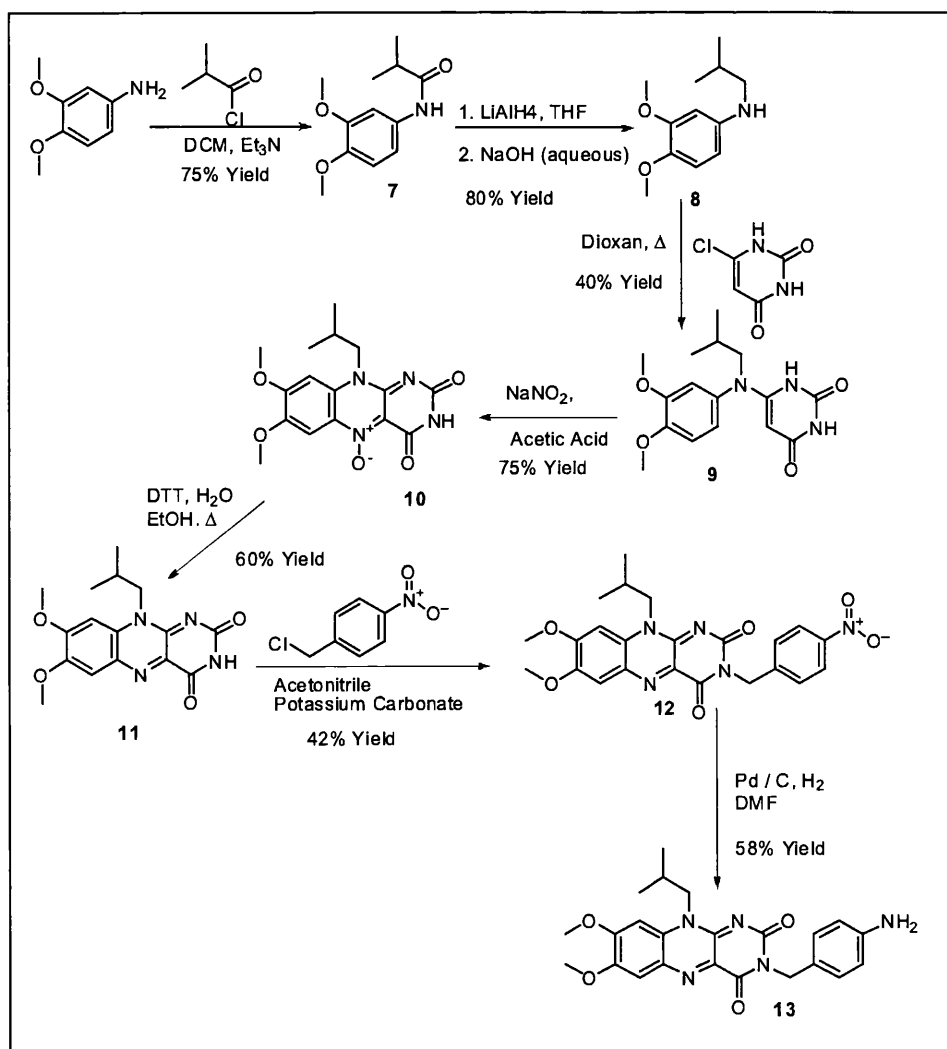


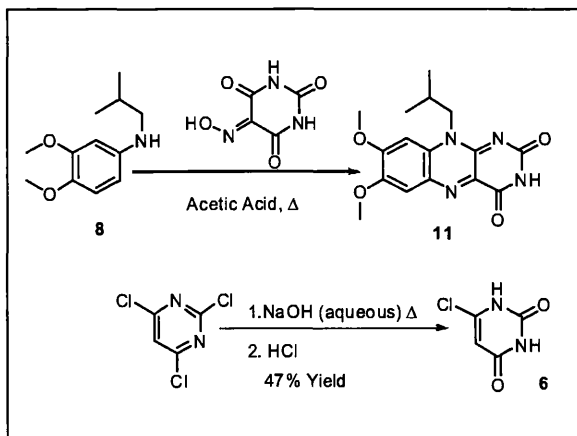
Figure 47. Possible mechanism for the conversion of (4) to (5)

2.2 The synthesis of the second half of the asymmetric axle

Scheme 7 below shows the overall reaction scheme for the second half of the asymmetric axle, starting from 3,4-dimethoxy aniline acylation.

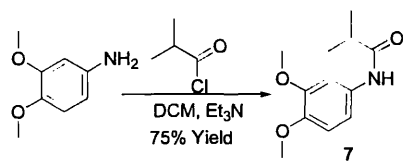


Scheme 7. The reaction scheme for the synthesis of dimethoxy flavin and its subsequent derivatisation.



Scheme 8. Showing the Formation of 6-chloropyrimidin-2,4-dione and the alternative dimethoxy flavin synthesis.

Acylation of 3,4-dimethoxy aniline.



Scheme 9. Acylation of 3,4-dimethoxy aniline

The acylation of 3,4-dimethoxy aniline with isobutyryl chloride gave a good yield and worked well with large quantities of reagents. Column chromatography removed impurities present to give an off white clean product in good yield.

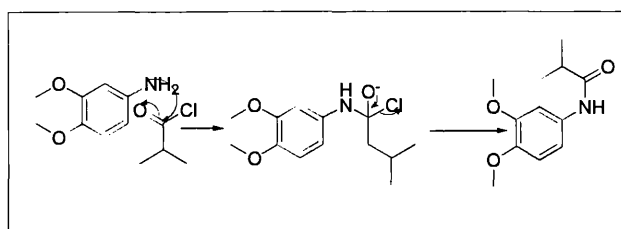
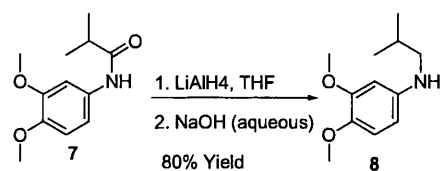


Figure 48. The possible mechanism for acylation.

Lithium Aluminium Hydride Reduction.



Scheme 10. Reaction scheme for the lithium aluminium hydride reduction.

The subsequent reduction of N-(3,4-dimethoxyphenyl)isobutyramide (7) with lithium aluminium hydride had variable yields and scale up was not so well suited to this reaction. Filtration of the lithium and aluminium salts was very slow as the large amounts of solvents were required to filter under gravity, and quickly blocked the filter paper. After filtration there was an extraction with DCM to recover the product from the aqueous extract. Drying with magnesium sulfate followed, where thorough washing of the drying agent was required to recover all the product. No purification was required after this point. However it was later found that filtration under vacuum through celite was possible, first washing with water to remove any unwanted impurities then washing with ethyl acetate to recover clean product.

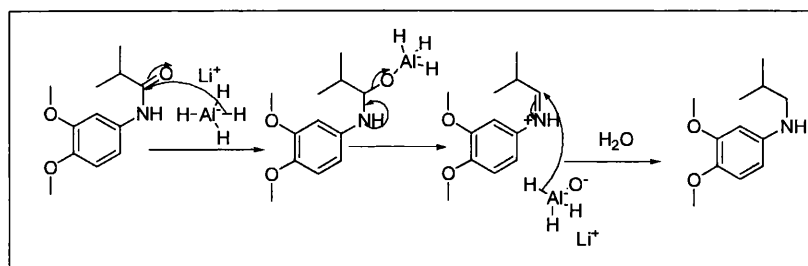
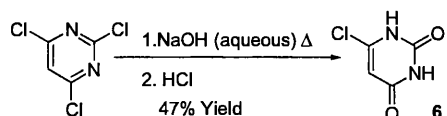


Figure 49. Mechanism for reduction with LiAlH₄

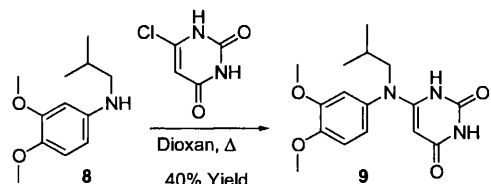
The formation of 6-chloropyrimidine-2,4-dione



Scheme 11. Formation of 6-chloropyrimidine-2,4-dione

6-chloropyrimidine-2,4-dione was formed by the hydrolysis of 2,4,6-trichloropyrimidine with sodium hydroxide. The reaction can handle large scales and re-crystallisation to remove an impurity was all that was required. The product was made in a moderate yield only, but with the ease of formation and large scales possible meant it wasn't a problem.

The synthesis of 6-Chloropyrimidine-2,4-dione addition.



Scheme 12. The reaction scheme for the addition of 6-chloropyrimidine-2,4-dione.

The reaction of 6-chloropyrimidine-2,4-dione with N-isobutyl-3,4-dimethoxyaniline (8) was poor yielding with about 40% yield. The separation by chromatography was straightforward as much of the impurities stayed on the baseline and did not move on the column even with elution with methanol. The compound fluoresced in solution to give a red-blue colour.

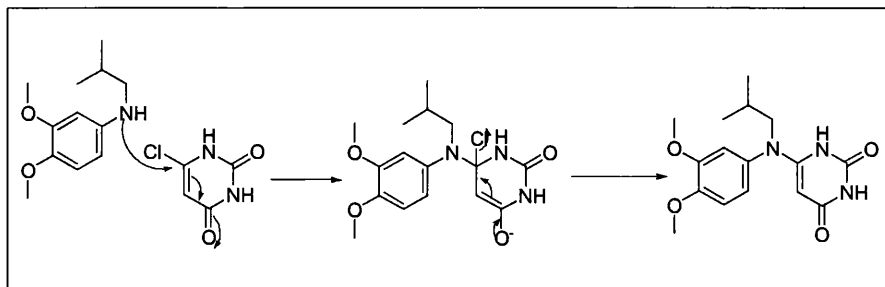
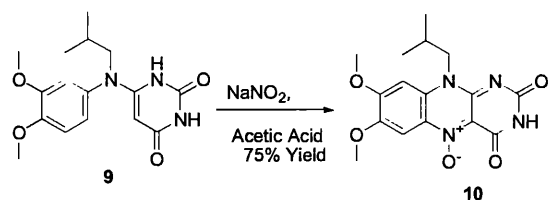


Figure 50. The possible mechanism for the addition of 6-chloropyrimidine-2,4-dione.

N-Oxide Formation.



Scheme 13. N-Oxide formation reaction.

The formation of the N-oxide with sodium nitrite was a high yielding transformation that was relatively free of impurities such that the crude product was taken onto the next stage without any purification.

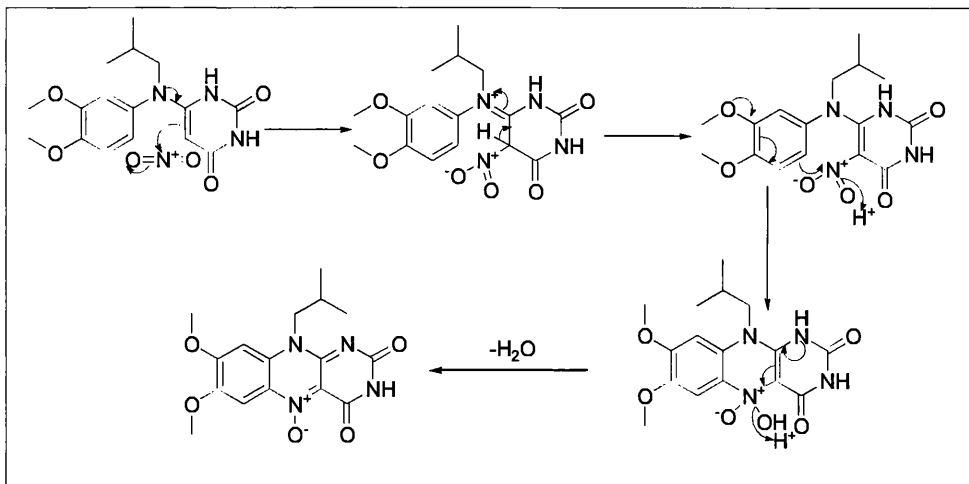
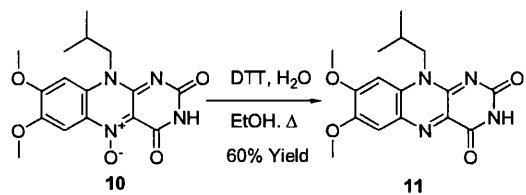


Figure 51. The possible mechanism for N-Oxide formation.

Reduction of N-Oxide with DTT.



Scheme 14. Reaction scheme for reduction with DTT.

The reduction of 10-isobutyl-7,8-dimethoxy-2,4-dioxo-2,3,4,10-tetrahydrobenzo[g]pteridine 5-oxide to yield the dimethoxy flavin, gave an incomplete transformation in a 60% yield. Separation of starting material and product was not possible as the two compounds ran at the same R_f value on tlc. The dithiothreitol was also difficult to completely remove from the product even after silica gel column chromatography. Nevertheless, with careful purification a yield of 60% could be achieved.

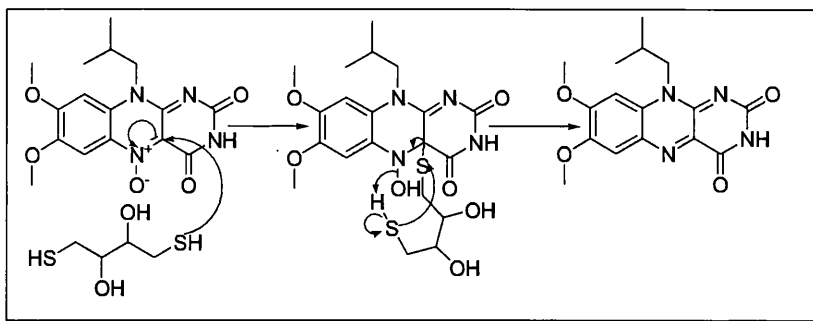
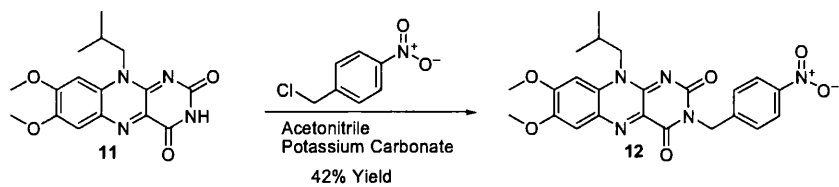


Figure 52. Possible mechanism for the reduction with DTT.

Alkylation of Dimethoxy Flavin With 4-Nitrobenzyl Chloride.



Scheme 15. Alkylation of dimethoxy flavin.

Scheme 15 shows the benzylation of compound (11). A reasonable yield of compound (12) was obtained using this method.

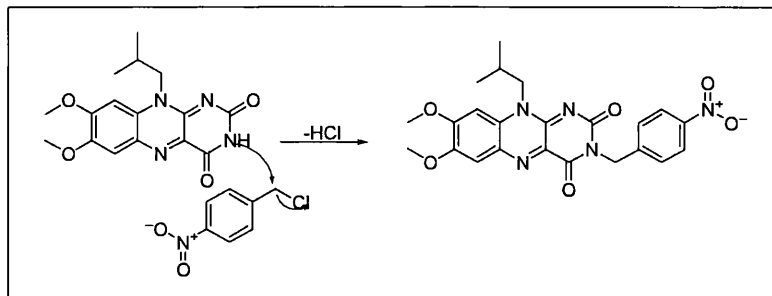
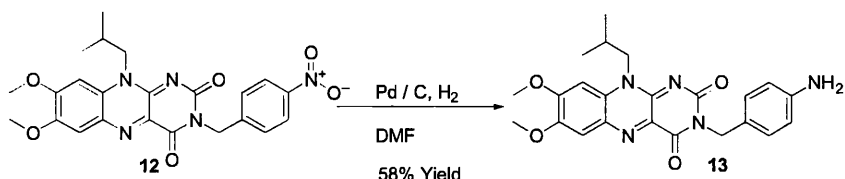


Figure 53. Possible mechanism for benzylation.

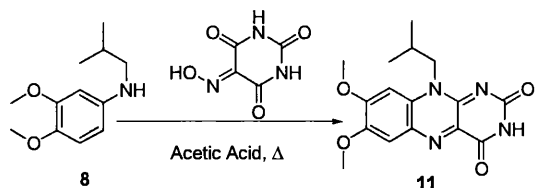
Palladium Reduction with Hydrogen gas.



Scheme 16. Reaction Scheme for reduction with Pd/C and H₂ gas

The reduction of the nitro group was initially carried out with the presence of ammonium formate, but for an unknown reason, it failed to give the desired compound and we could not recover the starting material. For this reason we then tried the reduction with hydrogen gas. The reaction worked relatively cleanly, though the DMF solvent caused problems when the crude material was separated by silica gel column chromatography, as incomplete removal caused the column to streak and separation of some impurities required a second chromatography.

Formation of dimethoxy flavin via violuric acid^[35]



Scheme 17. Conversion of (8) to dimethoxy flavin (11)

The alternative flavin synthesis via violuric acid can be carried out on larger scales and gives clean product in the form of orange crystals. Chromatography recovers product from the filtrate as some product does not fully crystallise out. The procedure was found late into the project, but was found to work well, cutting down the number of steps into the flavin from five to three, thereby decreasing the time taken to synthesise the flavin from basic starting materials, and increasing the

overall yield from ~11% to ~36%. It is believed that the reaction is successful due to the electron donating methoxy group *para* to the site of attack on the aromatic ring.

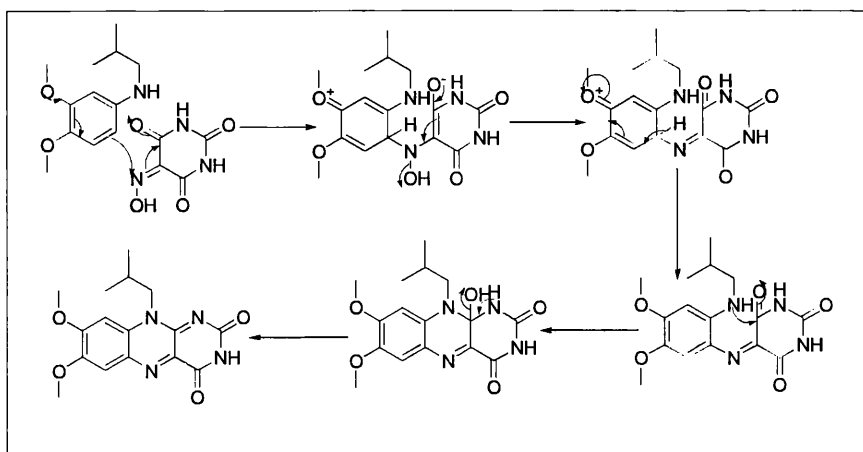
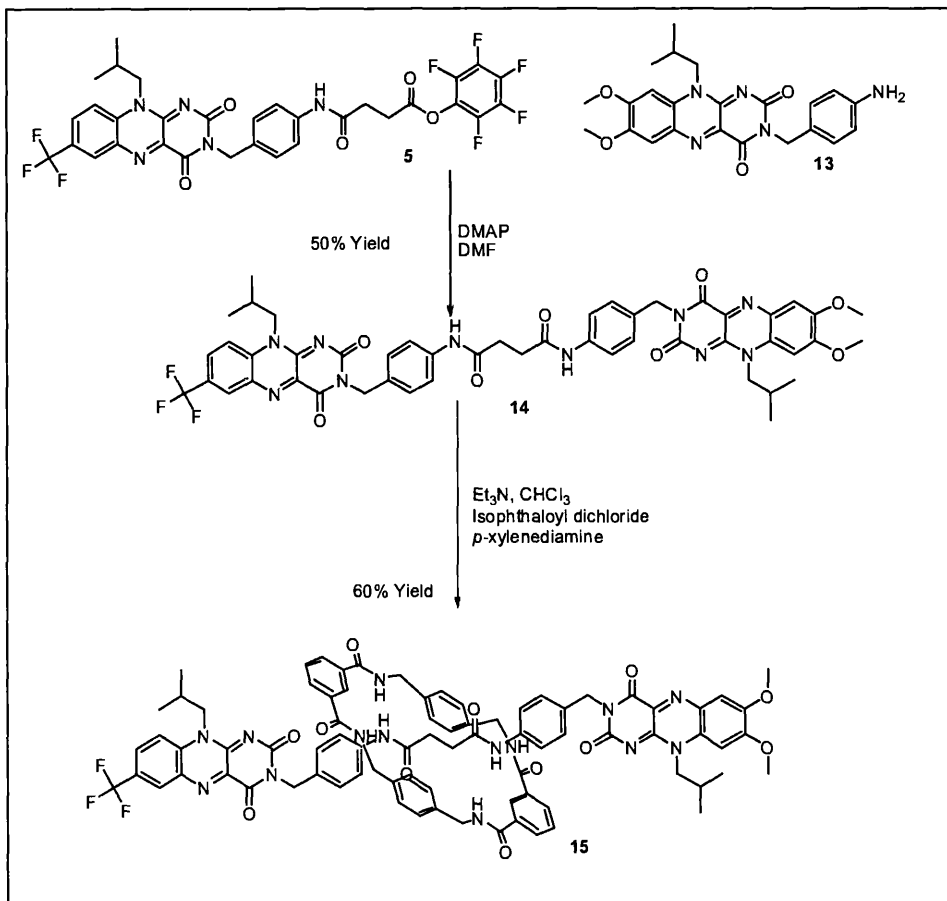


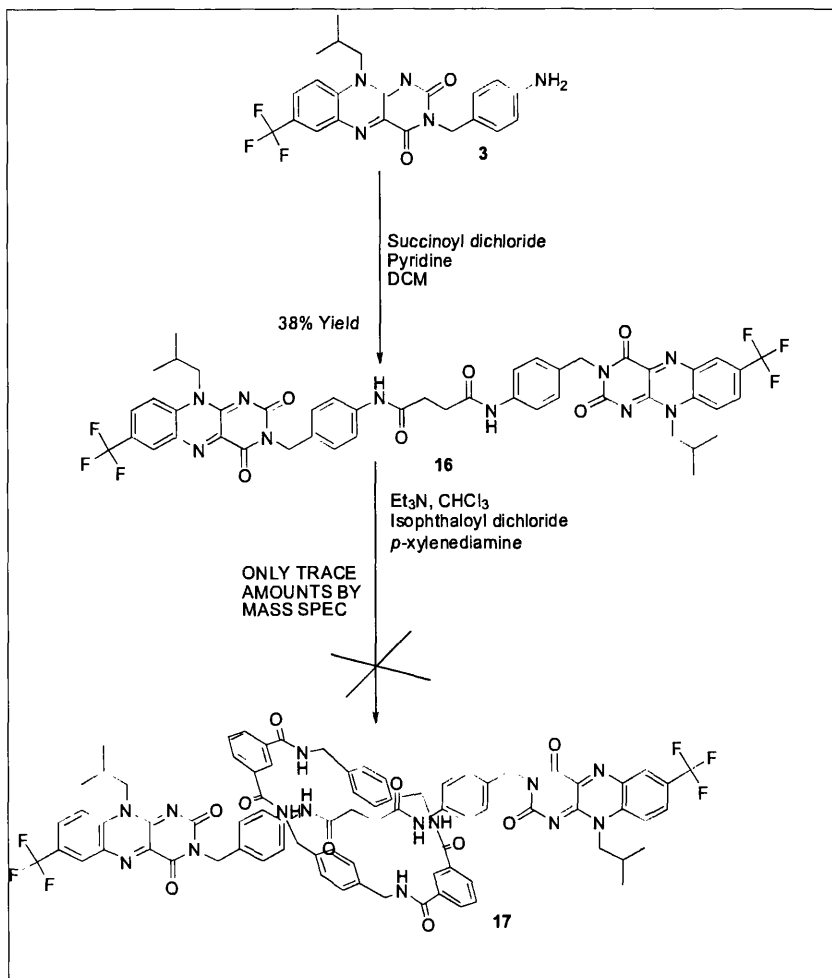
Figure 54. Possible mechanism for flavin formation.

2.3 The coupling to form the axle and subsequent rotaxane formation.

The scheme 18, below shows the reaction scheme for the coupling to form the axle, then the synthesis of the asymmetric rotaxane.

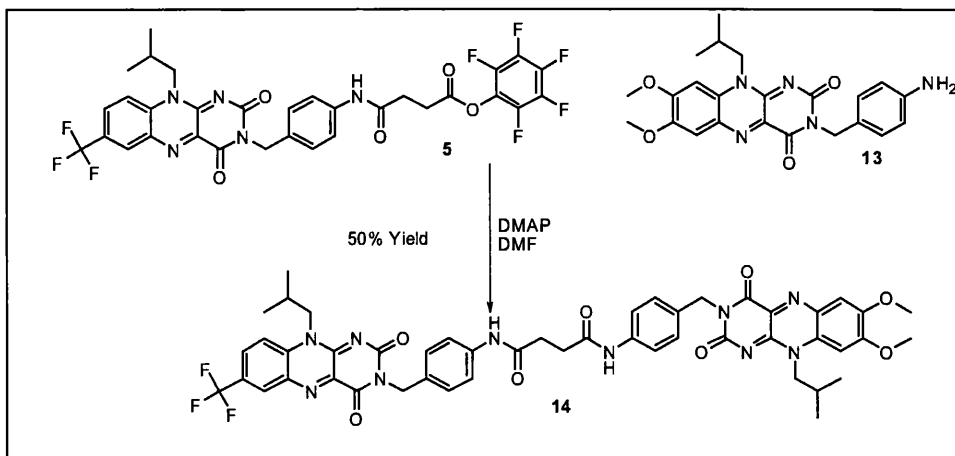


Scheme 18 shows the reaction scheme for the coupling of the two halves of the axle and the formation of the asymmetric rotaxane.



Scheme 19. Shows the formation of the symmetric axle and the rotaxane synthesis.

Formation of the asymmetric axle.



Scheme 20 The coupling to form the asymmetric axle

The solubility issues result in the use DMF as the reaction solvent for the coupling of the two halves of the axle. The axle is thermally unstable, and purification by column chromatography was not trivial. Nevertheless, a 50% yield was possible to achieve.

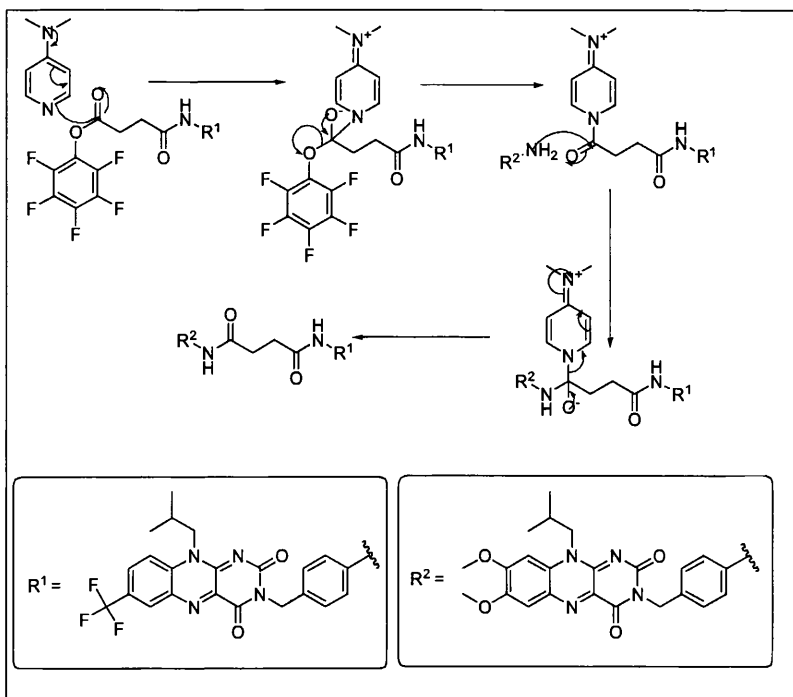
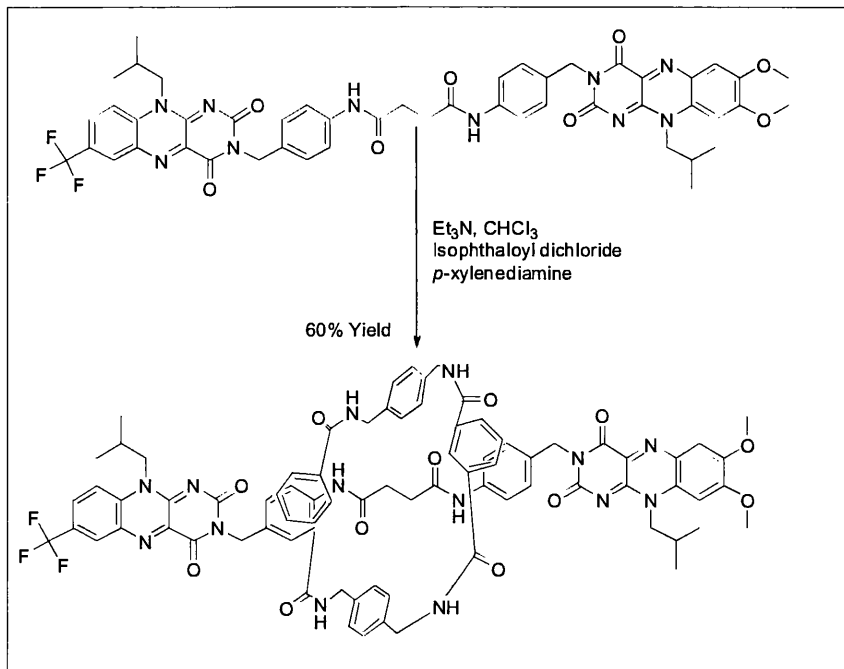


Figure 55. The possible mechanism for the coupling to form the axle.

Formation Of Asymmetric [2] Rotaxane.

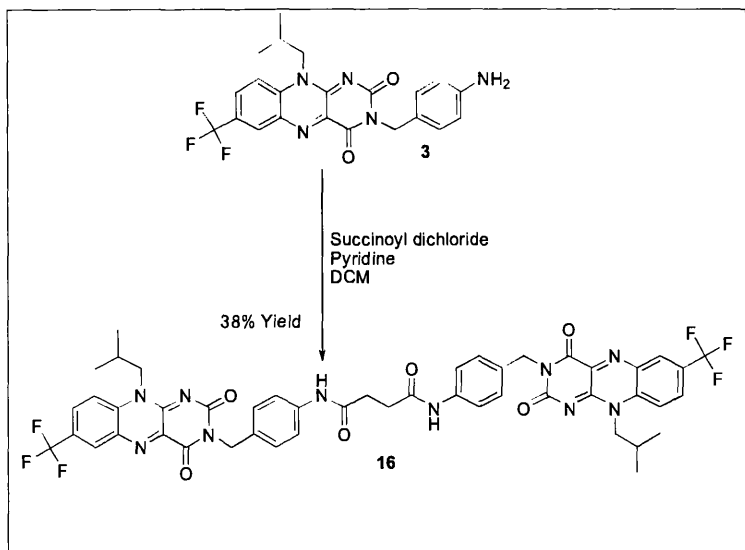


Scheme 21 Reaction to form the asymmetric rotaxane.

The asymmetric rotaxane synthesis was hampered by the solubility issues, in that the axle is sparingly soluble in chloroform, the solvent required for the reaction, and large amounts of solvent were required relative to the amount of starting material. The formation of polymers and interlocked structures from isophthaloyl dichloride and *p*-xylyenediamine were predominant due to the dispersion of the axle in solution. The un-reacted starting material and the product was recovered by column chromatography.

The rotaxanes formation was evident in the ^1H NMR, notably with a significant up field shift of 1.77ppm of the bridging succinyl protons of unsymmetrical axle from $\delta = 2.51$ in the axle to $\delta = 0.74$ for the rotaxane. Though it was difficult to integrate each individual peak due to the complexity of the molecule, a more generalised approach was taken for integration where individual peaks could not be assigned. Overall all the protons in the molecule were accounted for.

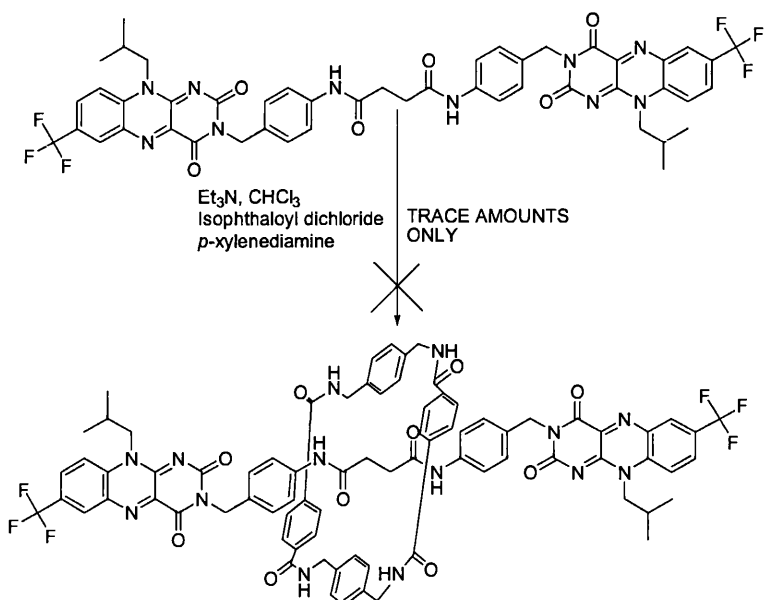
Formation of the symmetric axle.



Scheme 22. Reaction scheme for axle formation

The reaction shown in Scheme 22, was straight forward and no purification was required other than washing the crystals with acetone. Insolubility properties of the axle meant that precipitation out of solution occurred, whereby the product was free of impurities in a moderate yield of 38%.

Formation Of Symmetric [2] Rotaxane



Scheme 23. Reaction scheme for rotaxane formation.

The symmetric rotaxane was attempted using the symmetrical axle (16), but the starting material was even less soluble than the asymmetrical axle (14) and only trace amounts of product were recovered by column chromatography, as shown by Mass spectroscopy as the sodium adduct. Again polymeric and interlocked structures from the reaction of the isophthaloyl dichloride and the *p*-xylenediamine were the predominant formed by-products.

3.0 Conclusions and Future Work

3.1 Conclusions

We have successfully developed the methodology for the synthesis of symmetrically and asymmetrically functionalised flavin axle units. We have also developed a method for producing the interlocked hydrogen bonded rotaxane structures from these systems in reasonable yield.

3.2 Future Work.

The future work for this project is to synthesise more of the asymmetric rotaxane for ^1H NMR and CV studies, so as to identify the position of the macrocyclic ring relative to the axle, and study the possible shuttling motions of the ring when the flavin moieties are selectively reduced to their radical anion species.

The lack of solubility of the symmetric axle (16) in chloroform severely hindered the formation of the rotaxane. Therefore, more solubilising groups need to be incorporated into the axle unit.

4.0 Experimental.

4.1 General Experimental.

¹H NMR Spectra were performed on Bruker AC 200MHz, Bruker AC 375MHz, and Bruker AC 400MHz spectrometers. All NMR spectra used tetramethylsilane (TMS) as reference ($\delta = 0.0$ ppm)

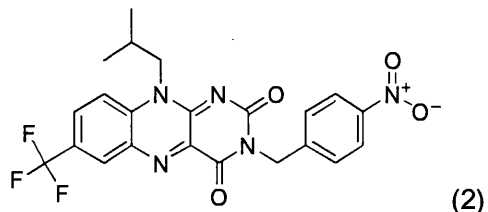
MS spectra were obtained from the EPSRC National Mass Spectrometry Service Centre, Chemistry Department, University of Wales, Swansea, or from the Mass Spectrometry laboratory in the Chemistry Department of the University of Glasgow. The MS carried out were either low resolution EI/CI MS or low resolution Fast Atom Bombardment (FAB)

Transmission IR spectra were recorded as thin films or KBr disks using a Perkin-Elmer RX FT-IR system.

All melting points recorded are uncorrected.

4.2 Chemical Experimental.

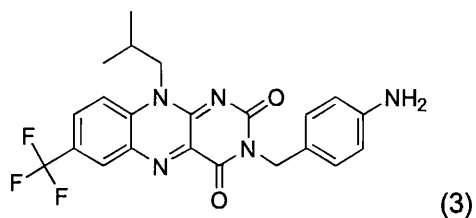
10-Isobutyl-3-(4-nitrobenzyl)-7-(trifluoromethyl)benzo[g]pteridine-2,4-dione. (2)^[32].



To a solution of 10-isobutyl-7-(trifluoromethyl)benzo[g]pteridine-2,4-dione (1) (1g, 3mmol) in acetonitrile was added 4-nitro benzyl chloride (1.01g, 6mmol) and potassium carbonate (0.882g, 9mmol). The reaction was then stirred at room temperature in the dark for one week. The reaction mixture was evaporated and then redissolved in dichloromethane and filtered to remove the potassium carbonate. The crude product was separated using silica gel column chromatography eluting with 100% DCM (1L) followed by 10% EtOAc / DCM (1L) then 20% EtOAc / DCM (1L) to yield the bright yellow product in 70% yield, 0.995g. Mp. = 184 -186 °C. ¹H NMR CDCl₃, 200 MHz : δ 8.54 (1H, d, J = 1.6 Hz), 8.10 (2H, d, J = 8.2 Hz), 7.98 (1H, dd, J₁=8.2 Hz, J₂=1.6 Hz), 7.70 (3H, d, J = 8.2 Hz), 5.31 (2H, s), 4.55 (2H, br.s), 2.40 (1H, sept, J = 8.0 Hz), 1.00 (6H, d, J = 8.0 Hz). ¹³C NMR CDCl₃, 400 MHz : δ 158.87, 154.66, 149.85, 147.48, 143.49, 138.36, 134.97, 134.89, 131.33, 130.76, 130.92, 130.36, 128.69, 122.83, 123.63, 116.79, 51.51, 44.61, 27.56, 20.00. IR (thin film on NaCl, v, cm⁻¹): 3363, 2966, 1715, 1666, 1596, 1560, 1528, 1451, 1343, 1323, 1255, 1224, 1169, 1129. MS m/z (accurate mass measurement, ES+) 474.1383 [M+H]⁺ (474.1384 calc.)

See Appendix 1 for ¹H NMR in CDCl₃ of compound (2)

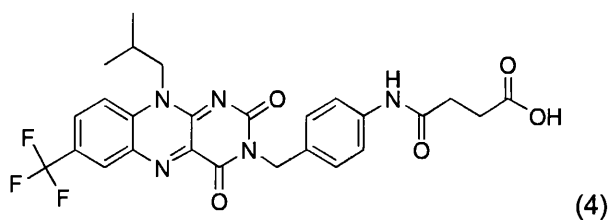
3-(4-Aminobenzyl)-10-isobutyl-7-(trifluoromethyl)benzo[g]pteridine-2,4-dione. (3).^[32]



To a solution of (2)(1g, 2.11mmol) in acetone was added ammonium formate (3.2g, 5.1mmol) in methanol and the solution was degassed with N₂ gas. To the reaction mixture was then added Pd/C (5mol%, 0.1g). The reaction was stirred under a nitrogen atmosphere for two hours at room temperature. The reaction mixture was then filtered under N₂ washing with acetone to remove the Pd/C. The filtrate was then evaporated *in vacuo* to yield a dark oil. The product was separated from the crude material by silica gel column chromatography eluting with 10% EtOAc / DCM (1L), followed by 20% EtOAc / DCM (1L), and finally 40% EtOAc / DCM (1L), to recover the product in a 70% yield 0.653g. Mp. 230 °C (dec). ¹H NMR CDCl₃, 200 MHz : δ 8.50 (1H, s), 7.95 (1H, dd, J₁ = 1.6 Hz, J₂ = 8.8 Hz), 7.66 (1H, d, J = 8.8 Hz), 7.35 (2H, d, J = 8.0 Hz), 6.50 (2H, d, J = 8.0 Hz), 5.07 (2H, s), 4.50 (2H, br.s), 3.45 (2H, br.s), 2.38 (1H, sept, J = 8.0 Hz), 0.99 (6H, d, J = 8.0 Hz). ¹³C NMR CDCl₃, 400 MHz,: δ 158.82, 155.07, 149.65, 145.98, 138.85, 135.01, 134.73, 131.30, 130.89, 130.69, 130.65, 128.22, 126.66, 122.67, 116.67, 114.88, 51.24, 44.84, 27.46, 20.05. IR (KBr disk, v, cm-1): 3461, 3356, 3095, 3037, 2963, 2926, 1709, 1662, 1592, 1558, 1536, 1449, 1428, 1321, 1258, 1225, 1186, 1169, 1132, 1074, 999, 920, 830, 811, 752, 569. MS m/z (accurate mass measurement, ES+) 444.1642 [M+H]⁺ (444.1643 calc.).

See Appendix 2 for ¹H NMR in CDCl₃ of compound (3)

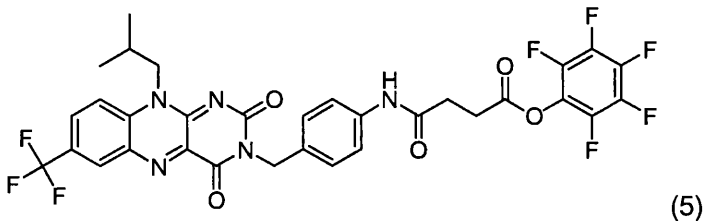
4-((4-((10-Isobutyl-2,4-dioxo-7-(trifluoromethyl)benzo[g]pteridin-3-yl)methyl)phenylamino)-4-oxobutanoic acid. (4).^[32]



To a solution of (3)(0.322g, 0.72mmol,) in pyridine 25 ml was added succinic anhydride (0.08g, 0.79mmol). The reaction was stirred over night at room temperature. The pyridine was removed *in vacuo*. The dark oil produced was then dissolved in dichloromethane and allowed to crystallise overnight. The mixture was filtered and the filtrate was evaporated and re-dissolved in a small amount of DCM and allowed to re-crystallise overnight. The crystals were recovered by filtration. 68% yield 0.275g. Mp. 145 °C (dec) ¹H NMR d₆-DMSO, 400 MHz : δ 12.08 (1H, br.s), 9.90 (1H, s), 8.52 (1H, s), 8.22 (1H, d, J=8 Hz), 8.16 (1H, d, J = 8 Hz), 7.48 (2H, d, J = 8.3 Hz), 7.29 (2H, d, J = 8.3), 5.03 (2H, s), 4.47 (2H, br.s), 2.51 (solvent signal, overlapping with some aliphatic proton signals, integration is not applicable), 2.33 (1H, m), 0.95 (6H, d, J = 7.4 Hz). ¹³C NMR d₆-DMSO 400 MHz : δ 173.77, 169.93, 159.03, 154.69, 150.32, 139.90, 138.36, 135.38, 134.20, 131.56, 129.41 (m), 127.69, 126.32, 125.09, 119.42, 118.90, 50.51, 43.78, 30.92, 28.74, 26.75, 19.74. IR (KBr pellet, ν, cm⁻¹): 3437, 2963, 1715, 1661, 1559, 1415, 1322, 1255, 1224, 1169, 1128, 1072, 1021, 921, 804. MS m/z (accurate mass measurement, ES+) 561.2068 [M+NH₄]⁺ (561.2074 calc).

See Appendix 3 for ¹H NMR in CDCl₃ of compound (4)

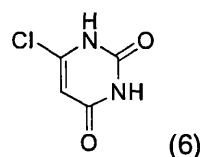
Perfluorophenyl 4-(4-((10-isobutyl-2,4-dioxo-7-(trifluoromethyl)benzo[g]pteridin-3-yl)methyl)phenylamino)-4-oxobutanoate. (5).



To a solution of compound (4) (0.09g, 0.165mmol) in DMF was added portionwise pentafluoro phenol (0.037mg, 0.2mmol) followed by EDCI (0.039g, 0.25mmol). The reaction mixture was stirred at room temperature for a week then heated to 60°C for several hours. The reaction mixture was allowed to cool over night. The solvent was removed *in vacuo* to leave a dark yellow oil. The crude product was separated by silica gel column chromatography eluting with 100% DCM (500ml) 10% EtOAc / DCM (500ml), 20% EtOAc / DCM (500ml), 30% EtOAc / DCM (500ml), 40% EtOAc / DCM (500ml). To yield the product as a yellow oil in a 43% yield. ^1H NMR, CDCl_3 , 400MHz; δ 8.50 (1H, s, CH), 7.96 (1H, dd, CH, $J_1 = 7.2\text{Hz}$, $J_2 = 2\text{Hz}$), 7.68 (3H, m, 3xCH), 7.16 (2H, d, 2xCH, $J = 8.4\text{Hz}$), 5.24(2H, s, CH_2), 4.516 (2H, br .s, $\text{CH}_2\text{-N}$), 2.82 (4H, d, 2x CH_2 , $J = 2\text{Hz}$), 2.38 (1H, sept, CH, $J = 6.8\text{Hz}$), 0.98 (6H, d, 2x CH_3 , $J = 6.8\text{Hz}$) ^{19}F NMR, CPD, CDCl_3 , 376.5MHz; δ -60.65, -62.13, -62.13, -62.34, -62.54, -62.61, -62.65, -62.70, -62.94. MS FAB/NOBA. m/z = 526.27 measured mass (loss of $\text{C}_6\text{F}_5\text{OH}$ as the major signal.), 526.17 (calculated mass with loss of $\text{C}_6\text{F}_5\text{OH}$)

See Appendix 4 for ^1H NMR, Appendix 5 for ^{13}C NMR, Appendix 6 for ^{19}F NMR, and, Appendix 7 for ^{19}F NMR CPD in CDCl_3 of compound (5).

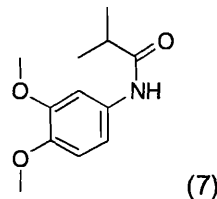
6-Chloropyrimidine-2,4-dione.^[34]



To a solution of 2,4,6-trichloropyrimidine (12.4g, 0.067mol) in water was added Sodium Hydroxide (10.8g, 0.268mol) and the reaction mixture was refluxed for 1½ hours. Cool conc HCl was added until the pH ~ 1. The product precipitated out of the solution as a white solid, the mixture was refrigerated overnight. The product was re-crystallised in water. 4.6g, 47% Yield. ^1H NMR, d₆-DMSO, 400MHz; δ 12.08 (1H, s, NH), 11.33 (1H, s, NH), 5.765 (1H, d, CH, J = 2Hz). Mp 149-150°C

See Appendix 8 for ^1H NMR in CDCl₃ of compound (6)

N-(3,4-Dimethoxyphenyl)isobutyramide. (7)^[33]

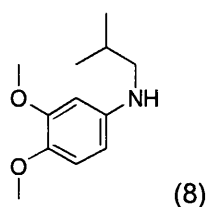


To a solution of 3,4-dimethoxy aniline (5g, 32.6mmol) in DCM (250ml) was added triethylamine (5.7ml, 40.5mmol) then isobutyryl chloride (5.1ml, 48.3mmol) dropwise. As the isobutyryl chloride was added the hydrochloric acid was given off. The reaction was then stirred at room temperature for three days. The solvent was removed *in vacuo*. The reaction mixture was then extracted with DCM (200ml) washing with water (3 x 60ml) followed by brine (3 x 60ml). The organic was dried over magnesium sulfate, filtered and evaporated. The crude product was separated by silica gel column chromatography, eluting with 10% ethyl acetate dichloromethane, followed by 20% ethyl acetate dichloromethane and finally 40% ethyl acetate dichloromethane. The product was

recovered in 75% yield. Mp 117-118°C ^1H NMR, CDCl_3 , 400MHz; δ 7.4 (1H, d, CH, J = 2Hz), 7.04 (1H, s, NH), 6.74 (2H, m, CH), 3.82 (3H, s, OMe), 3.79 (3H, s, OMe), 2.42 (1H, sept, CH, J = 6.8Hz), 1.19 (6H, d, 2xCH₃, J = 6.8Hz) MS m/z [M+H]⁺ 223

See Appendix 9 for ^1H NMR in CDCl_3 of compound (7)

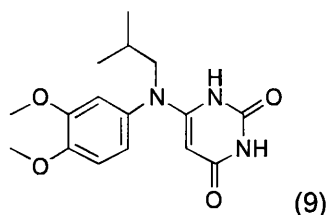
N-Isobutyl-3,4-dimethoxyaniline. (8).^[33]



To a solution of (7)(1g, 4.48mmol) in tetrahydrofuran (100ml) was added portion-wise solid lithium aluminium hydride (0.676g, 18mmol) under an atmosphere of N₂ and stirred for two days at room temperature. The reaction mixture was then cooled in an icebath and quenched drop-wise with water (100ml) followed by a 15% sodium hydroxide aqueous solution (100ml) then water (100ml). The reaction mixture was filtered under gravity to remove the aluminium salts and washed with DCM. The filtrate was then extracted washing the aqueous layer with DCM (3 x 100ml) then washing the organic layer with water (3 x 80ml). The organic layer was then dried over magnesium sulfate, filtered and evaporated to yield a dark red oil in 80% yield. Mp 186-188°C ^1H NMR, CDCl_3 , 400MHz; δ 6.67 (1H, d, CH, J = 18Hz), 6.21 (1H, d, CH, J = 2.4Hz), 6.07 (1H, dd, CH, J_1 = 5.6Hz, J_2 = 2.8Hz), 3.78 (3H, s, OMe), 3.74 (3H, s, OMe), 3.38 (1H, br .s, NH), 2.82 (2H, d, CH₂, J = 6.8Hz), 1.81 (1H, sept, CH, J = 6.8Hz), 0.92 (6H, d, 2xCH₃, J = 6.8Hz). MS m/z [M+H]⁺ 209

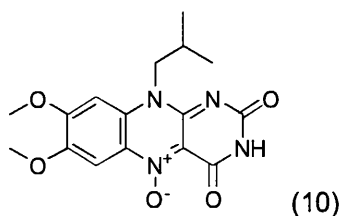
See Appendix 10 for ^1H NMR in CDCl_3 of compound (8)

6-((3,4-Dimethoxyphenyl)(isobutyl)amino)pyrimidine-2,4-dione. (9).^[33]



To (8) (0.82g, 3.9mmol) in dioxan 150ml was added 6-chlorouracil (0.291g, 2mmol) then refluxed over night. The reaction mixture was evaporated *in vacuo* to yield a dark residue which was loaded onto silica. The product was separated by silica gel column chromatography eluting with 100% acetone. The product was then collected in a 40% yield. Mp 187-188°C ¹H NMR d₆-DMSO, 400 MHz : δ, 10.394 (1H, br.s); 10.237 (1H, br.s); 7.081 (1H, s); 6.967 (1H, d, J=8.4); 6.814 (1H, d, J=2.4); 6.805 (1H, dd, J₁=9.6, J₂=2.4); 3.791 (3H, s); 3.755 (3H, s); 1.975 (1H, m); 0.994 (6H, d, J=6.8). MS m/z [M+H]⁺ 319

10-Isobutyl-7,8-dimethoxy-2,4-dioxo-2,3,4,10-tetrahydrobenzo[g]pteridine 5-oxide. (10).^[33]

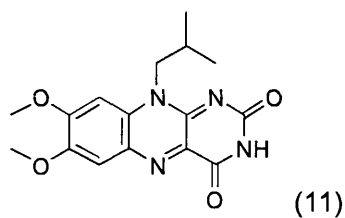


To compound (9) (0.393g, 1.23mmol) in acetic acid (15ml) cooled to 0°C was added portionwise sodium nitrite (0.255g, 3.7mmol). The reaction mixture was then allowed to warm to ambient temperature and stirred for 3 hours at room temperature monitoring by tlc. The reaction mixture was filtered, washing with ethanol. The filtrate was then evaporated to yield a dark orange solid. The solid was then washed with first DCM then diethyl ether to remove any residual acetic acid. The solid filtered off was

recovered and combined with the filtrate residue to yield the product in a 75% yield. Mp 285°C ^1H NMR d_6 -DMSO 400 MHz : δ 10.972 (1H, s); 7.706 (1H, s); 7.248 (1H, s); 4.559 (2H, br.s); 4.071 (3H, s); 3.937 (3H, s); 2.344 (1H, m); 0.996 (6H, d, $J=6.8$).

See Appendix 11 for ^1H NMR in CDCl_3 of compound (10)

10-Isobutyl-7,8-dimethoxybenzo[g]pteridine-2,4-dione. (11). ^[33]

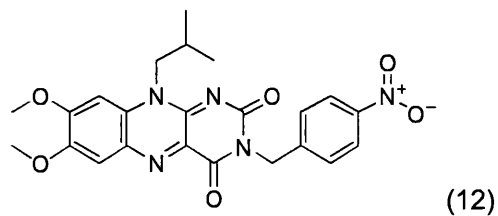


To (10) (410mg, 1.17mmol, 1 equiv) in ethanol was added dithiothreitol (813mg, 5.27mmol, 4.5 equiv) in water. The reaction mixture was refluxed under an atmosphere of nitrogen for two hours. The solution was then evaporated *in vacuo*. The product was separated by silica gel column chromatography, eluting with 100% acetone to yield the product in a 60% yield. Mp 293-294°C $^1\text{HNMR}$, CDCl_3 , 400MHz; δ 8.47 (1H, s, NH), 7.69 (1H, s, CH), 6.96 (1H, s, CH), 4.72 (2H, br.s, $\text{CH}_2\text{-N}$), 4.11 (3H, s, OMe), 4.04 (3H, s, OMe), 2.51 (1H, sept, CH, $J = 7.2\text{Hz}$), 1.11 (6H, d, $2\times\text{CH}_3$, $J = 7.2\text{Hz}$) MS FAB/NOBA $m/z = [\text{M}+\text{H}]^+ = 331.1406$ measured mass, $[\text{M}+\text{H}]^+$ 331.1362 (calculated mass)

See Appendix 12 for ^1H NMR in CDCl_3 of compound (11)

10-Isobutyl-7,8-dimethoxy-3-(4-nitrobenzyl)benzo[g]pteridine-2,4-dione.

(12)



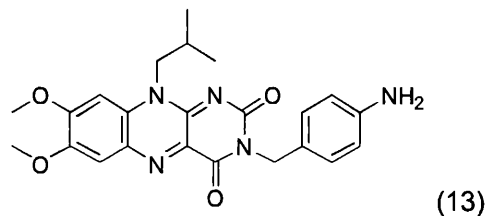
(12)

To a solution of (11) (0.225g, 0.77mmol) in acetonitrile (60ml) was added potassium carbonate (0.320g, 3.32mmol) and 4-nitro benzyl chloride (0.265g, 1.55mmol) and stirred at room temperature for 10 days. The solvent was evaporated *in vacuo*. The crude material was dissolved in dichloromethane then filtered to remove the potassium carbonate. The product was separated using silica gel column chromatography, eluting with 100% DCM, 10% EtOAc / DCM, 20% EtOAc / DCM then 40% EtOAc / DCM flushing with 100% acetone. 42% yield. ¹H NMR, CDCl₃, 400MHz; δ 8.07 (2H, d, 2xCH, J = 8.8Hz), 7.68 (2H, d, 2xCH, J = 8.4Hz), 7.57 (1H, s, CH), 6.68 (1H, s, CH), 5.47 (2H, s, CH₂), 4.56 (2H, br .s, CH₂-N), 4.05 (3H, s, OMe), 3.94 (3H, s, OMe), 2.40 (1H, sept, CH, J = 6.8Hz), 0.99 (6H, d, 2xCH₃, J = 6.8Hz) ¹³C NMR, DMSO-d₆, 400 MHz; δ 160.06; 159.59; 154.50; 149.09; 148.81; 146.51; 145.64; 133.48; 131.81; 130.31; 128.46; 123.36; 110.76; 97.71; 57.03; 56.30; 50.70; 43.77; 26.83; 19.94. IR (golden gate, v, cm⁻¹): 2936.1; 1698.0; 1650.8; 1581.3; 1541.8; 1510.0; 1418.4; 1339.3; 1250.6; 1214.9; 1172.5; 1013.4; 852.4; 807.06; 732.8. MS m/z (Accurate mass measurement, ES+) 466.1721 [M+H]⁺ (466.1718 calc.).

See Appendix 13 for ¹H NMR in CDCl₃ of compound (12)

3-(4-Aminobenzyl)-10-isobutyl-7,8-dimethoxybenzo[g]pteridine-2,4-dione.

(13)

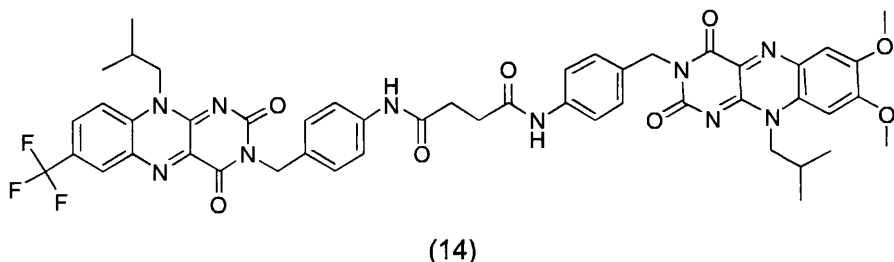


(13)

To compound (12) (0.066g, 0.14mmol) in DMF 50ml was added palladium on carbon (5% Pd on C, 0.1g). A balloon of hydrogen was attached and the mixture was stirred at room temperature for 2 hours. The reaction was then filtered and washed with DMF and acetone. The filtrate was evaporated down to yield an orange oil. Silica gel column chromatography was used to separate the compound eluting with 100% DCM 500ml, 10% acetone DCM 300ml, 20% acetone DCM 600ml, 30% acetone DCM, 40% acetone DCM 300ml. 58% Yield 0.035g.
¹H NMR, CDCl₃, 400MHz; δ 7.56 (1H, s, CH), 7.40 (2H, d, 2xCH, J = 8.4Hz), 6.83 (1H, s, CH), 6.54 (2H, d, 2x CH, J = 1.6Hz), 5.19 (2H, s, CH₂), 4.52 (2H, br .s, CH₂-N), 4.03 (3H, s, OMe), 3.93 (3H, s, OMe), 3.58 (2H, br .s, NH₂), 2.38 (1H, sept, CH, J = 6.8Hz), 0.97 (6H, d, 2xCH₃, J = 6.8Hz)
¹³C NMR d₆-DMSO, 400 MHz : 170.20; 159.87; 159.03; 156.64; 154.70; 154.61; 150.32; 148.91; 148.68; 139.89; 138.28; 138.13; 135.02; 134.19; 133.78; 132.06; 131.72; 131.59; 130.27; 129.84; 128.96; 128.23; 128.14; 118.73; 118.51; 110.73; 97.48; 56.98; 56.26; 50.54; 50.23; 43.98; 43.56; 31.13; 26.76; 19.91; 19.73. IR (golden gate, v, cm⁻¹): 3550.3; 3562.9; 3053.7; 2960.2; 1645.0; 1593.9; 1532.2; 1508.1; 1466.6; 1412.6; 1322.0; 1244.8; 1221.7; 1168.7; 1114.7; 1072.2; 1013.4; 921.8; 856.2; 803.2; 752.1; 622.4. MS m/z [M+H]⁺ 436.1982 measured mass, 436.197 calculated mass.

See Appendix 14 for ¹H NMR in CDCl₃ of compound (13)

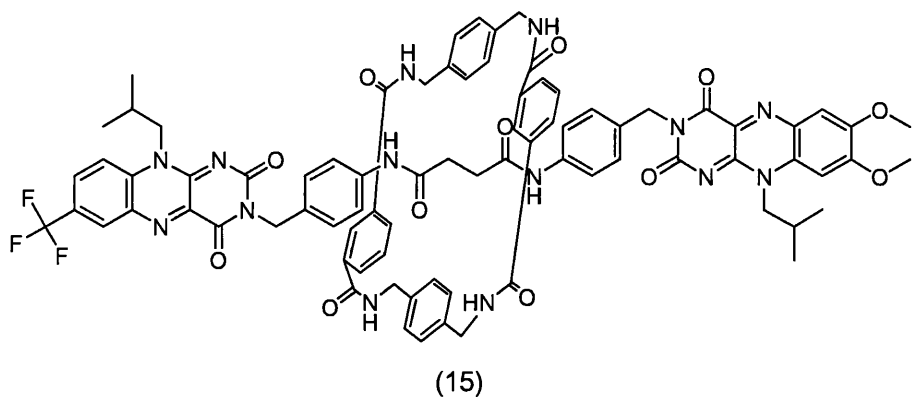
N1-((4-isobutyl-2,4-dioxo-7-(trifluoromethyl)benzo[g]pteridin-3-yl)methyl)-N4-((10-isobutyl-7,8-dimethoxy-2,4-dioxobenzo[g]pteridin-3-yl)methyl)phenyl)succinamide. (14)



To a solution of (5) (0.23g, 0.33mmol) in DMF was added (13) (0.146g, 0.33mmol) and DMAP (0.039g, 0.33mmol). The reaction was stirred over night in the dark at room temperature. The solvent was removed *in vacuo* to yield an orange oil. The product was separated by column chromatography eluting with 100% DCM, followed by a stepwise gradient of 10% Acetone DCM, 20% acetone DCM, 30% Acetone DCM, and 40% acetone DCM, finally flushing the column with 100% Acetone. 50% yield ¹H NMR, DMF, 400MHz; δ: 10.06 (1H, d, NH, J = 7.6Hz); 8.56 (1H, s, CH); 8.38 (1H, d, CH, J = 8.8 Hz); 8.26 (1H, d, CH, J = 8.8 Hz); 7.67 (1H, s, CH); 7.67-7.61 (4H, m, 4xCH); 7.48 (1H, s, CH); 7.41 (4H, d, CH, J = 8.4 Hz); 5.16 (4H, s, 2x CH₂); 4.76 (2H, s, CH₂-N); 4.66 (2H, s, CH₂-N); 4.22 (3H, s, OMe); 4.07 (3H, s, OMe); 2.73 (4H, s, 2xCH₂); 2.49 (2H, m, 2x CH); 1.04 (6H, d, 2xCH₃, J = 7.2 Hz); 1.02 (6H, d, 2xCH₃, J = 7.2 Hz) ¹H MNR, COSY GPSW, DMF, 400MHz; Coupling found between δ = 2.49 (2H, m, 2x CH) and 1.04 (6H, d, 2xCH₃, J = 7.2 Hz); 1.02 (6H, d, 2xCH₃, J = 7.2 Hz). ¹³C NMR d₆-DMSO, 400 MHz: δ 160.79; 155.90; 155.61; 149.03; 148.94; 134.71; 132.22; 131.27; 130.30; 127.47; 114.81; 111.77; 96.07; 56.75; 56.55; 51.41; 44.51; 30.96; 27.45; 20.31. IR (golden gate, v, cm⁻¹): 2936.1; 1698.0; 1650.8; 1581.3; 1541.8; 1510.0; 1418.4; 1339.3; 1250.6; 1214.9; 1172.5; 1013.4; 852.4; 807.06; 732.8

See Appendix 15 for ¹H NMR in d₆-DMSO of compound (14)

Asymmetric [2]Rotaxane. (15)

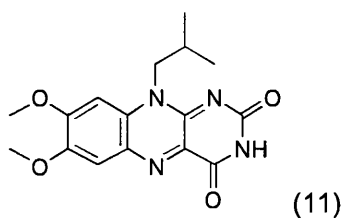


To (14) (0.075g, 0.07mmol) in chloroform (15ml) was added triethylamine (0.22ml). Solutions of *p*-xylenediamine (500mg, 3.7mmol) in chloroform (8ml) and isophthaloyl dichloride (800mg, 3.9mmol) in chloroform (8ml) were made up and added simultaneously over 3 hours. The reaction mixture was stirred for 24 hours. The reaction mixture was filtered and washed first with chloroform then with acetone. The solvent removed *in vacuo* to yield a yellow solid. The product was separated by silica gel column chromatography eluting with 100% dichloromethane, 10% acetone dichloromethane, 20% acetone dichloromethane, 25% acetone dichloromethane, 40% acetone dichloromethane. The product was collected and evaporated to yield a yellow solid in a 60% yield. Found, C 65.29, H 4.96, N 13.61. C₈₁H₇₅F₃N₁₄O₁₂ Requires C 65.14, H 5.06, N 13.13. MS m/z [M+H]⁺ 1493.5 measured mass, 1492.56 calculated mass. [M+Li]⁺ 1499.5 measured mass, 1499.6 calculated mass. Mp > 250°C ¹H NMR d₆-DMSO, 400MHz: δ 9.82 (1H, s, NH), 9.78 (1H, s, NH), 8.54 (1H, s, NH), 8.48 (1H, s, NH), 8.22 (4H, complex m, 4xCH), 8.08 (6H, d, 6xCH, J = 8 Hz), 7.7 (3H, t, 3xCH, J = 8Hz), 7.44 (6H, complex m, 6xCH), 7.24 (3H, m, 3xCH), 6.83 (7H, br. s, 7xCH), 6.67 (2H, br. s, 2xNH), 5.02 (2H, s, CH₂), 4.87 (2H, s, CH₂), 4.53 (4H, br. s, 2xCH₂), 4.37 (2H, br. s, CH₂), 4.35 (2H, br. s, CH₂), 4.19 (2H, br. s, CH₂), 4.16 (2H, br. s, CH₂), 4.1 (3H, s, OMe), 3.74 (3H, s, OMe), 2.34 (2H, m,

2xCH), 1.28 (3H, s, CH₃), 1.24 (3H, s, CH₃), 1.97 (6H, d, 2xCH₃, *J* = 6.4Hz), 0.74 (4H, br. s, 2xCH₂)

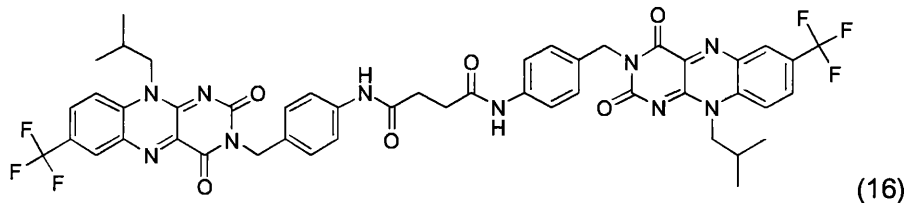
See Appendix 16 for ¹H NMR in d₆-DMSO of compound (15), and, Appendices 17 and 18 for the Mass Spectrum of (15).

Alternative Synthesis of 10-isobutyl-7,8-dimethoxybenzo[g]pteridine-2,4-dione.^[33,35]



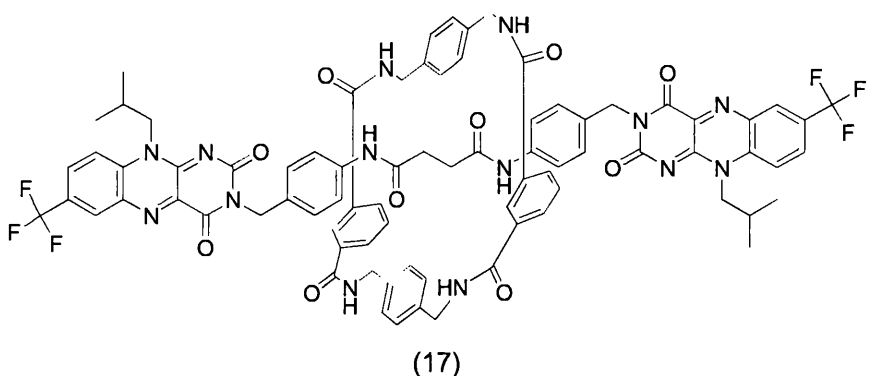
To a solution of (8) (0.3g, 1.4mmol) in acetic acid (50 ml) was added violuric acid monohydrate (0.251g, 1.4mmol). The reaction was refluxed for 30 minutes then allowed to cool for 2 hours. Once cool the reaction was filtered washing with water and a small amount of ethanol. The product was recovered as orange crystals. The filtrate was neutralised with saturated aqueous Sodium bicarbonate 500ml, extracting with DCM 3x 500mL. The organic layer was dried over MgSO₄, filtered and the solvent evaporated *in vacuo*. The product was then separated using column chromatography, eluting with 100% DCM, followed by 10% acetone DCM, 20% acetone DCM, 30% acetone DCM, 40% acetone DCM, 50% acetone DCM. The product was recovered as an orange solid in a 60 % yield. Mp 293-294°C ¹HNMR, CDCl₃, 400MHz; δ 8.47 (1H, s, NH), 7.69 (1H, s, CH), 6.96 (1H, s, CH), 4.72 (2H, br .s, CH₂-N), 4.11 (3H, s, OMe), 4.04 (3H, s, OMe), 2.51 (1H, sept, CH, *J* = 7.2Hz), 1.11 (6H, d, 2xCH₃, *J* = 7.2Hz) MS m/z [M+H]⁺ 331.1406 measured mass, 331.1362 (calculated mass)

N1,N4-bis(4-((10-isobutyl-2,4-dioxo-7-(trifluoromethyl)benzo[g]pteridin-3-yl) methyl)phenyl)succinamide (16)



A mixture of compound 3 (0.58g, 1.31mmol), succinoyl dichloride (0.0725 ml, 0.66 mmol) and pyridine (0.12 ml, 1.50mmol) in DCM (50 ml) was stirred at room temperature overnight. The precipitate was collected by filtration, washing with hot acetone (3 times) and dried to give yellow crystals in a 38% yield. The product is stable at temperatures up to 310 °C. ^1H NMR, CDCl_3 , 400 MHz : δ 8.548 (2H, s); 8.251 (2H, d, $J=8.8$); 8.195 (2H, dd, $J1=9.2$; $J2=2.0$); 7.629 (4H, d, $J=8.4$); 7.510 (4H, d, $J=8.4$); 5.041 (4H, s); 4.530 (4H, br. s); 2.510 (4H, m); 2.349 (2H, m); 0.981 (12H, d, $J=7.2$). ^{13}C NMR d_6 -DMSO, 400 MHz : δ 170.21; 152.02; 154.68; 150.31; 139.90; 138.26; 135.37; 134.19; 131.54; 131.26; 129.87; 128.23; 125.89; 118.74; 50.86; 43.28; 31.35; 26.74; 19.73. IR (golden gate, ν , cm^{-1}): 3312.1; 2959.2; 2876.3; 1705.7; 1653.7; 1593.9; 1556.3; 1529.3; 1450.2; 1407.8; 1321.0; 1253.5; 1221.7; 1168.7; 1138.7; 1071.3; 1002.8; 907.3; 825.4; 807.1; 646.0. MS m/z (Accurate mass measurement, ES+) 968.1387[M+H] $^+$ (968.3201 calc.).

Symmetric [2] Rotaxane. (17)

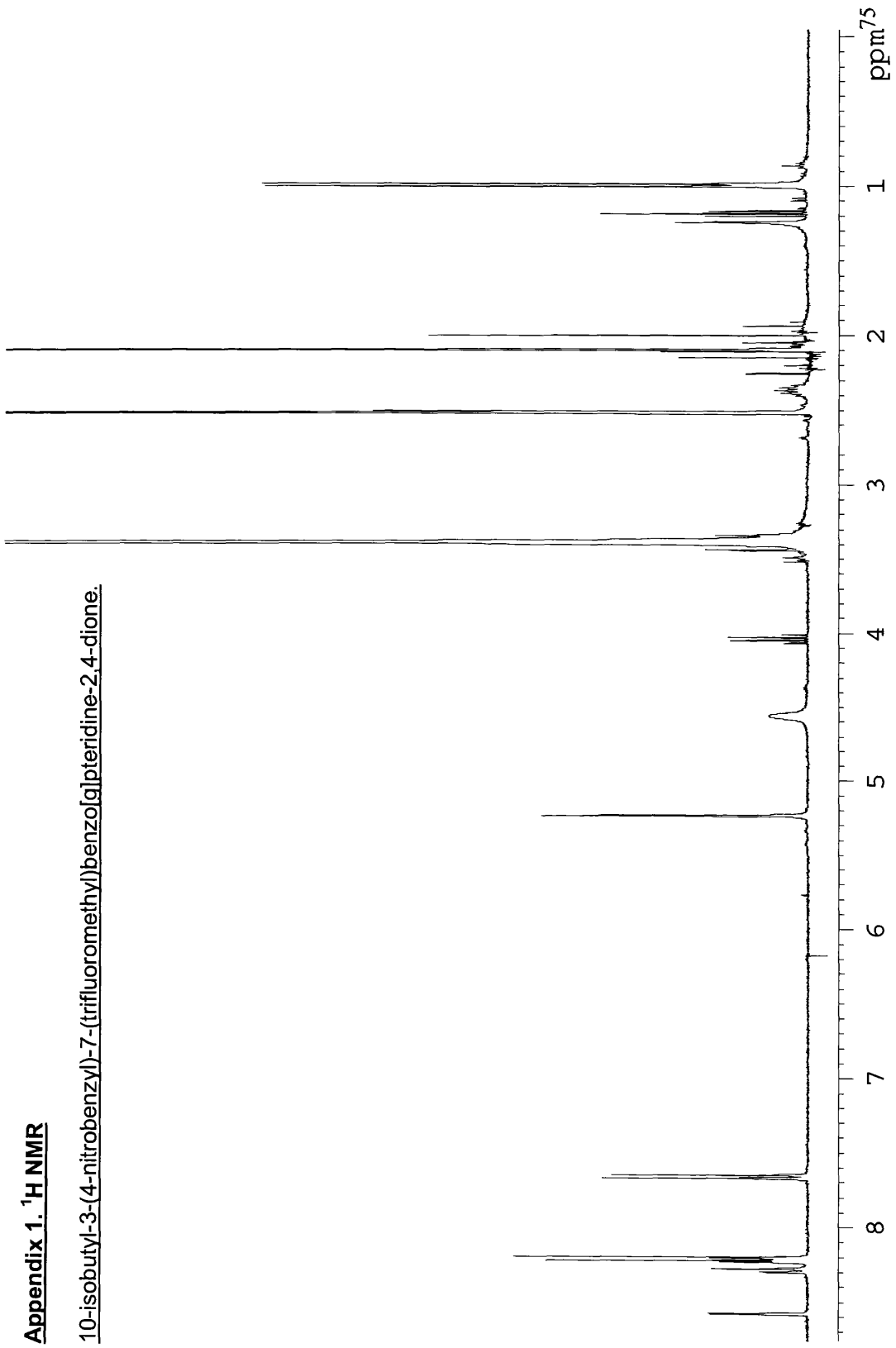


The symmetrical axle(16) (0.2g, 0.207mmol) was suspended in 200 ml of anhydrous CHCl₃. Triethylamine (3.30ml) was added to the mixture, and it was stirred at room temperature for 30 min. Solutions of *p*-xylenediamine (0.63g, 4.63mmol) in 5ml CHCl₃ and isophthaloyl dichloride (0.94g, 4.61mmol) in 5ml CHCl₃ were then added simultaneously over 4 hours at room temperature. The suspension was then stirred overnight at room temperature. Then precipitate was filtered and washed with chloroform. Solvent was removed *in vacuo*, and rotaxane was isolated by column chromatography on silica gel with 100% DCM, 10% acetone DCM, 20% acetone DCM, 30% acetone DCM, 35% acetone DCM 40% acetone DCM. Mass spectrum showed only traces of product was formed. MS MALDI [M+Na]⁺ = 1524.

See Appendix 19 for the Na⁺ adduct Mass Spectrum.

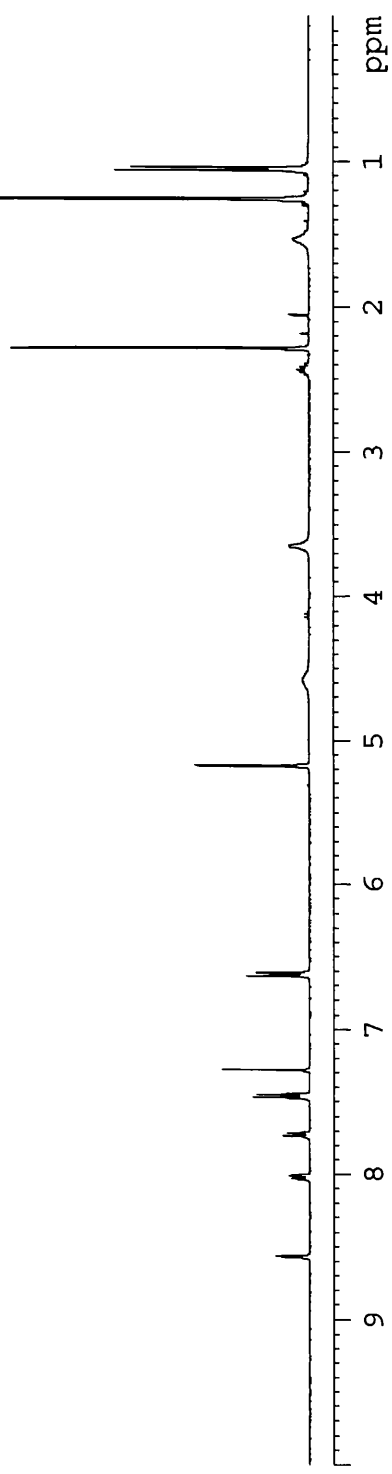
Appendix 1. ^1H NMR

10-isobutyl-3-(4-nitrobenzyl)-7-(trifluoromethyl)benzo[*g*]pteridine-2,4-dione.



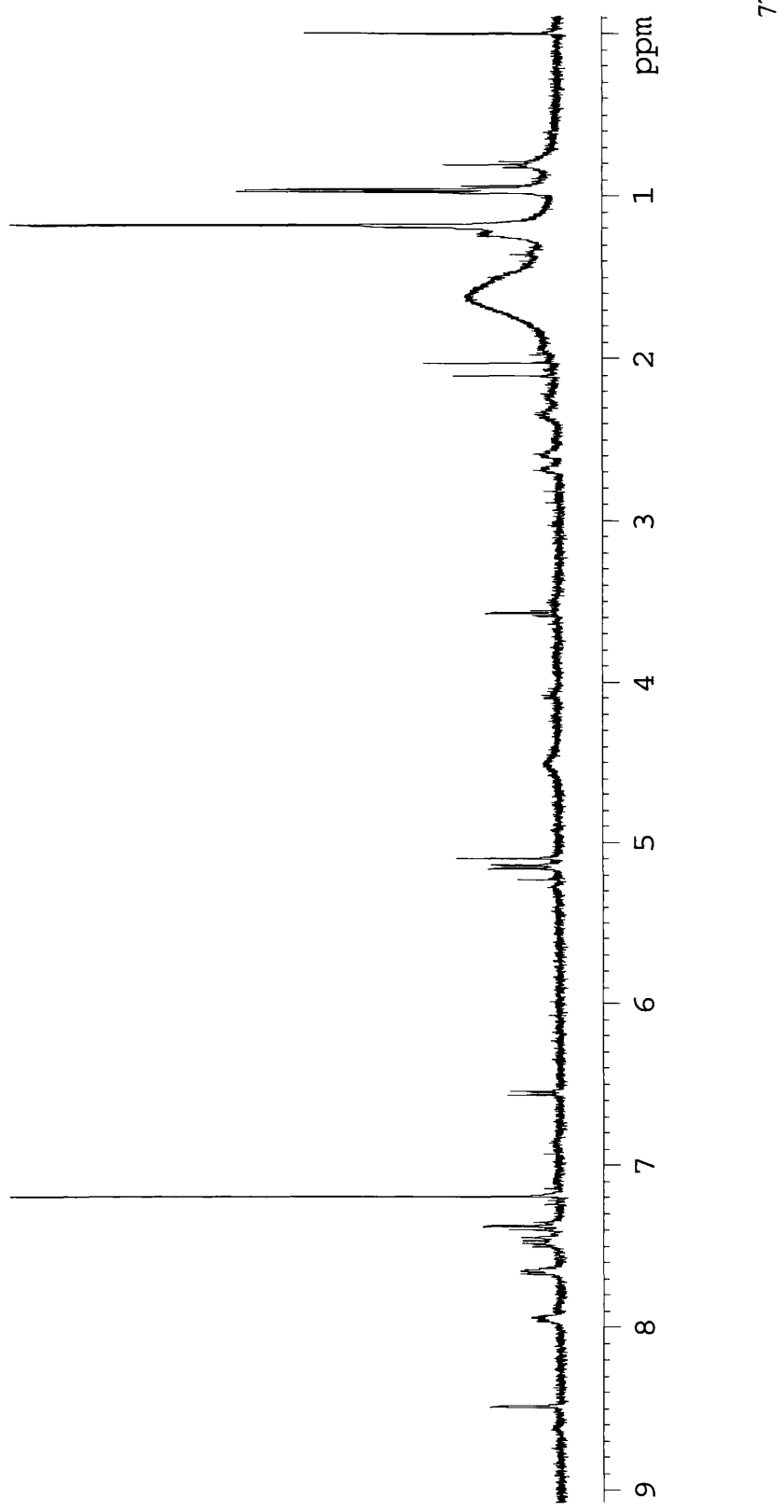
Appendix 2. ^1H NMR

10-isobutyl-3-(4-aminobenzyl)-7-(trifluoromethyl)benzoflpteridine-2,4-dione



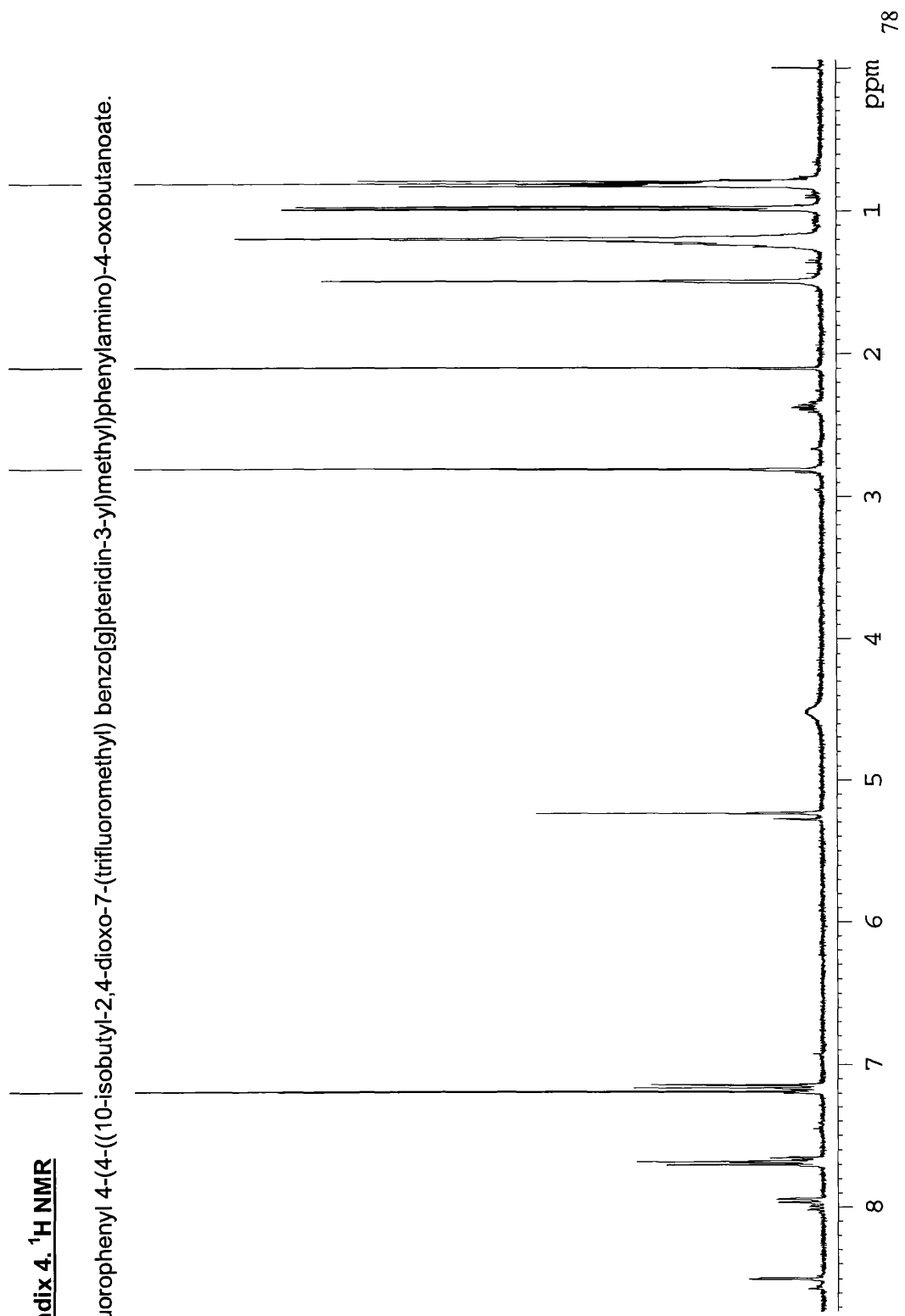
Appendix 3. ^1H NMR

4-(4-((10-isobutyl-2,4-dioxo-7-(trifluoromethyl)benzo[g]pteridin-3-yl)methyl)phenylamino)-4-oxobutanoic acid



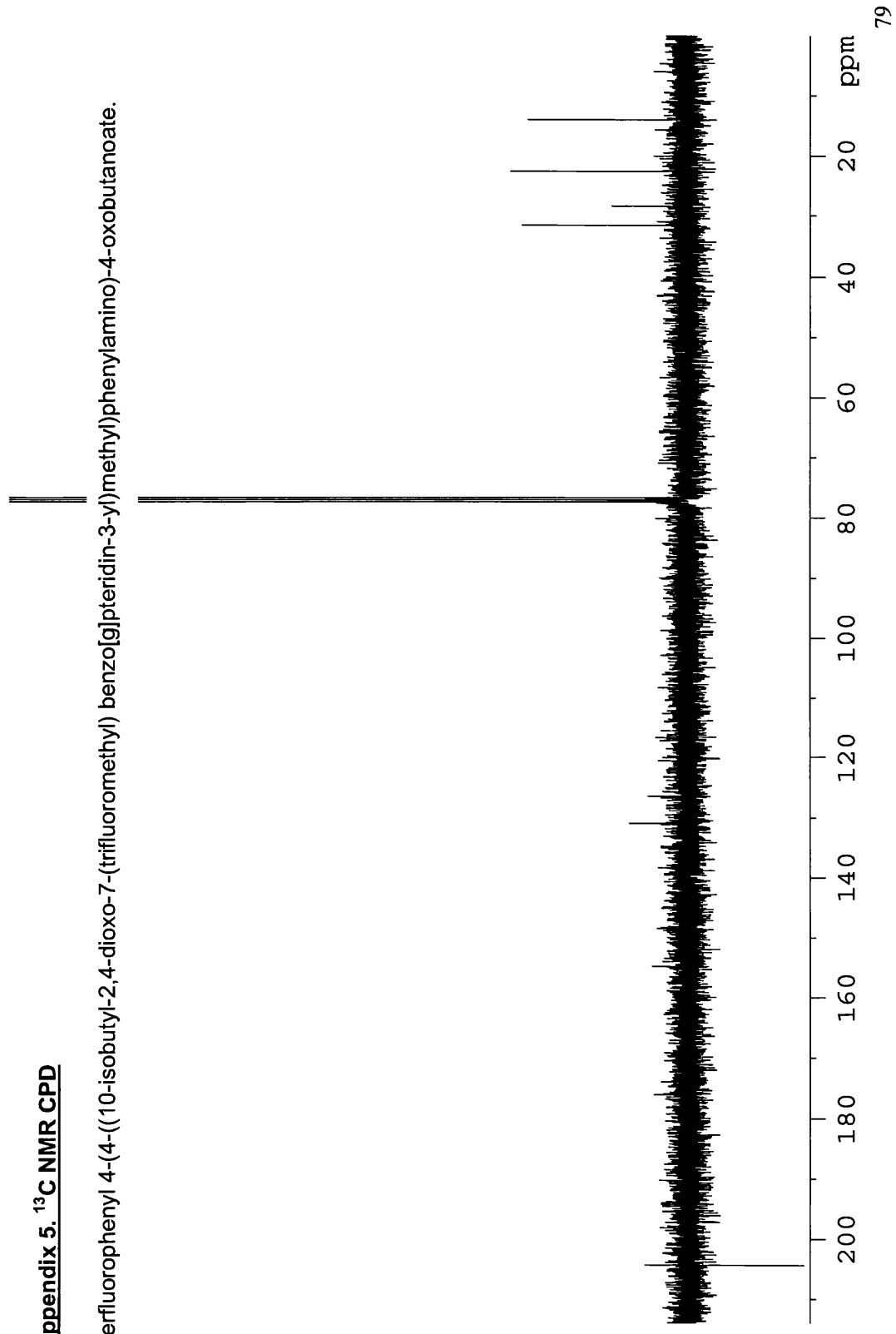
Appendix 4. ^1H NMR

Perfluorophenyl 4-(4-((10-isobutyl-2,4-dioxo-7-(trifluoromethyl) benzo[g]pteridin-3-yl)methyl)phenylamino)-4-oxobutanoate.



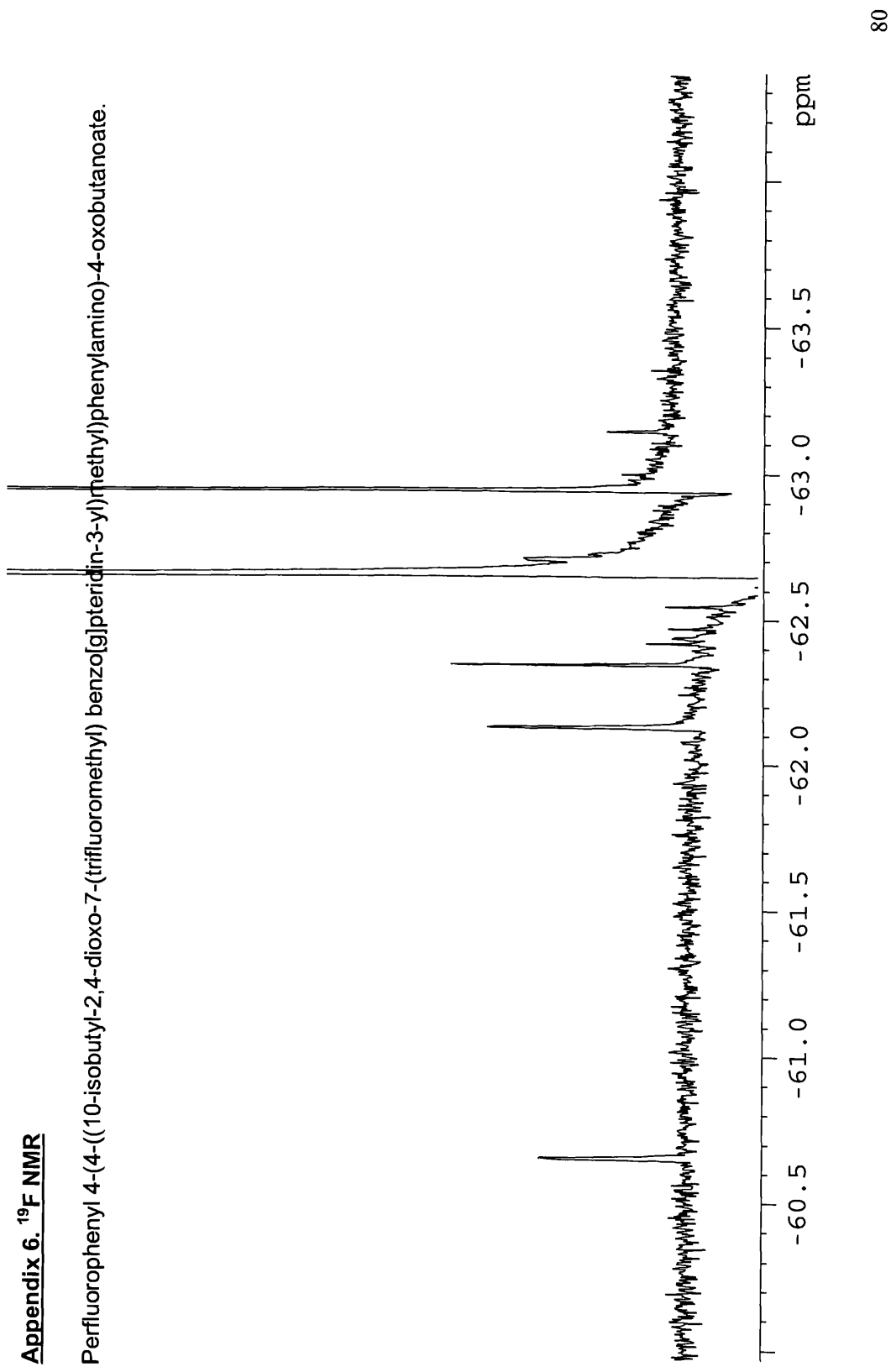
Appendix 5. ^{13}C NMR CPD

Perfluorophenyl 4-(4-((10-isobutyl-2,4-dioxo-7-(trifluoromethyl) benzo[g]pteridin-3-yl)methyl)phenylamino)-4-oxobutanoate.



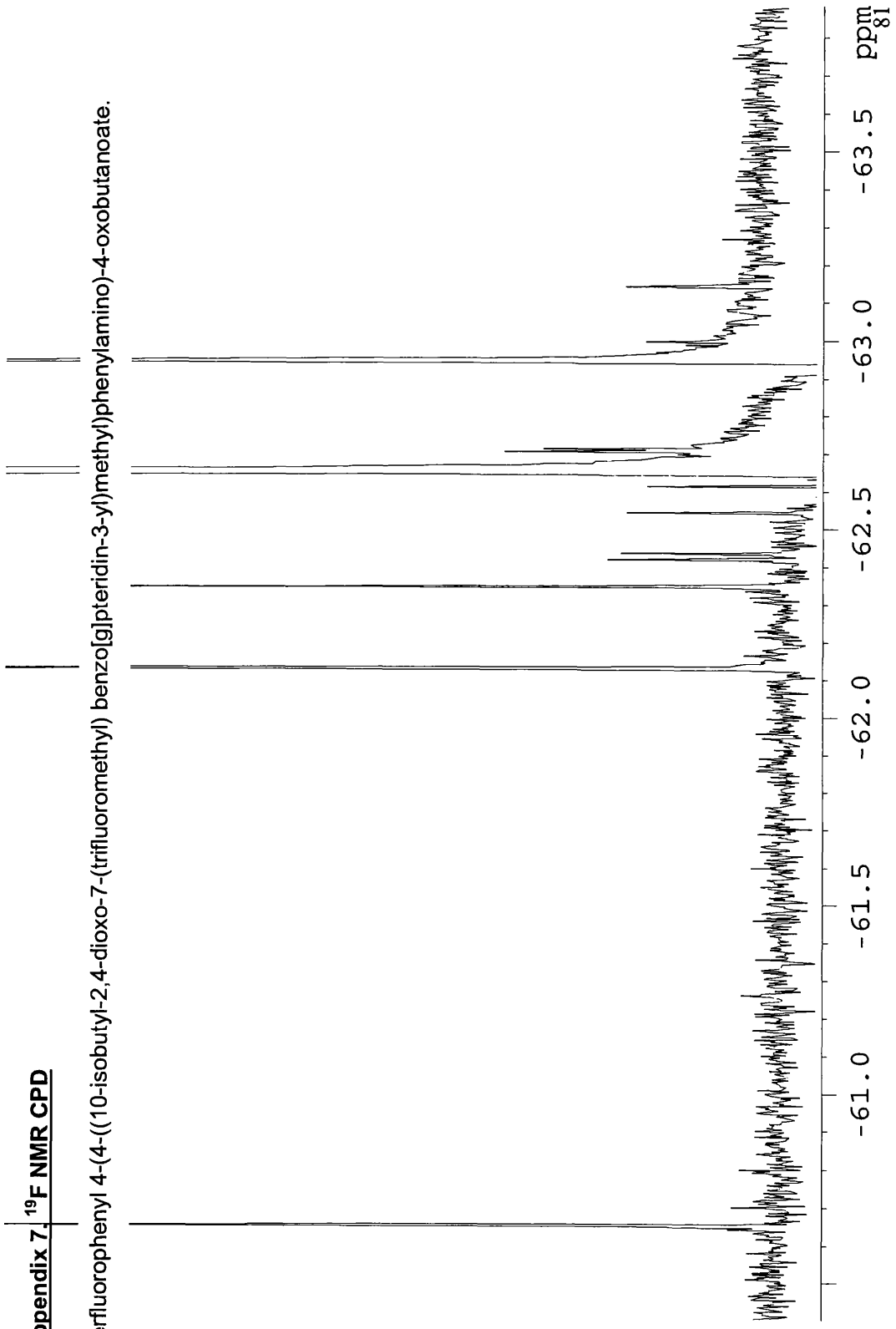
Appendix 6. ^{19}F NMR

Perfluorophenyl 4-(4-((10-isobutyl-2,4-dioxo-7-(trifluoromethyl) benzog[*g*]pteridin-3-yl)methyl)phenylamino)-4-oxobutanoate.



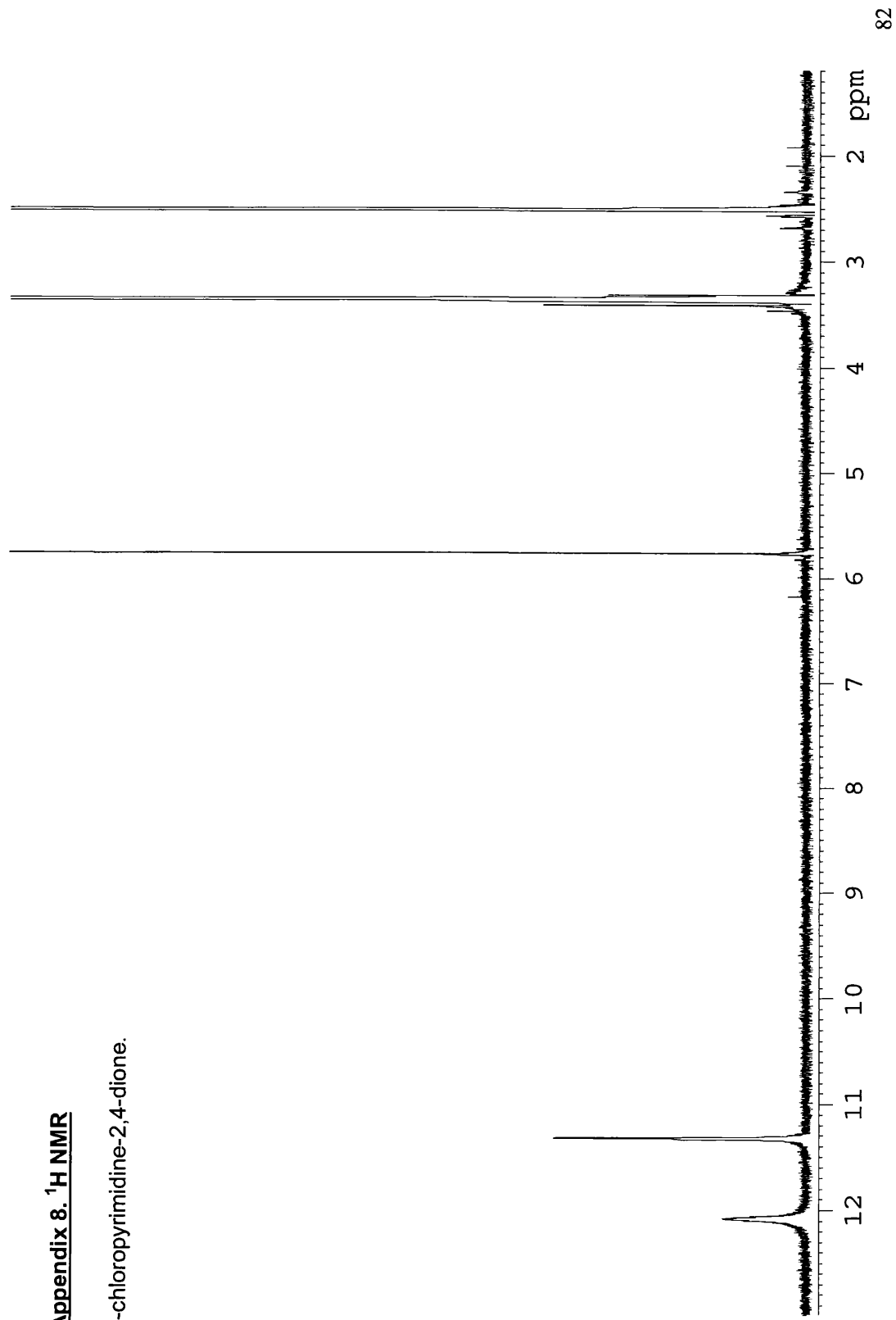
Appendix 7. ^{19}F NMR CPD

Perfluorophenyl 4-(4-((10-isobutyl-2,4-dioxo-7-(trifluoromethyl) benzo[g]pteridin-3-yl)methyl)phenylamino)-4-oxobutanoate.



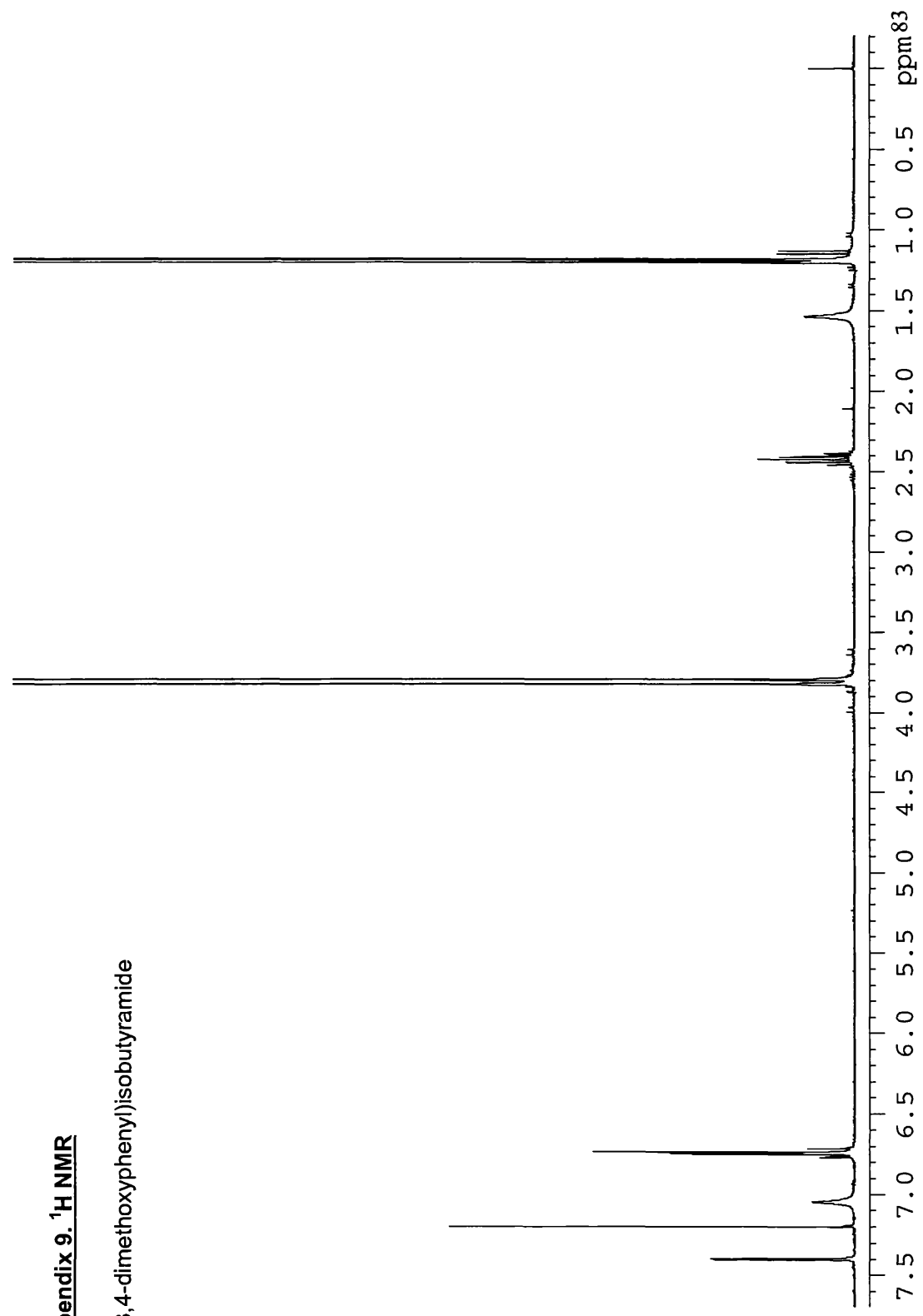
Appendix 8. ^1H NMR

6-chloropyrimidine-2,4-dione.



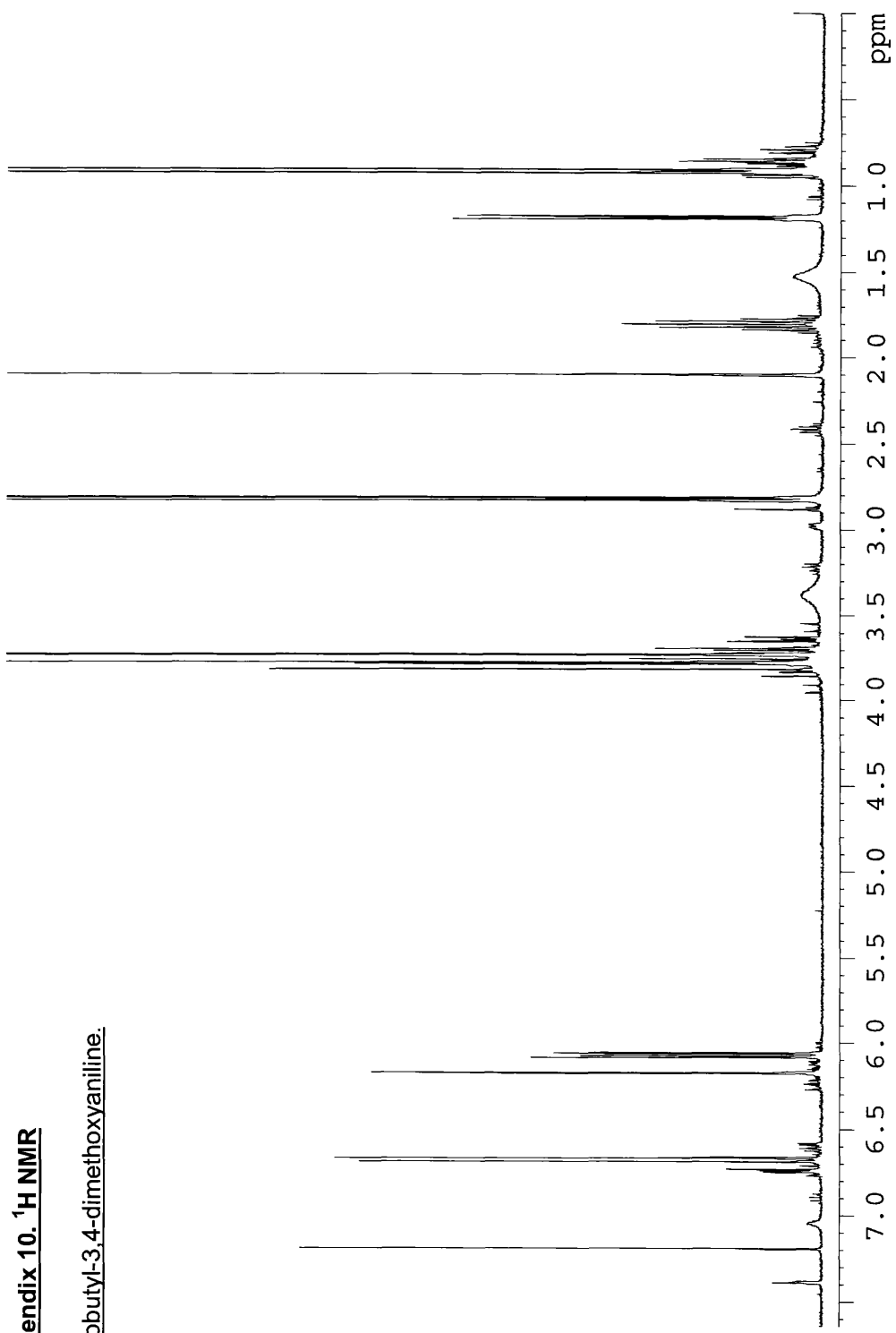
Appendix 9. ^1H NMR

N-(3,4-dimethoxyphenyl)isobutyramide



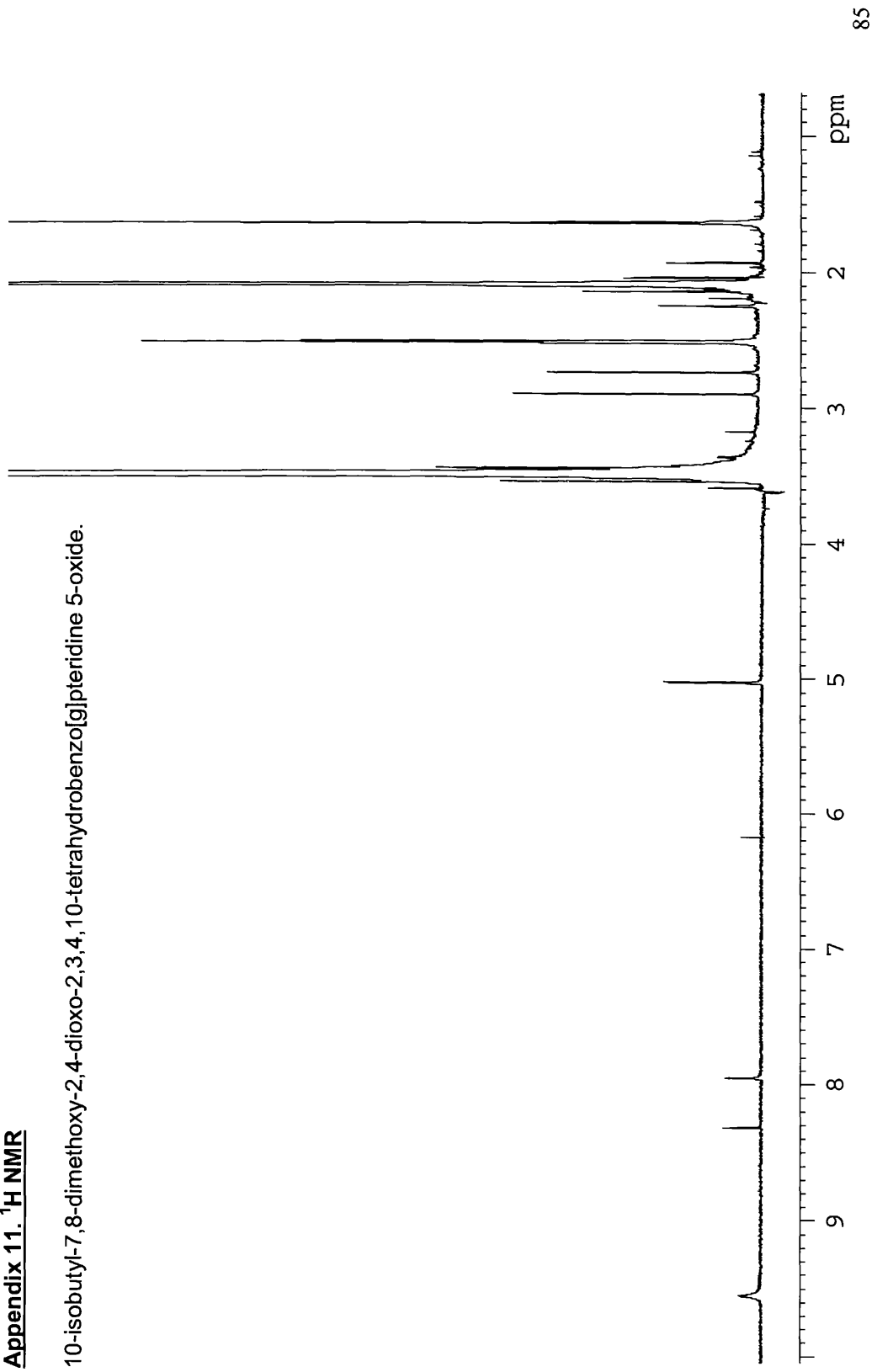
Appendix 10. ^1H NMR

N-isobutyl-3,4-dimethoxyaniline.



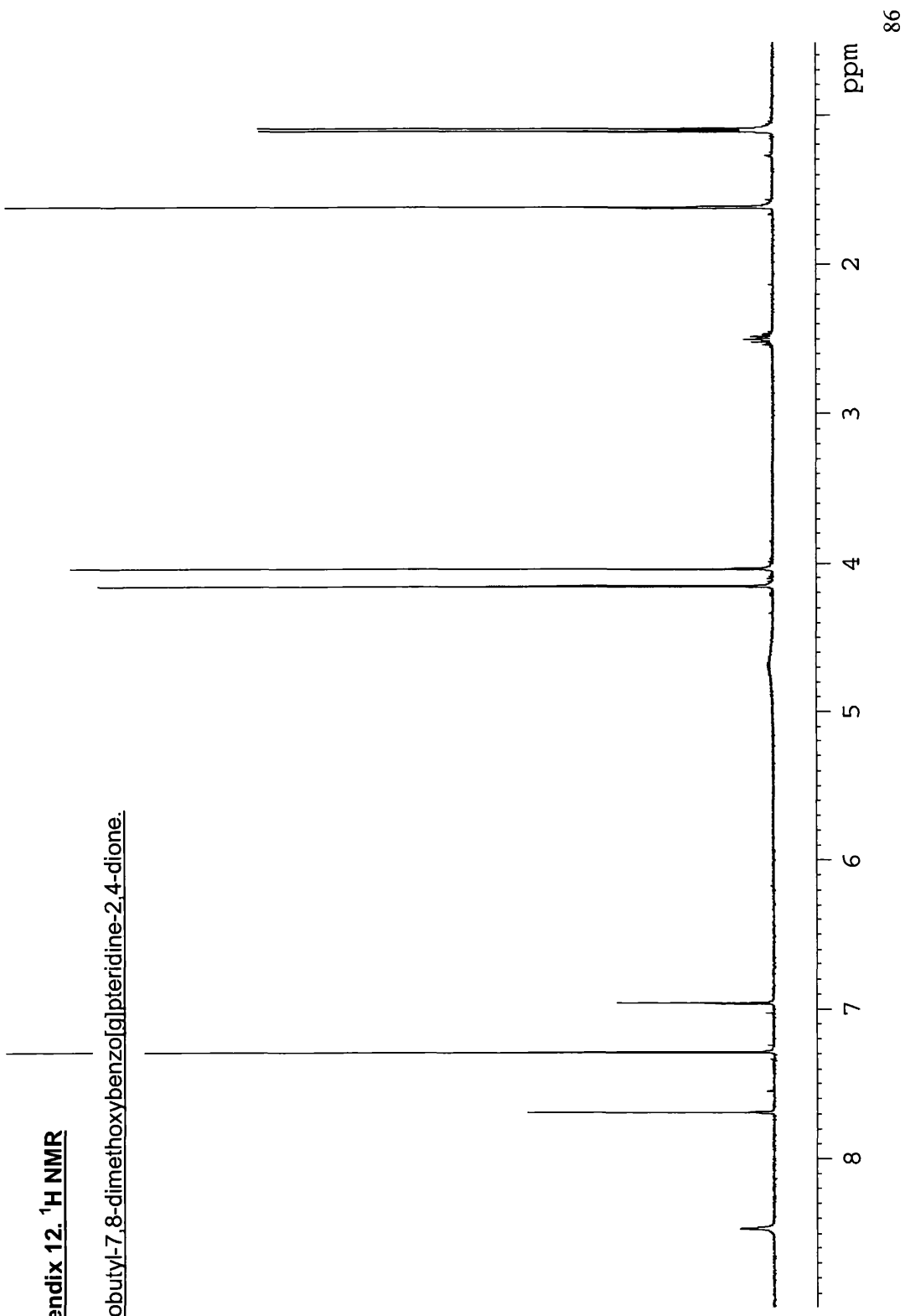
Appendix 11. ^1H NMR

10-isobutyl-7,8-dimethoxy-2,4-dioxo-2,3,4,10-tetrahydrobenzo[g]pteridine 5-oxide.



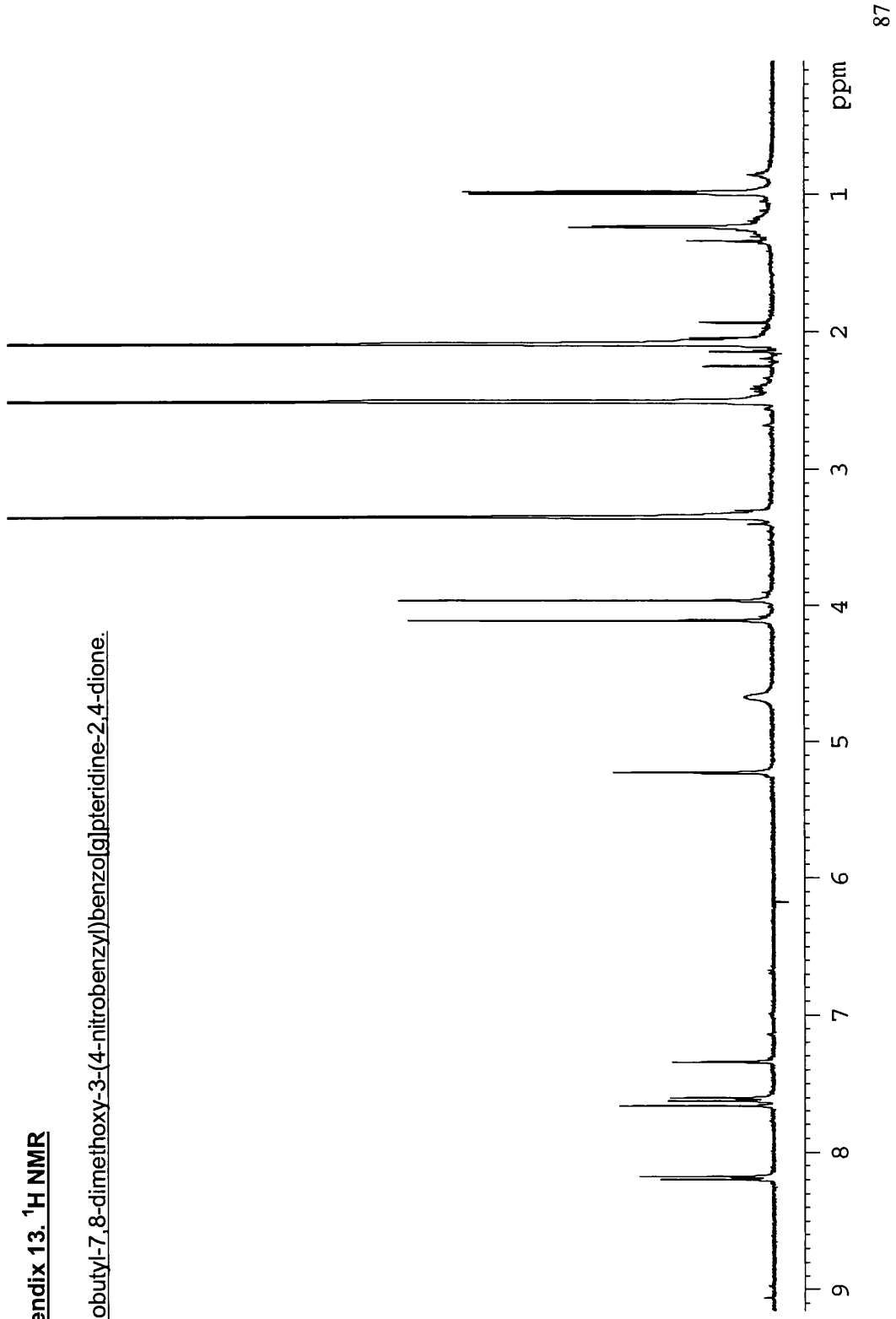
Appendix 12. ^1H NMR

10-isobutyl-7,8-dimethoxybenzo[*g*]pteridine-2,4-dione.



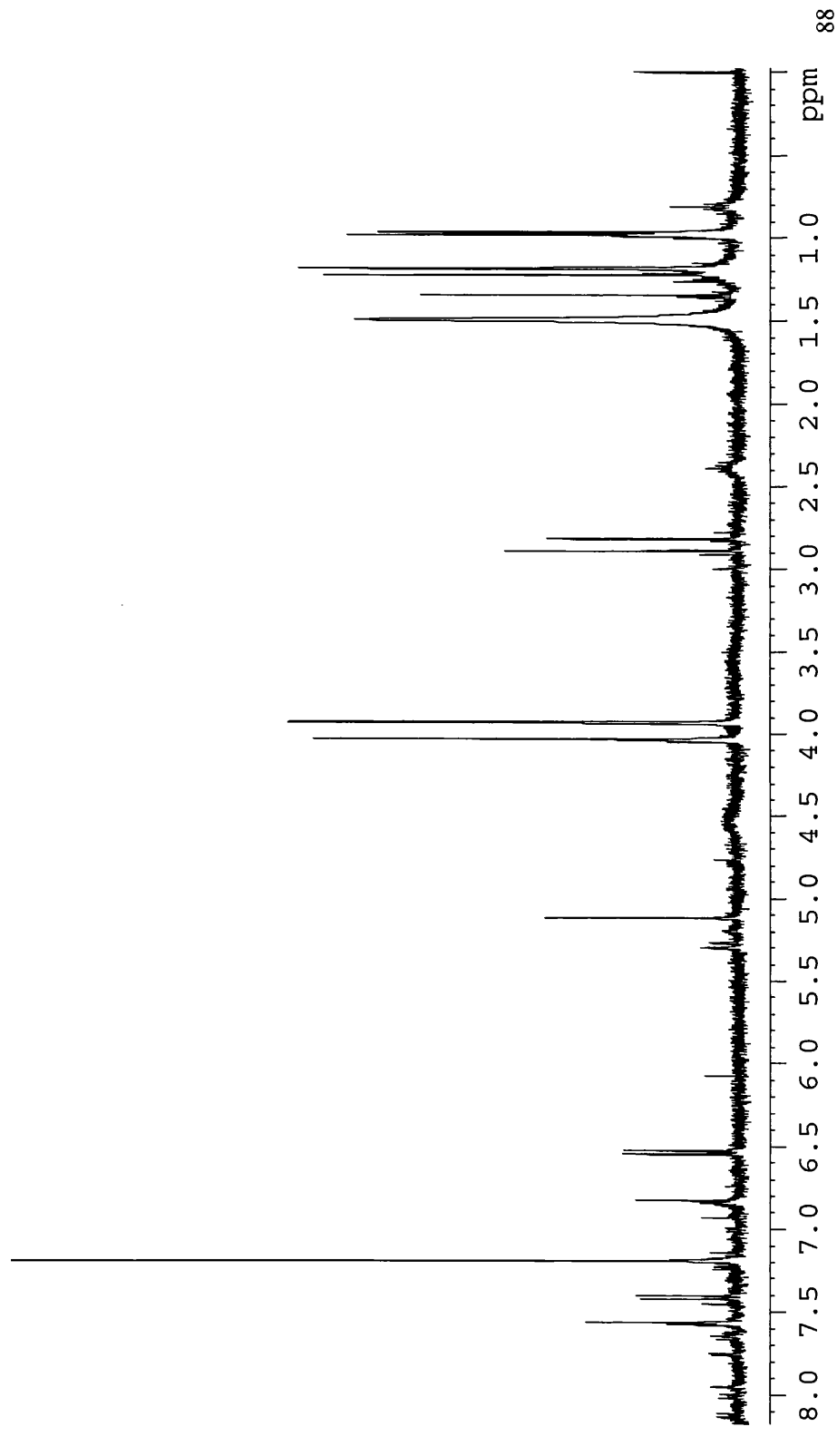
Appendix 13. ^1H NMR

10-Isobutyl-7,8-dimethoxy-3-(4-nitrobenzyl)benzo[*g*]pteridine-2,4-dione.



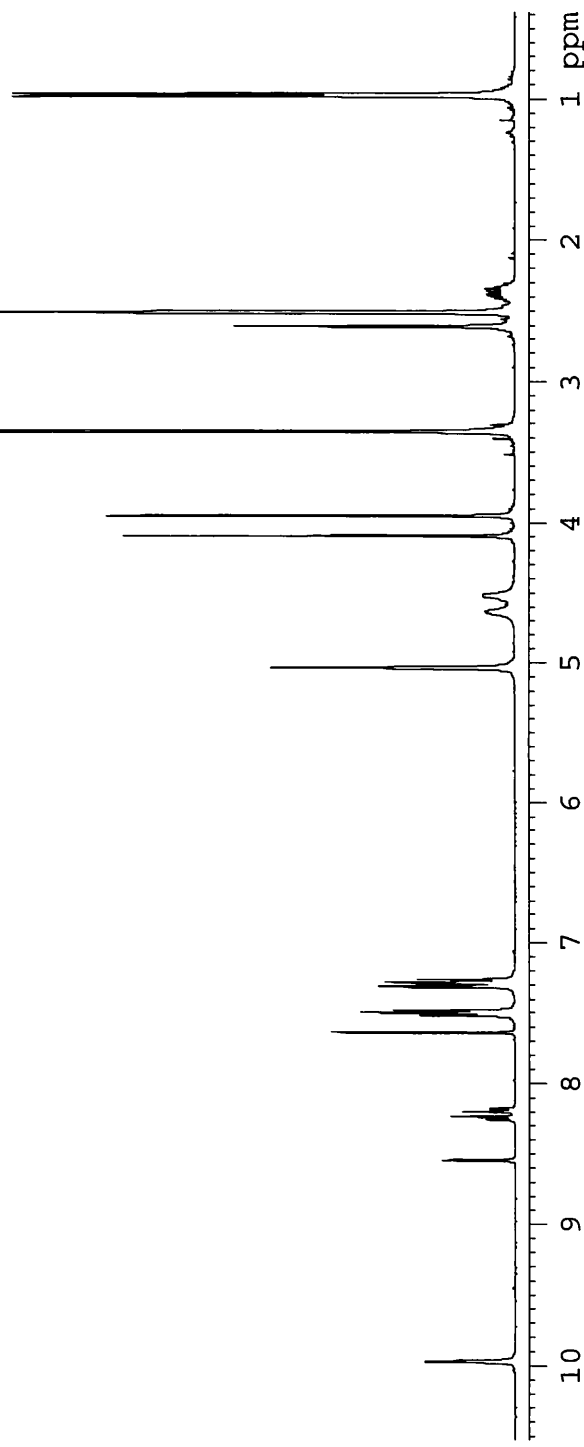
Appendix 14. ^1H NMR

10-(Isobutyl)-7,8-dimethoxy-3-(4-aminobenzyl)benzo[*g*]pteridine-2,4-dione.



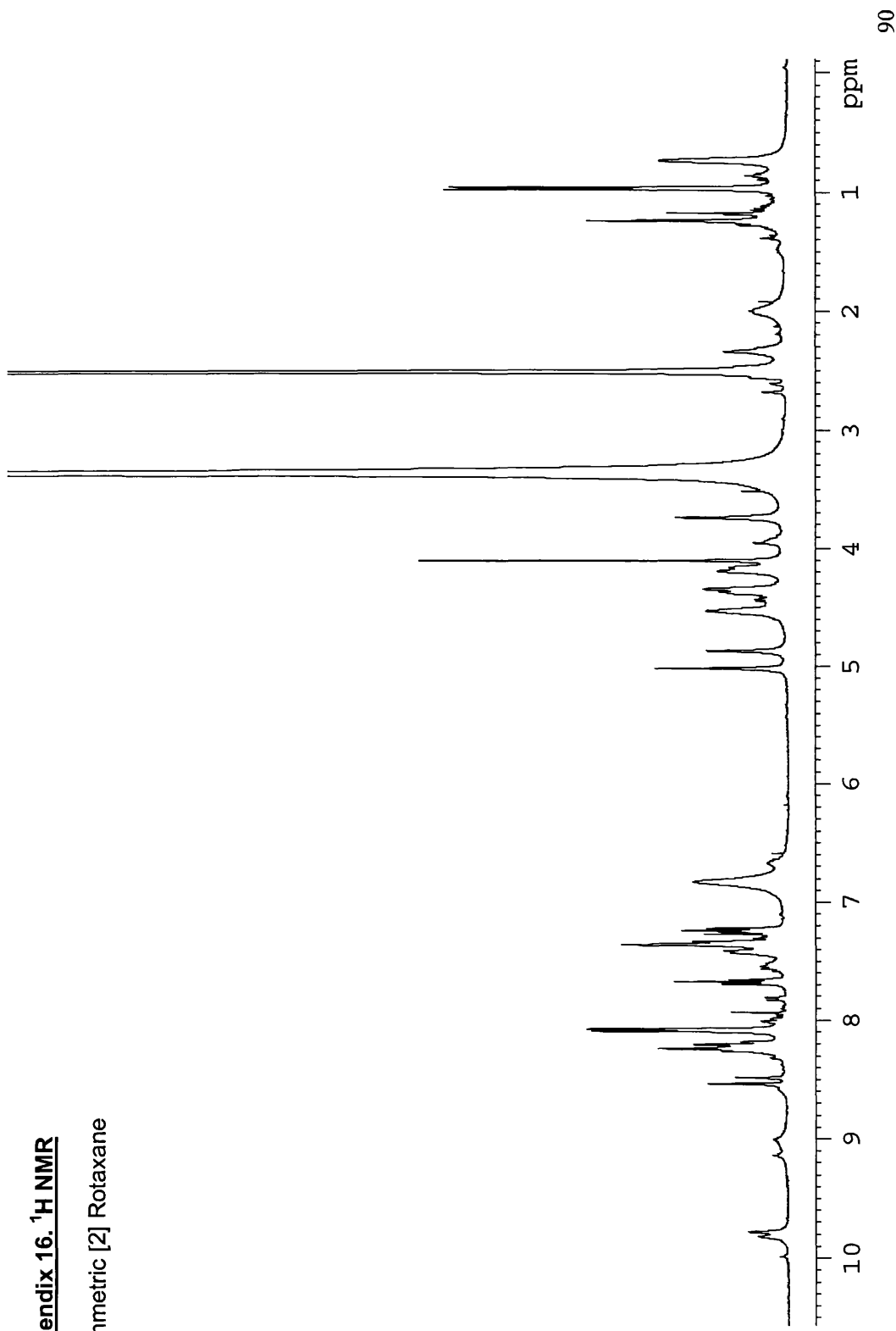
Appendix 15. ^1H NMR

N1-(4-((10-isobutyl-2,4-dioxo-7-(trifluoromethyl)benzo[g]pteridin-3-yl)methyl)phenyl)-N4-((10-isobutyl-7,8-dimethoxy-2,4-dioxobenzog[pteridin-3-yl)methyl)phenyl)succinamide.



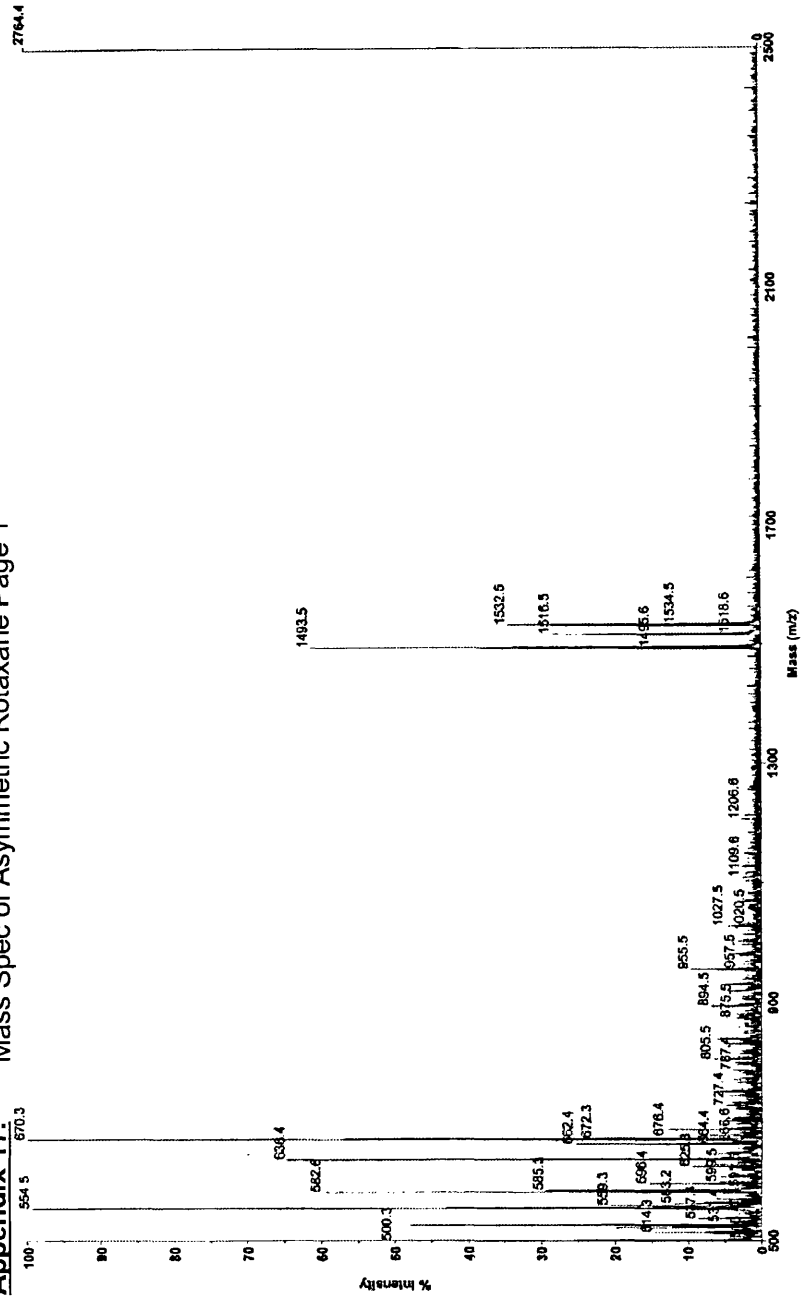
Appendix 16. ^1H NMR

Asymmetric [2] Rotaxane



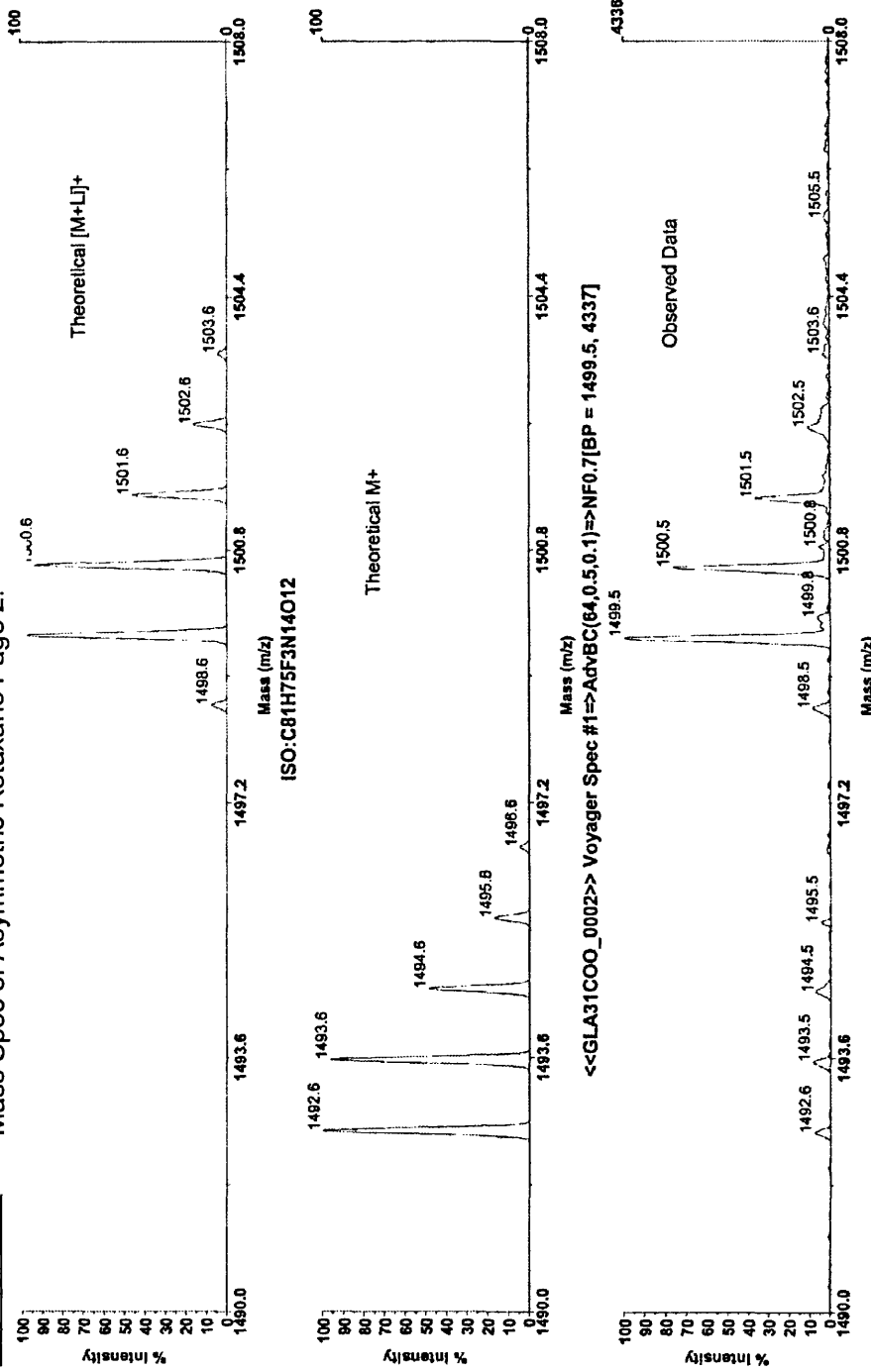
Appendix 17

Mass Spec of Asymmetric Rotaxane Page 1



Appendix 18.

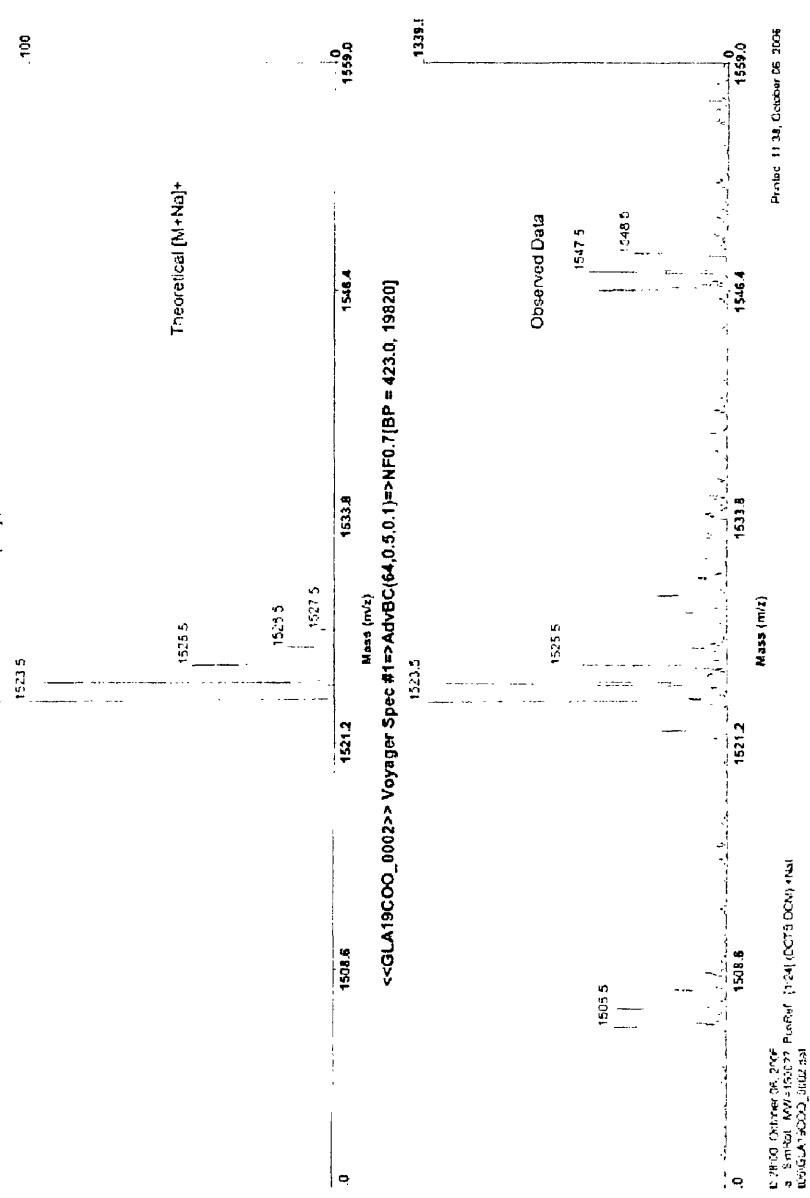
Mass Spec of Asymmetric Rotaxane Page 2.



Appendix 19 Mass Spectrum of the Symmetric Rotaxane.

EPSRC National Mass Spectrometry Service Centre (NMSSC), Swansea

ISO: C80H70N14O10F6 + [N3]1



References.

- [1] J. -M. Lehn. *Angew. Chem. Int. Ed. Engl.*, **1988**, 27,89.
- [2] D. J. Cram., *Angew. Chem. Int. Ed. Engl.*, **1988**, 27,1009.
- [3] P. D. Beer, P. A. Gale, D. K. Smith., *Supramolecular Chemistry Oxford Chemistry Primer.*, Oxford Science Publications., **1999**, pp 7-24.
- [4] J. W. Steed, J. L. Atwood., *Supramolecular Chemistry.*, John Wiley and Sons Ltd., **2002**, pp 9-14 , 20-30
- [5] J. Clayden, N. Greeves, S. Warren, P. Wothers., *Organic Chemistry. Third Edition.*, Oxford University Press., **2001**, pp 114-115.
- [6] R. A. Kelln, J. R. Gear., *BioScience.*, **1980**, 30, No.2
- [7] M. R. Kishan, A. Parham, F. Schelhase, A. Yoneva, G. Silva, X. Chen, Y. Okamoto, F. Vogtle., *Angew. Chem. Int. Ed.*, **2006**, 45, 7296.
- [8] P. Ghosh, G. Federwisch, M. Kogy, C. A. Schalley, D. Haase, W. Saak, A. Lutzen, and R. W. Gschwind., *Org. Biomol. Chem.*, **2005**, 3, 2691.
- [9] D. A. Leigh, A. Murphy, J. P. Smart, M. S. Deleuze, and F. Zerbetto., *J. Am. Chem. Soc.*, **1998**, 120, 6458.
- [10] G. J. Ashwell, B. Urasinska, C. Wang, M. R. Bryce, I. Grace, C. J. Lambert., *Chem. Commun.*, **2006**, 4706.
- [11] F. Cacailli, J. S. Wilson, J. J. Michels, C. Daniel, C. Silva, R. H. Friend, N. Severin, P. Samori, J. P. Rabe, M. J. O'Connell, P. N. Taylor, H. L. Anderson. *Nature Materials.*, **2002**, 1, 160.
- [12] M. A. Haidekker, E. A. Theodorakis. *Org. Biomol. Chem.*, **2007**, 5, 1669.

- [13] S. Flink, F. C. J. M. van Veggel, D. N. Reinhoudt., *Adv. Mater.*, **2000**, 12, 1315.
- [14] W. Q. Deng, A. H. Flood, J. F. Stoddart, and W. A. Goddard III., *J. Am. Chem. Soc.*, **2005**, 127, 15994.
- [15] V. Balzani, A. Credi, and M. Venturi., *Molecular Devices and Machines : A Journey Into The Nanoworld.*, Wiley – VCH Verlag GmbH & Co., **2003**, pp 272 – 274, 278 - 286.
- [16] E. R. Kay, D. A. Leigh, and F. Zerbetto., *Angew. Chem. Int. Ed.*, **2007**, 46, 72.
- [17] T. R. Kelly, J. P. Sestelo, and I. Tellitu., *J. Org. Chem.*, **1998**, 63, 3655.
- [18] M. M. Pollard, M. Lubomska, P. Rudolf, and B. L. Feringa., *Angew. Chem. Int. Ed.*, **2007**, 46, 1278.
- [19] T. R. Kelly, H. De Silva, R. A. Silva., *Nature.*, **1999**, 401, 150.
- [20] N. Koumura, R. W. J. Zijlstra, R. A. van Delden, N. Harada and B L. Feringa., *Nature.*, **1999**, 401, 152.
- [21] V. Serreli, C. F. Lee, E. R. Kay, and D. A. Leigh., *Nature.*, **2007**, 445, 523.
- [22] J. E. Green, J. W. Choi, A. Boukai, Y. Bunimovich, E. Johnston-Halperin, E. Delonno, Y. Luo, B. A. Sheriff, K. Xu, Y. S. Shin, H. R. Tseng, J. F. Stoddart, and J. R. Heath., *Nature.*, **2007**, 445, 414.
- [23] Y. Chen, G. Y. Jung, D. A. A. Ohlberg, X. Li, D. R Stewart, J. O. Jeppesen, K. A. Nielsen, J. F. Stoddart, R. S. Williams., *Nanotechnology*, **2003**, 14, 462.
- [24] S. J. Loeb, J A. Wisner., *Chem. Commun.*, **2000**, 1939.
- [25] C. M. Keaveney and D. A Leigh., *Angew. Chem. Int. Ed.* **2004**, 43, 1222.

- [26] S. Garaude, S. Silvi, M. Venturi, A. Credi, A. H. Flood, J. F. Stoddart., *Chem. Phys. Chem.*, **2005**, 6, 2145.
- [27] A. Altieri, F. G. Gatti, E. R. Kay, D. A. Leigh, D. Martel, F. Paolucci, A. M. Z. Slawin, J. K.Y. Wong., *J. Am. Chem. Soc.*, **2003**, 125, 8644.
- [28] G. Bottari, D. A. Leigh, E. M. Perez., *J. Am. Chem. Soc.*, **2003**, 125, 13360.
- [29] P. L. Anelli, N. Spencer, J. F. Stoddart., *J. Am. Chem. Soc.*, **1991**, 113, 5131.
- [30] A. Niemz, and V. M. Rotello., *Acc. Chem. Res.*, **1999**, 32, 44.
- [31] P. Hemmerich, C. Veeger, H. C. S. Wood., *Angew. Chem. Int. Ed.*, **1965**, 8, 671.
- [32] Y.-M. Legrand, M. Gray, G. Cooke, V. M. Rotello., *J. Am. Chem. Soc.*, **2003**, 125, 15789.
- [33] G. Cooke, J. F. Garety, B. Jordan, N. Kryvohyzha, A. Parkin, G. Rabani, and V. M. Rotello. *Org. Lett.*, **2006**, 8, 2297.
- [34] I. Ishikawa, Y. Nizuno, H. Ogura, and N. Kawahara., *Heterocycles*, **1990**, 31, 1641.
Synthesis and X – Ray Analysis of 1-Benzyl-6-Chlorouracil.
- [35] S. Kasai, B. J. Fritz, K. Matsui., *Bull. Chem. Soc. Jpn.*, **1987**, 60, 3041.